

**Membrane Spanning 4A Gene Family Expression and Function in Human
Mast Cells**

Thesis submitted for the degree of
Doctor of Philosophy
At the University of Leicester

by

Glenn Cruse BSc (Hons)

Department of Infection, Immunity and Inflammation,
Division of Respiratory Medicine,
University of Leicester Medical School, UK

2009

UMI Number: U559446

All rights reserved

INFORMATION TO ALL USERS

The quality of this reproduction is dependent upon the quality of the copy submitted.

In the unlikely event that the author did not send a complete manuscript and there are missing pages, these will be noted. Also, if material had to be removed, a note will indicate the deletion.



UMI U559446

Published by ProQuest LLC 2013. Copyright in the Dissertation held by the Author.
Microform Edition © ProQuest LLC.

All rights reserved. This work is protected against
unauthorized copying under Title 17, United States Code.



ProQuest LLC
789 East Eisenhower Parkway
P.O. Box 1346
Ann Arbor, MI 48106-1346

Declaration

The work presented in this thesis is the original work of the author, except where specific reference is made to other sources. It has not been submitted in part, or in whole for any other degree.

Glenn Cruse

Glenn Cruse

Membrane Spanning 4A Gene Family Expression and Function in Human Mast Cells

ABSTRACT

Mast cells are major effector cells of allergic and inflammatory disease. Thus understanding mechanisms of mast cell biology are of great interest to cell biology research. This study aimed to identify the expression and function of a newly identified gene family, the MS4A family, in human mast cells. This study identified 8 gene variants expressed in mast cells including 2 novel variants. All of the expressed genes were cloned and GFP and adenoviral constructs were generated. Quantitative RT-PCR demonstrated that all expressed gene variants were differentially regulated by mast cell stimulation with IgE, IgE/anti-IgE and stem cell factor (SCF) suggesting roles in mast cell biology. Transfections demonstrated that most proteins were trafficked to the cytoplasmic membrane, but some were trafficked to the nuclear membrane. This intracellular localisation of the MS4A family may be critical for their function. This was exemplified in this study by the function of a novel truncation (MS4A2_{trunc}) of MS4A2 (the beta chain of FcεRI). MS4A2_{trunc} was trafficked to the nuclear membrane, whereas MS4A2 was trafficked to the cytoplasmic membrane. Overexpression of MS4A2 using adenoviral transduction had no apparent effect on mast cell survival or proliferation. However, overexpression of MS4A2_{trunc} profoundly inhibited mast cell proliferation and induced apoptosis via G₂ phase cell cycle arrest. The removal of SCF from mast cell cultures upregulated the expression of MS4A2_{trunc}. In addition, the slowly replicating primary human lung mast cells, and the mast cell line LAD-2 expressed MS4A2_{trunc}. However, I was unable to demonstrate expression of MS4A2_{trunc} in the rapidly replicating c-KIT gain-of-function mutated mast cell line HMC-1. Thus loss of expression of MS4A2_{trunc} may be an important step in the development of mast cell neoplasia. This study has identified an entirely novel function for the MS4A2 gene and has opened numerous avenues for future research on the MS4A family.

Acknowledgements

I would like to thank everyone that participated and assisted in the completion of this work. Particularly: my supervisor Prof Peter Bradding; my co-supervisor Dr Mark Leyland; and Dr Su Li from Novartis Pharmaceuticals, Horsham.

I would also like to thank my thesis committee members, which in addition to those named above included Prof Chris Brightling and Dr Caroline Beardsmore.

I would also like to thank the staff at Glenfield Hospital in Respiratory Medicine, both past and present that have helped me along the way. Particular thanks to Dr Davinder Kaur and Dr S Mark Duffy for their help with methodology in FACS and electrophysiology, respectively. Thanks also to Prof Andrew Wardlaw for helpful input during data presentations. Finally thanks to technical staff and students that have helped with tissue culture and mast cell isolations, namely Abidan Muhayimana, Ryan Murray-Slater and Michelle Powell.

This study was funded by an unrestricted PhD Studentship from Novartis Pharmaceuticals, so thanks must also go to Novartis for funding this work.

Non standard abbreviations

Abbreviation	Definition
ASM	Airway smooth muscle
BAL	Bronchoalveolar lavage fluid
bFGF	Basic fibroblast growth factor
BHR	Bronchial hyper-responsiveness
BMMC	Bone marrow-derived mast cell
CBMC	Umbilical cord blood-derived mast cells
CD117	c-KIT – receptor for stem cell factor
Cdk	Cyclin-dependent kinase
CHO	Chinese hamster ovary
C _t	Cycle threshold
CTMC	Connective tissue mast cells
DC	Dendritic cell
DMEM	Dulbecco's modified Eagle's medium
FBS	Foetal bovine serum
FcεRI	High affinity IgE receptor
GAG	Glycosaminoglycan
GFP	Green fluorescent protein
GM-CSF	Granulocyte macrophage-colony stimulating factor
GOI	Gene of interest
HLMC	Human lung mast cell
HMT	Histamine- <i>N</i> -methyltransferase
IgE	Immunoglobulin E
IFN _γ	Interferon γ
IP ₃	Inositol triphosphate
ITAM	Immunoreceptor tyrosine-based activation motif
IU	Infective units
K _{Ca} 3.1	Intermediate conductance Ca ²⁺ -activated K ⁺ channel
Kir2.1	Inwardly-rectifying K ⁺ channel 2.1
LPS	Lipopolysaccharide
LTC ₄	Leukotriene C ₄
MC _C	Mast cell containing chymase

MC _T	Mast cell containing tryptase
MC _{TC}	Mast cell containing tryptase and chymase
MIRR	Multichain immune recognition receptor
MMC	Mucosal mast cells
MOI	Multiplicity of infection
MS4A	Membrane spanning 4 A gene
NGF	Nerve growth factor
NTC	No template control
ORF	Open reading frame
PAR	Protease-activated receptor
PGD ₂	Prostaglandin D ₂
PLA ₂	Phospholipase A ₂
PLC	Phospholipase C
RBL	Rat basophil leukaemia
RER	Rough endoplasmic reticulum
RSV	Respiratory syncytial virus
SAM	S adenosyl methionine
SCF	Stem cell factor
SH2	Src homology 2
SHIP	Src homology 2-containing inositol phosphatase
SOCC	Store-operated calcium channel
SOCE	Store-operate calcium entry
TGF- β	Transforming growth factor β
TLR	Toll-like receptor
T _m	Melting temperature
TNF α	Tumour necrosis factor α
tPA	tissue plasminogen activator
TRAIL	Tumour necrosis factor-related apoptosis inducing ligand
VEGF	Vascular endothelial growth factor
VP	Virus particles

List of Figures

	Page
1.1 Ontogeny of mast cells	5
1.2 The contribution of mast cell mediators to inflammatory cell recruitment	18
1.3 Mast cell interactions with structural airway cells in the pathogenesis of asthma	23
1.4 Simplified schematic of mast cell signaling events leading to degranulation and mediator production	27
1.5 IgE-dependent and –independent mechanisms of mast cell activation	33
2.1 Multiple sequence alignment of proteins with high amino acid sequence similarity to MS4A2	48
2.2 Map of the pGEM [®] -T Easy Vector	60
2.3 Map of the pEGFP-N1 Vector	63
2.4 Map for Adapt6 Vector	65
3.1 RT-PCR for MS4A gene expression in human mast cells	85
3.2 RT-PCR cloning of the full length open reading frame of MS4A gene family members and their splice variants in LAD-2 cells	88
3.3 Restriction enzyme digests of cDNA obtained from transformed <i>E. coli</i>	89
3.4 RT-PCR cloning of the full length open reading frame of MS4A gene family members and their splice variants in HLMC	90
3.5 Restriction enzyme digests of cDNA excised from the gel of Figure 3.4 and cloned into JM109 <i>E. coli</i>	91
3.6 The full open reading of MS4A2	92
3.7 The full open reading of MS4A2 _{trunc}	93
3.8 The full open reading of MS4A4 variant 1	94
3.9 The full open reading of MS4A6 variant 1	95
3.10 The full open reading of MS4A4 variant 1 polymorphism	96
3.11 The full open reading of MS4A6 novel variant	97
3.12 The full open reading of MS4A7 variant 1	98
3.13 The full open reading of MS4A7 variant 2	99
3.14 LAD-2 products using qualitative real time RT-PCR	102

3.15	LAD-2 products using qualitative real time RT-PCR	103
3.16	HMC-1 products using qualitative real time PCR	105
3.17	HLMC products using qualitative real time PCR	106
3.18	HLMC products before and after IgE stimulation	107
3.19	Fibrocyte products using real time PCR	108
3.20	Dissociation curves for MS4A2 and MS4A2 _{trunc}	111
3.21	Dissociation curves for MS4A4 and MS4A6 Variant 1	112
3.22	Dissociation curves for MS4A6 polymorphism and MS4A6 novel variant	113
3.23	Dissociation curves for MS4A7 variants	114
3.24	Dissociation curves for β -actin	115
3.25	Efficiency of MS4A2 QPCR reaction	117
3.26	Efficiency of MS4A2 _{trunc} QPCR reaction	117
3.27	Efficiency of MS4A4 variant 1 QPCR reaction	118
3.28	Efficiency of MS4A6 variant 1 QPCR reaction	118
3.29	Efficiency of MS4A6 polymorphism QPCR reaction	119
3.30	Efficiency of MS4A6 novel variant QPCR reaction	119
3.31	Efficiency of MS4A7 short variant QPCR reaction	120
3.32	Efficiency of MS4A7 long variant QPCR reaction	120
3.33	SCF down-regulates the expression of MS4A2 _{trunc}	123
3.34	Regulation of expression of MS4A4 variant 1	124
3.35	Regulation of MS4A6 gene variants in mast cells	127
3.36	Regulation of MS4A7 gene variants in mast cells	129
3.37	MS4A family localisation in LAD-2 cells using nucleofection	131
3.38	MS4A family localisation in HMC-1 cells using lipofection	133
3.39	Effects of MS4A gene family transfection on baseline currents in CHO cells	135
3.40	The K _{Ca} 3.1 opener 1-EBIO induces a K _{Ca} 3.1-like current in CHO cells after transfection with MS4A4 variant 1	137
3.41	Human mast cells express a novel truncation of MS4A2	138
3.42	MS4A2 _{trunc} sequencing	139
3.43	Transmembrane domain predictions	141
3.44	MS4A2 and MS4A2 _{trunc} can be successfully transduced into human mast cells	144

3.45	MS4A2 _{trunc} localizes to the nuclear membrane rather than the cytoplasmic membrane	146
3.46	MS4A2 _{trunc} prevents proliferation of HMC-1 cells and initiates cell death	149
3.47	Transduction of MS4A2 _{trunc} induces apoptosis	151
3.48	The antiproliferative effect of MS4A2 _{trunc} was due to G ₂ /M phase arrest	154
3.49	Overexpression of MS4A2 _{trunc} decreases FcεRI expression in HLMC	156

List of Tables

	Page
1.1 Mast cell sub-type characteristics	8
1.2 The classical human mast cell mediators and their biological effects	12
1.3 In vitro biological effects of human mast cell cytokines	13
1.4 In vitro biological effects of human mast cell chemokines	14
2.1 Cell line characteristics	43
2.2 Primers designed for RT-PCR of MS4A family members to confirm expression in human mast cells	52
2.3 Primers designed for quantitative real time RT-PCR of expressed MS4A family members and splice variants in human mast cells	55
2.4 Primers designed for cloning of MS4A family members and splice variants in human mast cells	58
2.5 Primers designed for producing MS4A : eGFP chimeric proteins	63
2.6 Primers designed for producing MS4A adenoviral constructs	65
2.7 Antibodies used	81
3.1 Summary of MS4A gene family expression	109

CONTENTS

	Page
Declaration	I
Abstract	II
Acknowledgements	III
Non standard abbreviations	IV
List of figures	VI
List of tables	IX
Contents	X
1 Chapter 1: Introduction	1
1.1 Introduction	2
1.2 Mast cell biology	2
1.2.1 Mast cell development	2
1.2.2 Mast cell heterogeneity	6
1.2.3 General morphology and biology	9
1.3 Role of mast cells in health	15
1.3.1 Mast cells in wound repair and angiogenesis	15
1.3.2 Mast cells and inflammation	17
1.3.3 Parasite infection	19
1.3.4 Defence against bacterial and viral infection	19
1.4 Mast cell interactions with the specific immune system	20
1.4.1 Mast cells and antigen presentation	20
1.5 The role of mast cells in allergic diseases	21
1.5.1 Mast cells in asthma	22
1.6 Mechanisms of mast cell activation	25
1.6.1 IgE-dependent activation	25
1.6.2 Monomeric IgE-dependent mast cell activation	29
1.6.3 Non-immunological stimuli	30
1.7 Novel targets for therapies in asthma	34
1.7.1 The membrane spanning 4A gene family	35
1.7.1.1 Possible functions of the MS4A gene family	36
1.7.2 Project aims	38

2	Chapter 2: Materials and methods	40
2.1	Cells	41
	2.1.1 Cell lines	41
	2.1.2 Human lung mast cell isolation	42
2.2	MS4A gene expression analysis	44
	2.2.1 Isolation of total RNA from human mast cells	44
	2.2.2 RT-PCR	44
	2.2.3 Quantitative real-time PCR	53
2.3	Molecular biology	56
	2.3.1 MS4A family cloning	56
	2.3.2 Generation of green fluorescent protein - MS4A chimeric constructs	60
	2.3.3 Generation of adenoviral constructs	64
2.4	MS4A protein trafficking	66
	2.4.1 Transfection of GFP tagged MS4A proteins into LAD-2 cells	66
	2.4.2 Transfection of GFP tagged MS4A proteins into HMC-1 cells	66
	2.4.3 Transduction of MS4A gene family members into HLMC	67
	2.4.3.1 Transduction of HLMC using Ad5C01Att01 adenovirus	67
	2.4.3.2 Transduction of HLMC using Ad5C20Att01 Adenovirus	68
	2.4.4 Immunofluorescence of MS4A gene products in HLMC	69
	2.4.5 Confocal microscopy	70
2.5	Mediator release assays	70
	2.5.1 Mast cell challenge experiments	70
	2.5.2 Histamine radioenzymatic assay	71
2.6	Electrophysiology	73
	2.6.1 Single cell patch clamping	73
	2.6.1.1 Patch clamping solutions	73
2.7	Cell survival/proliferation and cell cycle assays	74
	2.7.1 Trypan blue method	74
	2.7.2 Apoptosis assays	75

2.7.3	Proliferation assays – ³ H-thymidine uptake	76
2.7.4	Cell cycle analysis	77
2.8	Protein expression assays	78
2.8.1	Flow cytometry	78
2.8.1.1	Intracellular staining for flow cytometry	78
2.8.1.2	Extracellular staining for flow cytometry	79
2.8.2	Western blotting	80
3	Chapter 3: Results	82
3.1	RT-PCR	83
3.1.1	MS4A gene family expression in human mast cells	83
3.2	Identification, cloning and sequencing of MS4A gene family	86
3.2.1	MS4A gene family cloning	86
3.2.2	Cloned sequences of the MS4A gene family	91
3.3	Qualitative and quantitative real time PCR and gene regulation	100
3.3.1	Qualitative real time RT-PCR for gene expression	100
3.3.1.1	Qualitative MS4A gene expression in LAD-2 cells	100
3.3.1.2	Qualitative MS4A gene expression in HMC-1 cells	104
3.3.1.3	Qualitative MS4A gene expression in HLMC	105
3.3.2	Quantitative real time RT-PCR	109
3.3.2.1	Confirming specificity of QPCR amplification	109
3.3.2.2	Determining the efficiency of the QPCR reaction	116
3.3.3	Quantitative real time RT-PCR for regulation of gene expression	121
3.3.3.1	MS4A2 variants	121
3.3.3.2	MS4A4	124
3.3.3.3	MS4A6 variants	125
3.3.3.4	MS4A7 variants	128
3.4	Protein trafficking and sub-cellular localisation	130
3.4.1	Localisation of MS4A – eGFP chimeric proteins in LAD-2 cells	130
3.4.2	Localisation of MS4A – eGFP chimeric proteins in HMC-1 cells	132
3.5	MS4A electrophysiology	134

3.5.1	Electrophysiology of baseline currents in transfected CHO cells	134
3.5.2	Transfection of MS4A4 into CHO cells induces a $K_{Ca}3.1$ -like current with the addition of the $K_{Ca}3.1$ opener 1-EBIO	136
3.6	Effects of MS4A2 on human mast cell function	138
3.6.1	Identification of MS4A2 truncation	138
3.6.2	Regulation of expression of MS4A2 gene variants	142
3.6.3	Transduction and overexpression of the MS4A2 variants in human mast cells	143
3.6.4	MS4A2 _{trunc} traffics preferentially to the nuclear membrane	145
3.6.5	Transduction of MS4A2 _{trunc} into human mast cells inhibits cell proliferation and survival	147
3.6.6	MS4A2 _{trunc} induces apoptosis in human mast cells	150
3.6.7	The anti-proliferative effects of MS4A2 _{trunc} are mediated via G2 cell cycle arrest	152
3.6.8	MS4A2 _{trunc} decreases surface FcεR1α expression	155
4	Chapter 4: Discussion	157
4.1	Future work	167
4.2	Future aims	168
5	Chapter 5: References	170
6	Chapter 6: Appendix	204
6.1	Solutions	205

CHAPTER 1: INTRODUCTION

1.1 INTRODUCTION

Since their discovery over a century ago, the role of mast cells in human pathophysiology has been the subject of much debate. Mast cells are ubiquitous throughout connective tissues and mucosal surfaces, particularly at the interface with the external environment such as the skin, respiratory tract and gastrointestinal tract. At these sites they are well placed and well-equipped to deal with a multitude of tissue insults. Mast cells contribute to the maintenance of tissue homeostasis with examples including roles in wound repair ^(1;2), revascularisation ⁽³⁾, and protective roles in acquired and innate immune responses to bacterial infection ⁽⁴⁾. They are also implicated in many diverse diseases such as asthma and related allergies, pulmonary fibrosis, connective tissue disease, multiple sclerosis and atherosclerosis. Mast cells can therefore be considered to represent a double-edged sword.

1.2 MAST CELL BIOLOGY

1.2.1 Mast Cell Development

Mast cells derive from pluripotent haematopoietic stem cells in the bone marrow (**Figure 1.1**). Mast cell-committed progenitors are released into the systemic circulation as agranular, undifferentiated, CD34⁺ mononuclear cells which then migrate into their destination tissue where they terminally differentiate (mature) under the influence of the local cytokine milieu (for review of mast cell ontogeny see ⁽⁵⁾). In addition, interactions with the cell matrix and resident cells such as fibroblasts profoundly alters their phenotype ⁽⁶⁻¹¹⁾. The vital growth factor for

mast cells is the stromal cell and fibroblast-derived cytokine, stem cell factor (SCF)⁽¹²⁾. Previously known as steel factor, SCF is the ligand for the receptor tyrosine kinase CD117, encoded by the proto-oncogene *c-kit*⁽¹³⁾. SCF exists as both a cell membrane-bound protein and a soluble protein which can be detected in the blood⁽¹⁴⁾. The activation of *c-kit* by SCF is vital for the growth and survival of mast cells which undergo apoptosis on SCF withdrawal⁽¹⁵⁾. Mast cells can also undergo apoptosis in the presence of SCF since they have been found to have tumour necrosis factor-related apoptosis inducing ligand (TRAIL) receptors which initiate apoptosis⁽¹⁶⁾. Activation of *c-kit* on mast cells regulates expression levels of *c-kit*⁽¹⁷⁾, induces immature cell proliferation, promotes chemotaxis and suppresses apoptosis thus enhancing survival and promoting recruitment and growth⁽¹⁸⁾. The activation of *c-kit* also has a regulatory role in mast cell activation. At 10 ng/ml it potentiates IgE-dependent mast cell mediator and cytokine release, while at 100 ng/ml it directly activates the cells⁽¹⁹⁻²⁶⁾.

SCF is the critical growth factor responsible for mast cell growth and differentiation in humans. Mast cells will grow *in vitro* with SCF as the only exogenous factor although the cells remain immature and are predominantly of the tryptase-only (MC_T) phenotype⁽²⁷⁾. However, cells that are grown in suspension culture in a medium supplemented with serum, SCF, and IL-6 are more mature in terms of their nuclear morphology and granular structure but remain as the MC_T phenotype⁽²⁸⁻³¹⁾. Cells grown on a fibroblast or endothelial cell monolayer have a tryptase⁺ chymase⁺ (MC_{TC}) phenotype and resemble skin mast cells^(27;31-33). In addition, bone marrow- derived mast cells (BMMC) and umbilical cord blood-derived mast cells (CBMC) grown in conditioned medium

from a cell strain derived from a patient with systemic mastocytosis together with SCF yielded fully mature cells containing chymase only (MC_C phenotype)⁽³⁴⁾. These observations suggest that factors other than SCF are required for complete mast cell maturation. The phenotypic differences could be due, in part, to the presence of IL-4 which dramatically increases chymase expression in CBMC⁽³⁵⁾. It is also possible that the expression of chymase is part of a maturation pathway with MC_T phenotypes maturing into MC_{TC} phenotypes⁽¹⁸⁾.

There are co-factors that can enhance or inhibit the effects of SCF, which appear to be dependent upon the origin of the mast cells⁽³⁶⁾. Nerve growth factor (NGF)⁽³⁷⁾, IL-3, IL-6, IL-9, IL-10^(28;38) and thrombopoietin enhance SCF-dependent mast cell growth. Conversely, granulocyte macrophage-colony stimulating factor (GM-CSF)⁽³⁹⁾, retinoids, interferon γ (IFN γ) and transforming growth factor β (TGF- β) inhibit the growth and differentiation of mast cells⁽⁴⁰⁾.

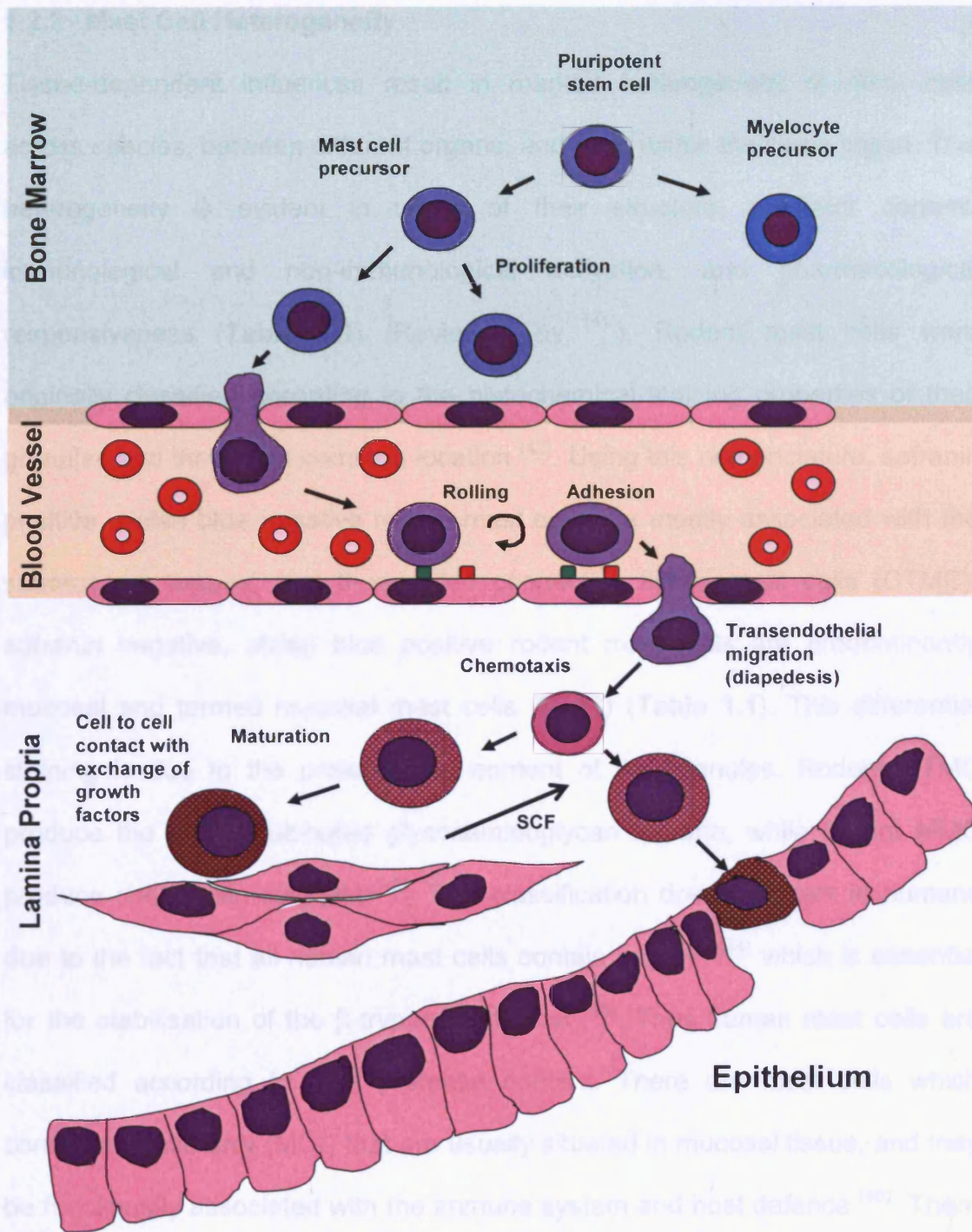


FIGURE 1.1: Ontogeny of mast cells. Mast cells originate from pluripotent hematopoietic stem cells in the bone marrow. They enter the bloodstream as mast cell-committed CD34+ progenitor cells. Mast cells differentiate after tissue recruitment within the tissue itself, which accounts for much of their heterogeneity. For more details, see text.

1.2.2 Mast Cell Heterogeneity

Tissue-dependent influences result in marked heterogeneity of mast cells across species, between different organs, and even within the same organ. This heterogeneity is evident in terms of their structure, mediator content, immunological and non-immunological activation, and pharmacological responsiveness (**Table 1.1**) (Reviewed by ⁽⁴¹⁾). Rodent mast cells were originally classified according to the histochemical staining properties of their granules and their most common location ⁽⁴²⁾. Using this nomenclature, safranin positive, alcian blue negative rodent mast cells are mostly associated with the submucosal tissues, and thus called connective tissue mast cells (CTMC); safranin negative, alcian blue positive rodent mast cells are predominantly mucosal and termed mucosal mast cells (MMC) (**Table 1.1**). This differential staining is due to the proteoglycan content of the granules. Rodent CTMC produce the highly sulphated glycosaminoglycan heparin, while rodent MMC produce chondroitin sulphate ⁽⁴³⁾. This classification does not work in humans due to the fact that all human mast cells contain heparin ⁽⁴⁴⁾ which is essential for the stabilisation of the β -tryptase tetramer ⁽⁴⁵⁾. Thus human mast cells are classified according to their protease content. There are mast cells which contain tryptase only (MC_T) that are usually situated in mucosal tissue, and may be functionally associated with the immune system and host defence ⁽⁴⁶⁾. There are also tryptase, chymase, carboxypeptidase A and cathepsin G containing mast cells (MC_{TC}) (**Table 1.1**), which are normally situated in the skin and submucosal connective tissue, and are proposed to be involved in tissue repair, fibrotic reactions and angiogenesis ^(47,48). There are also reports of mast cells containing chymase and carboxypeptidase (MC_C) without tryptase ⁽⁴⁹⁻⁵¹⁾ which

vary in location, and whose function has yet to be elucidated. The heterogeneity of mast cells also extends to their cytokine content. The expression of IL-4 and IL-13 is predominantly in MC_{TC} whilst IL-5 and IL-6 are almost exclusively in MC_T^(49;52), again suggesting distinct roles for these phenotypes.

TABLE 1.1: Mast cell sub-type characteristics

Characteristics	Rodent Mast Cells		Human Mast Cells	
	MMC	CTMC	MC _T	MC _{TC}
Protease Content	Chymase (rat mast cell protease 2)	Chymase (rat mast cell protease 1)	Tryptase	Tryptase Chymase Carboxypeptidase Cathepsin G
Proteoglycan Content	Chondroitin sulphate	Heparin	Heparin	Heparin
Predominant granule patterning evident with electron microscopy			Scroll	Lattice
Common Location	Mucosa	Submucosal tissues	Epithelium	Lamina propria, connective tissue and skin
Staining Characteristics	Alcian Blue +	Safranin +	Safranin +	Safranin +
Suggested Primary Role	Host defence	Tissue repair	Host defence	Tissue repair
Relative Histamine Content	Low	High	Low	High
Relative Leukotriene C ₄ release	High	Absent	High	Skin low
Relative Prostaglandin D ₂ release	Low	Low	High	Skin high
Cytokine Profile			IL-4 (low) IL-5 (High) IL-6 (High) IL-13 (low)	IL-4 (High) IL-13 (High)
Activated by antigen	Yes	Yes	Yes	Yes
Activated by substance P	No	Yes	No	Yes
Responds to C5a			No	Yes
Inhibited by sodium cromoglycate	No	Yes	Yes (weak effect)	No

1.2.3 General Morphology and Biology

Despite the heterogeneity of mast cells, their general morphology is similar regardless of the tissue site they reside in. Ultrastructurally, the cell membrane contains finger-like projections, and while immature mast cells may have a multi-lobed nucleus, mature cells have a mono-lobed nucleus with no apparent nucleoli and little condensed chromatin. They have few mitochondria and ribosomes, as well as an inconspicuous Golgi apparatus, scant rough endoplasmic reticulum (RER), and in contrast to basophils, a lack of cytoplasmic glycogen aggregates (Reviewed by ⁽⁵³⁾). In fact, the only cytoplasmic structures that are prominent are the electron dense granules. Unusually, mature human mast cells have ribosomes closely associated with these secretory granules, and little association between ribosomes and RER ⁽⁵⁴⁾. This suggests that the secretory granules play a significant role in ribonucleic acid (RNA) metabolism in human mast cells. The granules are membrane bound and contain preformed mediators, while dense lipid bodies are a store of arachidonic acid. The membrane bound secretory granules contain crystalline structures that resemble scrolls, lattices, crystals or whorls ⁽⁵³⁾. These structures are more visible in MC_T subtypes as the sheer volume of protease in the MC_{TC} subtype masks their appearance. Despite this, electron microscopy can show that MC_T granules contain predominantly scroll patterns and MC_{TC} granules contain predominantly lattice patterns (**Table 1.1**)⁽⁵⁵⁾.

Mast cells have basophilic cytoplasm which stains pink when using Wright's or May-Grunwald's Giemsa, with a purple/blue nucleus and blackish granules. Mast cells can have an irregular shape in tissues but can be identified by

selective staining using cationic dyes (such as aniline dyes) that bind to sulphated glycosaminoglycans (GAGs) specific to the mast cell granules. Using stains that utilise the anionic property of the mast cell granules to identify their presence is a useful tool. However, in humans the most effective way to identify the location and subtype of mast cells histologically is to use immunohistochemistry with antibodies raised against the mast cell specific enzymes tryptase and chymase ⁽⁵⁶⁾.

The proteoglycans of the granules are the backbone of the granule matrix. They are a long single peptide with GAGs attached. In human mast cells, the proteoglycan content of the granules is mainly heparin and chondroitin E. Neutral proteases, acid hydrolases and histamine molecules are attached to the proteoglycans by ionic linkage to the sulphate groups on the GAGs ⁽⁵⁷⁾. The sulphate groups generate an acidic environment within the granules which maintains the mediators in an inactive state ⁽⁵⁸⁾. IgE-dependent activation of the mast cell induces granule swelling, crystal dissolution, granule fusion, both with surrounding granules as well as the cell membrane, followed by exocytosis with release of mediators into the extracellular space ⁽⁵⁹⁾. This process is termed compound exocytosis, or anaphylactic degranulation. Once in the extracellular space, the neutral pH activates the mediators ^(59;60). However, in many diseased tissues including asthmatic bronchial mucosa, the ultrastructural appearance of mast cells typically demonstrates piecemeal degranulation ⁽⁶¹⁻⁶³⁾, in which there is variable loss of granule contents although the granules and their membranes remain intact. The mechanisms leading to piecemeal degranulation in mast cells are poorly understood and require further research. The effects of

TABLE 1.2: The classical human mast cell mediators and their biological effects

<u>Preformed</u>	<u>Effects</u>
Histamine	Bronchoconstriction; tissue oedema; mucus secretion; fibroblast proliferation; collagen synthesis; endothelial proliferation, dendritic cell activation
Heparin	Anticoagulant; storage matrix for mast cell mediators; fibroblast activation; protects growth factors from degradation and potentiates their action; endothelial cell migration
Trypsase	Generates C3a and bradykinin; degrades neuropeptides; increases BHR; indirectly activates collagenase; fibroblast proliferation and collagen synthesis; bone remodelling, epithelial activation, potentiates mast cell histamine release
Chymase	Mucus secretion; extracellular matrix degradation, type I procollagen processing, converts angiotensin I to angiotensin II, inhibits T cell adhesion to airway smooth muscle, activates IL-1 β , degrades IL-4, releases membrane-bound SCF.
<u>Newly generated</u>	
PGD ₂	Bronchoconstriction; tissue oedema; mucus secretion; dendritic cell activation; chemotaxis of eosinophils, Th2 T cells and basophils via the CRTH2 receptor
LTC ₄ /D ₄	Bronchoconstriction; tissue oedema; mucus secretion; enhances IL-13-dependent airway smooth muscle proliferation; dendritic cell maturation and migration; eosinophil IL-4 secretion, mast cell IL-5, IL-8 and TNF α secretion; tissue fibrosis

TABLE 1.3: In vitro biological effects of human mast cell cytokines

Cytokine	Target cells	Biological effects
IL-4	B cells	IgE production; proliferation; MHC class II, CD40, and CD25 expression; IL-6 production Proliferation; induction of TH2 cell phenotype ↑ VCAM-1 and ↓ ICAM-1 expression; proliferation ↓ generation of H ₂ O ₂ and O ₂ ·, ↓ parasite killing and ↓ tumouricidal activity; ↓ IL-1, -6, -8, and TNFα production. ↑ MHC class II and CD23 expression; monocyte → macrophage differentiation; 15-lipoxygenase expression Transendothelial migration Proliferation, chemotaxis and matrix protein secretion; ↑ ICAM-1 expression ↑ FcεRI expression, ↑ ICAM-1 expression
	T cells	
	Vascular endothelial	
	Monocyte/macrophages	
	Eosinophils	
IL-3, IL-5, and GM-CSF	Eosinophils	Growth, adhesion, transendothelial migration, chemotaxis, activation, and prolonged survival.
	Fibroblasts	
IL-6	B cells	Immunoglobulin secretion including ↑ IgE synthesis Growth, differentiation and activation Airway glandular Mucus secretion Survival
	T cells	
	Mast cells	
IL-13	B cells	IgE synthesis As for IL-4 Activation, ↑ survival ↑ VCAM-1
	Monocyte/macrophages	
	Eosinophils	
	Vascular endothelial	
IL-16	T cells	Chemotaxis
TNFα	Monocyte/macrophages	Enhanced cytotoxicity; chemotaxis and prolonged survival Class II antigen and IL-2R expression; proliferation Chemotaxis, enhanced cytotoxicity Enhanced cytotoxicity and oxidant production Histamine and tryptase secretion E-Selectin, ICAM-1, and VCAM-1 expression. Adhesion and transendothelial migration of most leucocytes. Growth and chemotaxis; ↓ collagen synthesis but ↑ Airway glandular mucus secretion
	T cells	
	Neutrophils	
	Eosinophils	
	Mast cells	
	Vascular endothelial	
SCF	Mast cells	Growth, differentiation, survival, chemotaxis
NGF	Mast cells	Differentiation, survival, activation, mediator release Differentiation, proliferation, Ig synthesis Differentiation, proliferation Proliferation Activation, mediator release Chemotaxis, survival, mediator release Proliferation, mediator release Migration, contraction Migration, contraction, proliferation
	B cells	
	T cells	
	Eosinophils	
	Basophils	
	Neutrophils	
	Monocyte/macrophages	
	Fibroblasts	
	Smooth muscle cells	
TGFβ	Smooth muscle cells	Differentiation, activation Inhibition of proliferation Induces angiogenesis
	Epithelial cells	
	Endothelial cells	
basic FGF	Fibroblasts	Proliferation Stimulates angiogenesis
	Vascular endothelial	

TABLE 1.4: In vitro biological effects of human mast cell chemokines

Chemokine	Target cells	Biological effects
CCL1	T cells	Chemotaxis (Selective for Th2), survival?
CCL2	T cells Mast cells Eosinophils Monocytes Fibrocytes Epithelial cells Basophils	T cell polarisation towards Th2 phenotype, Chemotaxis Chemotaxis Chemotaxis Chemotaxis Proliferation, chemotaxis Activation, mediator release
CCL3	Macrophages Neutrophils Eosinophils Monocytes Mast cells Basophils T cells	Differentiation Chemotaxis (<i>in vivo</i>) and cytotoxicity Chemotaxis Chemotaxis Activation, mediator release Activation, mediator release Chemotaxis (selective for Th1), polarisation towards Th1 phenotype
CCL4	Eosinophils Neutrophils T cells	Chemotaxis Chemotaxis (<i>in vivo</i>) Chemotaxis (selective for Th1), polarisation towards Th1 phenotype
CCL5	Mast cells Eosinophils Monocytes T cells	Chemotaxis? Chemotaxis Chemotaxis Chemotaxis (selective for Th1), polarisation towards Th1 phenotype
CCL7	Eosinophils Monocytes Basophils	Chemotaxis Chemotaxis Activation, mediator release
CCL12	Fibrocytes Monocytes Eosinophils Lymphocytes	Chemotaxis Chemotaxis Chemotaxis Chemotaxis
CCL17	T cells	Chemotaxis (selective for Th2)
CCL19	Airway smooth muscle	Chemotaxis
CCL20	Dendritic cells T cells	Chemotaxis Chemotaxis
CCL22	T cells	Chemotaxis (selective for Th2)
CXCL5	Neutrophils	Chemotaxis
CXCL8	Neutrophils Mast cells Endothelial cells Eosinophils	Chemotaxis Inhibition of chemotaxis, inhibition of mediator release, Proliferation, survival, chemotaxis, angiogenesis Chemotaxis after priming with IL-3, IL-5 or GM-CSF

1.3 ROLE OF MAST CELLS IN HEALTH

Interest in the function of mast cells in disease often takes precedence over their role in health. However, mast cells may play a significant role in the healing of wounds and defence against bacterial and parasitic infection, participating in both innate and adaptive immunity. They are also major effector cells in inflammatory processes attracting leucocytes to the area of insult which contributes to host defence and repair. It is likely, therefore, that their primary role is to sense the external environment, ready to respond to a variety of diverse tissue insults with an early and appropriate program of gene expression and mediator release aimed at initiating inflammation and then repair. When the insult becomes chronic, then it is our view that their continuing activation contributes to tissue dysfunction and remodelling. In addition, through the misguided generation of allergen-specific IgE by host B cells, they have the potential to induce acute, sometimes life-threatening symptoms on exposure to allergen.

1.3.1 Mast Cells in Wound Repair and Angiogenesis

Due to the biological actions of their mediators (**Tables 1.2, 1.3 and 1.4**), mast cells have been thought to be involved in the healing of wounds. Early studies using metachromatic staining showed that mast cells “disappear” at the wound edge in the first few days, possibly due to degranulation, then increase two-fold over baseline by 10 days before returning to normal ⁽⁶⁷⁾. However, studies using mast cell-deficient mice have provided conflicting results. Egozi and co-workers found that mast cells modulated the early inflammatory response to wound healing and angiogenesis, but were not required for the late phase proliferative

response to injury and had no effect on collagen deposition and re-epithelialisation ⁽⁶⁸⁾. In contrast, Iba and co-workers showed that mast cells contributed to the late phase remodelling in wound healing and that collagen fibrils were more interwoven in wild type mice than mast cell deficient mice (*Kit^w/Kit^{w-v}*) ⁽¹⁾. The differing results between these studies may be due to the experimental models used. However, neither study showed any real convincing evidence of a major role for mast cells in wound repair. In contrast, a study by Weller and colleagues suggested that mast cell deficient (*Kit^w/Kit^{w-v}*) mice have significant retardation of wound closure when compared to wild type, and that mast cells are required for normal wound healing ⁽²⁾.

Mast cells may potentially inhibit thrombosis within damaged tissues through the release of heparin, tryptase, chymase and tissue plasminogen activator (tPA), allowing perfusion and nutrition to the site of injury ^(69;70). In support of this, mast cell-deficient mice are more susceptible to lethal thrombogenic stimuli than wild-type mice.

Neovascularisation occurs in a number of physiological and pathological situations including wound healing and tumour growth respectively. Mast cells are usually found at sites of neovascularisation such as around the periphery of solid tumours ⁽⁷¹⁻⁷³⁾. Rodent mast cells and the human mast cell line HMC-1 induce proliferation of microvessels ⁽⁷⁴⁾. Several cytokines identified in human mast cells have potential roles in angiogenesis including TNF α , basic fibroblast growth factor (bFGF), and vascular endothelial growth factor (VEGF). Supernatants from unstimulated HMC-1 cells induce proliferation of human

microvascular endothelial cells which is largely mediated by VEGF ⁽⁷⁵⁾. In a model of vascular tube formation, human dermal microvascular endothelial cells exposed to HMC-1 cell supernatants or co-cultured with HMC-1 cells rapidly differentiate and mature into vascular tubes ⁽⁷⁶⁾. This effect is reproduced by exposure of vascular cells to purified human tryptase, and inhibited approximately 80% following pre-treatment of HMC-1 supernatants with the specific tryptase inhibitor BABIM.

1.3.2 Mast cells and inflammation

Mast cells can contribute to the inflammatory response at various stages. The mechanisms controlling leucocyte recruitment to sites of inflammation includes a series of steps and mast cells can contribute to all of these processes. In addition, mast cells can also activate effector cells for mediator secretion. Thus mast cell mediators and cytokines have the potential to control inflammation at all stages (**Figure 1.2**)(**Tables 1.3 and 1.4**). Indeed, a wealth of evidence suggests that this is the case (reviewed by ⁽³¹⁾).

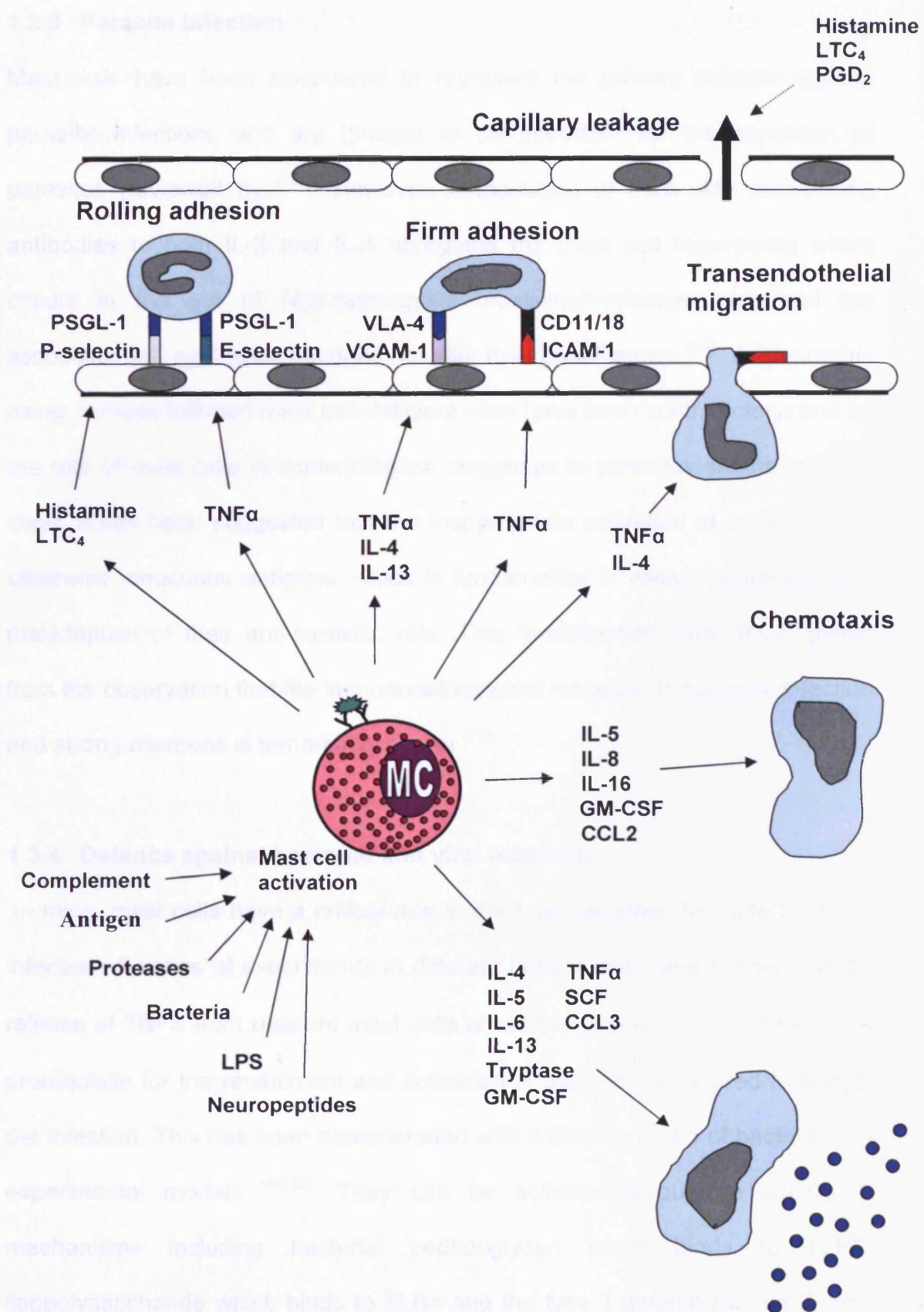


FIGURE 1.2: The contribution of mast cell mediators to inflammatory cell recruitment. See text for definition of abbreviations. Figure modified from ⁽⁷⁷⁾.

1.3.3 Parasite Infection

Mast cells have been considered to represent the primary defence against parasitic infections and are thought to be important for the expulsion of parasites (reviewed by ⁽⁷⁸⁾). However, inoculation of mice with neutralising antibodies to both IL-3 and IL-4 abrogates the mast cell hyperplasia which occurs in the gut of *Nippostrongylus brasiliensis*-infected mice and the associated IgE synthesis, but does not alter the clinical course ⁽⁷⁹⁾. Experiments using parasite-infected mast cell-deficient mice have been contradictory, and so the role of mast cells in immunological responses to parasites seems far from clear. It has been suggested that the inappropriate activation of mast cells by otherwise innocuous antigens, which is fundamental in allergic reactions, is a maladaptation of their anti-parasitic role. This “maladaptation hypothesis” stems from the observation that the immunopathological response to parasitic infection and strong allergens is remarkably similar ⁽⁷⁸⁾.

1.3.4 Defence against bacterial and viral infection

In mice, mast cells have a critical role in the host response to acute bacterial infection. A series of experiments in different laboratories have shown that the release of TNF α from resident mast cells at various tissue sites is an essential prerequisite for the recruitment and activation of neutrophils required to control the infection. This has been demonstrated with a diverse range of bacteria and experimental models ⁽⁸⁰⁻⁸²⁾. They can be activated through a variety of mechanisms including bacterial peptidoglycan which binds to TLR2, lipopolysaccharide which binds to TLR4 and the type 1 fimbrial subunit (FimH) which binds to CD48 ^(83;84). Mast cells can also ingest opsonised bacteria, and

potentially kill them following oxidative burst ⁽⁸⁴⁾, and are activated following ligation of TLR3 indicating a likely role in the host response to viral infection ⁽⁸⁵⁾. These studies provide a clear example of where mast cells, in mice at least, provide an important protective role for the host. This role in the defence against local infection perhaps explains why mast cells are so widely distributed throughout the human body, particularly at mucosal sites and within the skin which provide a ready portal of entry for foreign organisms.

1.4 MAST CELL INTERACTIONS WITH THE SPECIFIC IMMUNE SYSTEM

1.4.1 Mast cells and antigen presentation

In addition to the innate mechanisms of mast cell activation, mast cells are capable of presenting soluble antigens to T cells initiating their proliferation ^(86;87). Both rodent and human mast cells express class II MHC antigens which are required for antigen presentation. In rat mast cells, this antigen presentation is enhanced by IL-4 and GM-CSF and inhibited by IFN γ ⁽⁸⁷⁾. Since IL-4 is required for the differentiation of the Th2 subset of T cells mast cell-derived IL-4 could provide the right microenvironment for T cell polarisation ⁽⁸⁸⁾. Indeed, it has been reported that rat mast cells can shift the differentiation of T cells towards the Th2 phenotype ⁽⁸⁹⁾. Therefore, mast cells could contribute to T cell skewing towards a Th2 phenotype with both antigen presentation and IL-4 secretion.

1.5 THE ROLE OF MAST CELLS IN ALLERGIC DISEASES

Despite the potential physiological roles that mast cells perform they are still synonymous with allergy. Mast cells play many roles in a number of diverse diseases. Allergic diseases are IgE-mediated and include asthma, allergic rhinitis and conjunctivitis, eczema, urticaria, and systemic anaphylaxis. Allergic diseases are increasing in prevalence⁽⁹⁰⁻⁹³⁾, although the aetiology is uncertain. It is evident from **Tables 1.2 and 1.3** and the above discussion that mast cells secrete a plethora of pleiotropic mediators including autacoids, proteases and cytokines. These mediators are linked to the pathophysiology of allergic diseases, and many of these are released via both IgE-dependent and non-dependent mechanisms. Depending on the site of mediator release, symptoms manifest clinically as rhinitis, conjunctivitis, urticaria, angioedema, erythema, bronchospasm, diarrhoea, vomiting and hypotension which can be fatal in severe reactions (such as anaphylactic shock).

In some of these diseases such as seasonal allergic rhinoconjunctivitis and anaphylaxis the role of IgE and allergen is well understood and widely acknowledged. However, diseases with more complex aetiology and pathophysiology such as chronic asthma and atopic eczema, have much less obvious involvement of IgE and mast cells, and therefore many other factors must contribute to the disease phenotype. Since I will be using primary human lung mast cells for this study, this report will focus in detail on the immunopathology of asthma: although many of the principles discussed are also applicable to the immunopathology of related allergic diseases.

1.5.1 Mast Cells in Asthma

Asthma is a complex disease which is characterised by the presence of variable and reversible airway obstruction. In terms of symptomatology, asthma is characterised by the symptoms of wheeze, dysnoea, cough and chest tightness. Asthma exacerbations may be triggered by a number of different stimuli, which will differ between individuals who will normally have one or more that will predominate. Airflow obstruction is a result of smooth muscle contraction, mucosal oedema, airway inflammation, and airway wall remodelling. In this section I will concentrate on the evidence for mast cells playing a role of central effector cells in asthma pathophysiology, their ongoing mediator release, and tissue infiltration of key structures within the airways (Figure 1.3).

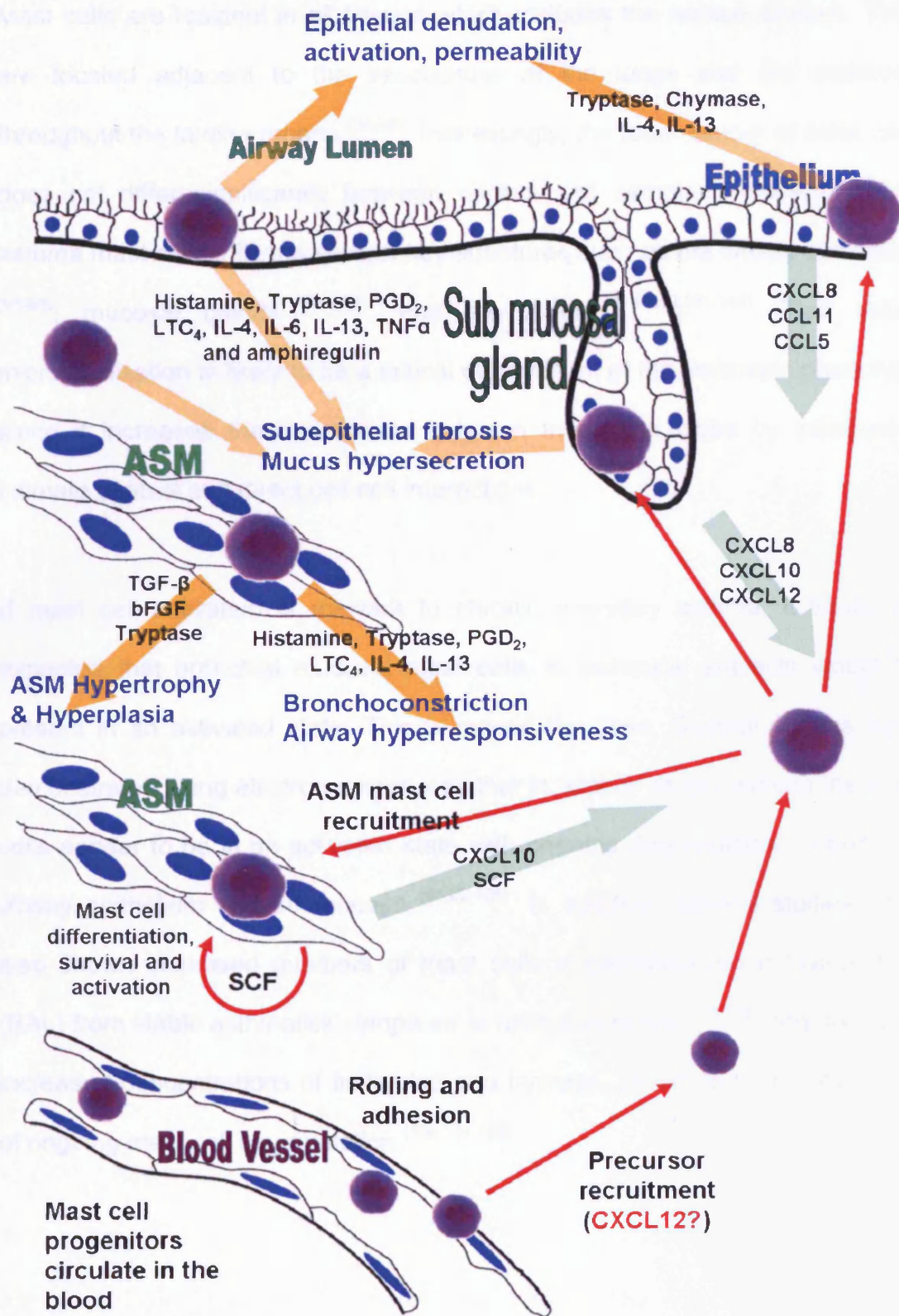


FIGURE 1.3: Mast cell interactions with structural airway cells in the pathogenesis of asthma.

Mast cells are resident in all tissues which includes the normal airways. They are located adjacent to the vasculature of the lungs and are scattered throughout the lamina propria ⁽⁹⁴⁻⁹⁶⁾. Interestingly, the total number of mast cells does not differ significantly between normal and asthmatic airways, but in asthma mast cells infiltrate several key structures such as the airway epithelium ⁽⁹⁶⁻⁹⁸⁾, mucosal glands ⁽⁹⁹⁻¹⁰¹⁾, and the ASM ^(61;97;99;101-104). This tissue microlocalisation is likely to be a critical determinant of the asthmatic phenotype since it increases the interactions between these cell types by introducing intimate contact and direct cell-cell interactions.

If mast cell activation is relevant to chronic everyday asthma, it would be expected that bronchial mucosal mast cells in asthmatic subjects would be present in an activated state. This is indeed the case. Several studies have demonstrated using electron microscopy that in “stable” atopic asthma the mast cells appear to be in an activated state with ongoing degranulation in both the airway epithelium and submucosa ^(61;62;105). In addition, several studies have also shown increased numbers of mast cells in bronchoalveolar lavage fluid (BAL) from stable asthmatics compared to normal controls ⁽¹⁰⁶⁻¹⁰⁸⁾, together with increased concentrations of histamine and tryptase, providing further evidence of ongoing mast cell degranulation ^(106;107;109).

1.6 MECHANISMS OF MAST CELL ACTIVATION

1.6.1 IgE-Dependent Activation

The best studied mechanism of mast cell activation, and that considered most relevant to allergic disease is activation through the high affinity IgE receptor Fc ϵ RI (reviewed by ^(110;111)). Most of the downstream signalling events identified following Fc ϵ RI engagement have been defined in rodent models, with relatively little known about events in human mast cells. Where human cells have been investigated, some important differences in signalling have been observed ⁽¹¹²⁾. Fc ϵ RI is a tetrameric structure from the multichain immune recognition receptor (MIRR) family. It is comprised of an α chain (Fc ϵ RI α) which binds IgE, a β chain signalling subunit (Fc ϵ RI β), and two γ subunits which exist as a homodimer signalling subunit (Fc ϵ RI γ) (**Figure 1.4**). A detailed description of the multiple signalling cascades activated following receptor activation is beyond the scope of this chapter but is summarised in **Figure 1.4** (for reviews see ^(110;111)). In terms of the proximal signalling pathways, the γ signalling subunits contain an immunoreceptor tyrosine-based activation motif (ITAM)⁽¹¹³⁾ within their cytoplasmic C-terminal domains, which bind to Syk tyrosine kinases initiating phosphorylation. The β chain of Fc ϵ RI also contains an ITAM. However, the Fc ϵ RI β ITAM contains a non-canonical tyrosine residue which prevents binding of Syk kinase. Instead, Fc ϵ RI β signals through the activation of the lipid raft-associated Lyn tyrosine kinase which in turn activates Syk kinase (**Figure 1.4**)⁽¹¹¹⁾.

Signalling *in vivo* is initiated when multivalent allergen binds to allergen-specific IgE bound to the FcεRIα chain. This promotes FcεRI aggregation and can be mimicked *in vitro* by the use of anti-IgE antibodies. Receptor aggregation initiates the association of the receptor with lipid rafts containing Lyn, a membrane anchored member of the Src family of protein tyrosine kinases (reviewed by ⁽¹¹⁴⁾). Lyn kinase transphosphorylates tyrosine residues in the ITAMs before binding strongly to the phosphorylated FcεRIβ ITAM through the Src homology 2 (SH2) domain (reviewed by ⁽¹¹⁵⁾). Syk protein tyrosine kinases are recruited to the rafts and bind the doubly phosphorylated ITAMs. They are themselves phosphorylated by recruited Lyn and Syk kinases promoting the Syk activation loop which results in a fully activated Syk with adjacent tyrosine phosphorylation that begins a cascade of events leading to the activation of inositol triphosphate (IP₃). The generation of IP₃ induces calcium mobilisation from intracellular rough endoplasmic reticulum (RER) stores, which initiates the influx of extracellular calcium *via* store operated calcium channels (**Figure 1.4**)⁽¹¹⁶⁾. In terms of IgE-dependent mediator release in both rodents and humans, influx of extracellular Ca²⁺ is a critical requirement for the release of both pre-formed and newly generated mediators ^(117;118).

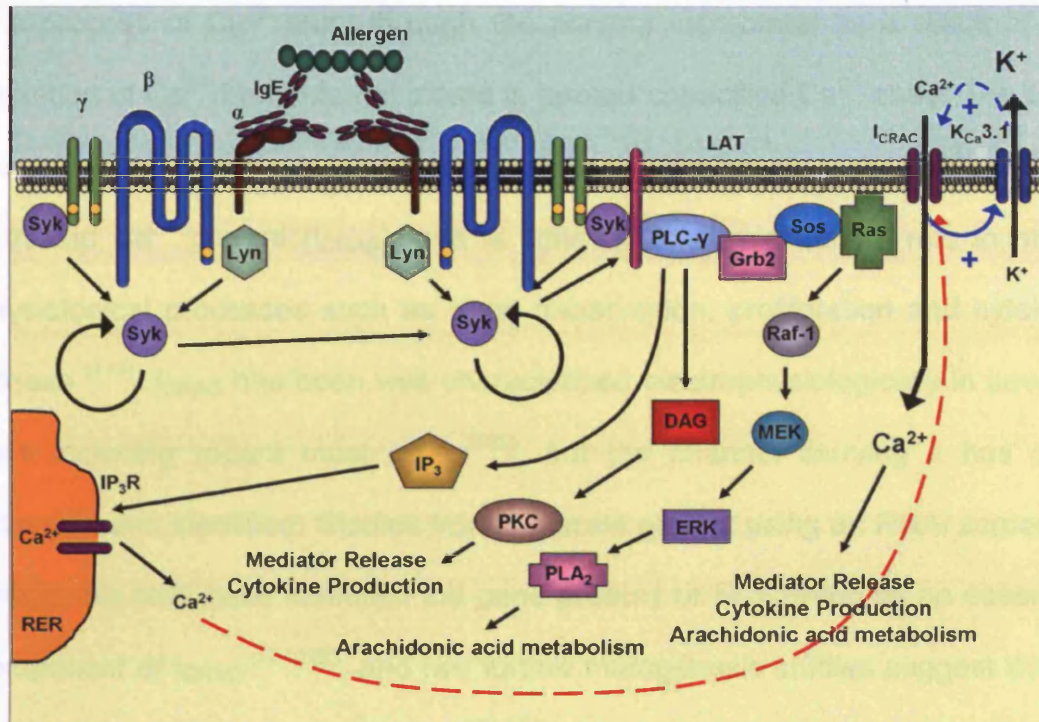


FIGURE 1.4: Simplified schematic of mast cell signaling events leading to degranulation and mediator production. Cross-linking of IgE molecules bound to FcεRI initiates ITAM phosphorylation at the cytoplasmic termini of the dimeric γ signaling subunits of the receptor (depicted in green). Syk kinases are recruited to the activated ITAMs, which autophosphorylate and recruit more Syk kinases (along with other kinases) leading to a cascade of signaling events. The β chain of the receptor (depicted in blue) also contains an ITAM, which binds to the lipid raft-associated Lyn kinase which in turn recruits, to the lipid rafts, and activates Syk kinases, thus amplifying receptor signaling. Syk kinases activate the membrane-associated LAT, which activates phospholipase C (PLC)- γ leading to the release of intracellular calcium stores from the rough endoplasmic reticulum via inositol trisphosphate (IP_3) and its receptor. PLC- γ also leads to activation of protein kinase C (PKC), which induces mediator release and cytokine production. In addition, PLC- γ initiates the Grb2/Sos/Ras pathway, which leads to extracellular regulated kinase (ERK) activation that initiates arachidonic acid metabolism via activation of phospholipase A₂ (PLA₂) and subsequent eicosanoid production and release. Mast cell degranulation is dependent on influx of extracellular calcium through store-operated calcium channels (SOCC) such as I_{CRAC} , which is initiated by the release of calcium from internal stores (depicted by red dashed line). This influx of calcium activates the intermediate conductance Ca^{2+} -activated K^+ channel, $\text{K}_{\text{Ca}3.1}$ (depicted by blue arrow), leading to an efflux of K^+ which counteracts the membrane depolarization induced by Ca^{2+} influx, thus increasing the driving force for Ca^{2+} entry.

The process of Ca^{2+} entry through the plasma membrane as a result of the depletion of Ca^{2+} from internal stores is termed capacitive Ca^{2+} entry. The Ca^{2+} current passing through the plasma membrane is known as the Ca^{2+} release activated Ca^{2+} current (I_{CRAC}), and is believed to play a central role in many physiological processes such as gene transcription, proliferation and cytokine release ⁽¹¹⁹⁾. I_{CRAC} has been well characterized electrophysiologically in several cells including rodent mast cells ⁽¹²⁰⁾, but the channel carrying it has only recently been identified. Studies from separate groups using an RNAi screen in *Drosophila* cells have identified the gene product of *FLJ 14466* as an essential component of I_{CRAC} ^(121;122), and two further mutagenesis studies suggest this is indeed the pore forming protein ^(123;124). The gene product has been given different names (Orai1, CRACM1). I will refer to it as CRACM1. Although it is generally accepted that Ca^{2+} influx following store release is required for mediator release from human and rodent mast cells following immunological activation, whether CRACM1 channels alone control granule exocytosis is not clear, and has not been investigated in human mast cells. One study in rat basophil leukaemia (RBL) cells, which combined measurements of I_{CRAC} with membrane capacitance measurements to monitor exocytosis found I_{CRAC} did not provide sufficient Ca^{2+} to support granule fusion ⁽¹²⁵⁾, however it may well contribute to the production of lipid mediators in these cells ⁽¹²⁶⁾. Human mast cells also express several members of the transient receptor potential family of ion channels which also have the potential to contribute to Ca^{2+} influx following immunological activation ⁽¹²⁷⁾.

K⁺ channels have the potential to modulate Ca²⁺ influx and hence mediator release due to their profound effects on the cell membrane potential. K⁺ channels hyperpolarise the plasma membrane when open and thus increase the electrical driving force for Ca²⁺ entry ⁽¹²⁸⁾, but perhaps more importantly, CRACM1 conducts larger currents at negative membrane potentials ⁽¹²⁰⁾. In both RBL cells and rat IL-3-dependent bone marrow-derived mast cells, an inwardly-rectifying K⁺ channel (Kir2.1) is open when the cells are at rest ^(129;130). However, the K⁺ channels present in human mast cells differ to those in rodents highlighting an example of species-dependent heterogeneity. Of note no Kir current has ever been seen in any human mast cell ^(112;131-135). Thus the majority of HLMC and human peripheral blood-derived mast cells are electrically “silent” at rest with a resting membrane potential of around 0 mV. Following IgE-dependent activation, human mast cells rapidly open the intermediate conductance Ca²⁺-activated K⁺ channel K_{Ca}3.1 ^(112;136) which has not been described in rodent mast cells. The K_{Ca}3.1 channel indirectly enhances Ca²⁺ influx and histamine release, but is not critical for secretion, and can thus be considered as increasing the gain of an immunological stimulus ⁽¹³³⁾. This channel is closed by compounds which inhibit mast cell secretion such as β₂-adrenoceptor agonists, providing a mechanism for the coupling of receptor activation and impaired secretion. Interestingly, this effect appears to act through a cAMP-independent mechanism ⁽¹³²⁾.

1.6.2 Monomeric IgE-dependent mast cell activation

In addition to the cross-linking of FcεRI by allergen, the binding of monomeric IgE alone to FcεRI can initiate intracellular signalling events and Ca²⁺ influx

(22;137-146). In rodents this results in the release of granule-derived mediators and the secretion of cytokines including IL-6^(137;138;141). This IL-6 acts in an autocrine manner and prolongs mast cell survival following growth factor withdrawal⁽¹³⁸⁾. In human cord blood-derived mast cells, monomeric IgE alone induces the release of the cytokines I-309, GM-CSF and MIP-1 α without histamine release⁽¹⁴⁷⁾. However, in human lung mast cells (HLMC) that have been maintained in culture, IgE induces the secretion of histamine, LTC₄ and IL-8, which is markedly enhanced in the presence of SCF⁽²²⁾. Interestingly, in both rodent mast cells and HLMC, on-going signalling is dependent on the presence of “free” IgE, and this ceases immediately when free IgE is removed, suggesting that these findings are physiologically relevant^(22;142). The mechanisms behind this are uncertain but in part are thought to involve Fc ϵ RI aggregation. These observations are of great interest because SCF and free IgE concentrations are elevated in asthmatic airways, and there is a robust correlation between total serum IgE, and the presence of asthma and bronchial hyperresponsiveness⁽¹⁴⁸⁻¹⁵¹⁾. This provides a mechanism for the ongoing activation of mast cells through Fc ϵ RI in the absence of allergen, and could explain in part the efficacy of anti-IgE therapy in chronic allergic disease⁽¹⁵²⁻¹⁵⁵⁾.

1.6.3 Non-immunological stimuli

Mast cells may also be activated through a plethora of non-IgE-dependent mechanisms (**Figure 1.5**). These include proteases (including tryptase)^(156;157), cytokines (e.g stem cell factor, TNF α , IFN γ)^(21;158-160), complement^(161;162), adenosine⁽¹⁶³⁾, toll-like receptor ligands^(85;164), neuropeptides (particularly skin mast cells)^(21;165), and hyperosmolality⁽¹⁶⁶⁻¹⁶⁹⁾. For example, The C5a receptor

CD88 was not thought to be expressed on HLMC, but recent work demonstrates that it is in fact expressed on the MC_{TC} subset of HLMC ⁽¹⁷⁰⁾. Elevated C5a concentrations have been identified in the induced sputum of asthmatic subjects ⁽¹⁷¹⁾, thus providing an alternative means of mast cell activation, and of particular relevance to those mast cells (MC_{TC}) within the ASM bundles (see below).

Human progenitor-derived mast cells and mouse mast cells express Toll-like receptors (TLRs) 1-7 and -9 ^(172;173). These play an important role in the innate host response to pathogens, activating diverse programmes of gene expression depending on the stimulus. For example, in mouse mast cells functional responses to TLR2 (the receptor for bacterial peptidoglycan) results in production of TNF α , IL-4, -5, -6, -13 and IL-1 β , while activation of TLR4 (the receptor for LPS) induces production of TNF α , IL-1 β , IL-6, and IL-13, but not IL-4 or IL-5. In addition, activation of TLR-2 but not TLR-4 induces Ca²⁺ mobilisation, degranulation and LTC₄ production ^(81;174;175). Examination of the gene expression profile from human cord blood-derived mast cells using high density oligonucleotide probe arrays following activation with LPS compared to anti-IgE demonstrates that both induce a core response, plus an LPS or anti-IgE specific program of gene expression ⁽¹⁷⁶⁾. Perhaps of more relevance to asthma is mast cell activation via TLR3, the ligand for which is double-stranded viral RNA ⁽⁸⁵⁾. Poly:IC, a synthetic activator of TLR3, induces the specific release of IFN α as does exposure to RSV and influenza virus. Since viruses are a common cause for asthma exacerbations, the mast cell anti-viral response may be an important contributor to the deteriorating airway physiology.

A further interesting area of study is the role of immunoglobulin (Ig) free light chains. These are present in serum in normal subjects and their production is augmented in inflammatory diseases such as rheumatoid disease. In mice, Ig free light chains can confer mast cell-dependent hypersensitivity through an unknown mechanism, and antigen-specific light chains can mediate mast cell-dependent bronchoconstriction following antigen challenge ⁽¹⁷⁷⁾. Concentrations of Ig free light chains are elevated in the sera of asthmatic compared to normal subjects suggesting they may be relevant to the pathophysiology of human asthma ⁽¹⁷⁷⁾.

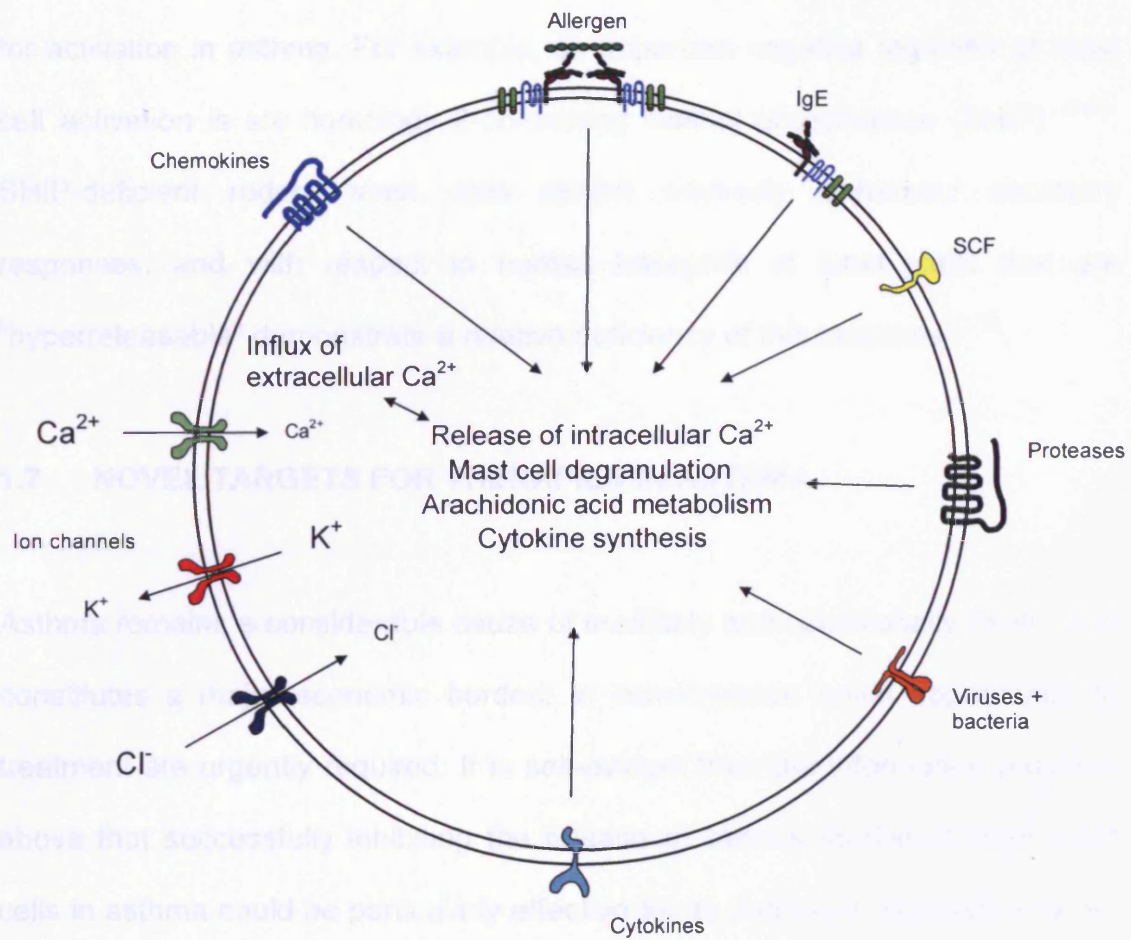


FIGURE 1.5: IgE-dependent and –independent mechanisms of mast cell activation. See text for definition of abbreviations.

Finally, there are likely to be genetic factors which lower the mast cell threshold for activation in asthma. For example, an important negative regulator of mast cell activation is src homology 2-containing inositol phosphatase (SHIP) ⁽¹⁴⁶⁾. SHIP-deficient rodent mast cells exhibit markedly enhanced secretory responses, and with respect to human basophils at least, cells that are “hyperreleasable” demonstrate a relative deficiency of this molecule ⁽¹⁷⁸⁾.

1.7 NOVEL TARGETS FOR THERAPIES IN ASTHMA

Asthma remains a considerable cause of morbidity and occasionally death, and constitutes a major economic burden: in consequence novel approaches to treatment are urgently required. It is self-evident from the information provided above that successfully inhibiting the release of various mediators from mast cells in asthma could be particularly effective for its treatment. A possible target for treatment has already been tested clinically. The non-anaphylactogenic humanised monomeric antibody omalizumab which prevents IgE from binding to its high (FcεRI) and low (CD23) affinity receptors by binding to an epitope on the C_H3 domain of IgE ⁽¹⁷⁹⁾ is partially effective and now licensed for the treatment of asthma in many countries. However, this approach is not without drawbacks and the treatment is only partially effective. Thus other targets which could modulate mediator release are still of great interest. One such target that may prove effective is the MS4A gene family.

1.7.1 The membrane spanning 4A gene family

The MS4A gene family was recently identified when MS4A3 (also known as HTm4) was found to have high sequence homology to both MS4A1 (also known as CD20, or the B cell receptor) and MS4A2 (also known as FcεRIβ, the β subunit of FcεRI) ⁽¹⁸⁰⁾. Since this discovery, several further family members have been identified ⁽¹⁸¹⁻¹⁸³⁾. Thus the MS4A gene family now comprises of at least 12 known family members in humans which share a high degree of sequence homology and are all located at chromosome 11q12 ⁽¹⁸⁴⁾. According to our own bioinformatical analyses, they usually have 4 transmembrane domains with cytoplasmic amino and carboxyl termini, and their expression is largely restricted to immunological cells. MS4A1, MS4A2 and MS4A3 are the most characterised proteins in the family and share about 20% homology. Importantly, their structure is conserved across species with high similarity and significant sequence identity between human, mouse and rat proteins, particularly in the first 3 transmembrane regions. Functionally, almost all of the MS4A gene family remain unexplored with a Pubmed search for “MS4A gene” yielding only 6 results. However, MS4A1 and MS4A2 have been studied, but still only to a small degree.

Analysis of transcript expression in the mouse suggests that CD20 expression is restricted to cells of the B cell lineage ⁽¹⁸⁵⁾ and since the mouse and human isoforms are so well conserved (73% amino acid identity) it is likely that this would be the case in human expression. MS4A1 is an integral part of the B cell receptor, and is functionally associated with the regulation of cell cycle progression and signal transduction in B lymphocytes ^(186;187). Thus MS4A1 acts

as a transmembrane component of a multimeric receptor complex which is involved in signal transduction of the receptor. This property may be a feature of the gene family since proline rich regions in the cytoplasmic N- and C-termini of most of the gene family members suggests that they may well form receptor complexes. Indeed, MS4A2 is an integral part of the human tetrameric IgE receptor complex FcεRI which is critical for IgE-dependent mast cell activation. In this complex MS4A2 performs important signalling events which affect mast cell function, although its expression is not essential for IgE receptor signalling⁽¹⁸⁸⁾. However, MS4A2 is known to act as an amplifier of FcεRI signalling⁽¹⁸⁹⁾.

1.7.1.1 Possible functions of the MS4A gene family

Although there is some knowledge of the rudimentary function of the better known MS4A gene family members, there are even fewer mechanistic reports. However, one possible mechanism behind the roles of MS4A gene products in signal transduction is that they may regulate ionic conductance. Indeed, MS4A1 has been proposed to act as a distinct and highly selective Ca²⁺ channel in B lymphocytes⁽¹⁹⁰⁾. This hypothesis was drawn after the discovery that transfection of MS4A1 cDNA into human K562 erythroleukaemia cells and mouse NIH-3T3 fibroblasts induced an identical transmembrane Ca²⁺ conductance which was very similar to the native current evident in B cells⁽¹⁹⁰⁾. More recently, Li and colleagues⁽¹⁹¹⁾ demonstrated that MS4A1 may actually act as a store-operated calcium channel (SOCC) which associates within lipid rafts to couple B cell receptor signalling to store-operated calcium entry (SOCE) in cholesterol-dependent lipid microdomains⁽¹⁹¹⁾. This theory is interesting since FcεRI in mast cell signalling has been proposed to work in a similar way (see

section **1.6 Mechanisms of mast cell activation**). In addition, incorporation of complexes of FcεRI and a molecule called cromolyn binding protein into lipid bilayers caused calcium conductance which was blocked by cromolyn ^(192;193). The calcium conductance was not induced with the incorporation of either FcεRI or cromolyn binding protein alone ⁽¹⁹³⁾ suggesting that FcεRI directly modulated the opening of the channel forming unit of the complex which was the cromolyn binding protein. However, the identity of the cromolyn binding protein has never been determined (to the best of our knowledge).

Calcium signalling and influx are associated with many functions including cell activation, migration, survival, proliferation and apoptosis ^(194;195). The regulation of cell cycle progression and proliferation which is attributable to MS4A1 is associated with calcium influx which speeds up progression through the G₁ phase when transfected into Balb/c 3T3 cells ⁽¹⁹⁶⁾. In addition, MS4A12 has been reported to act as a distinct SOCC (or modulate an as-yet-unknown calcium channel) in colonic epithelial cells ⁽¹⁹⁷⁾. Importantly, the expression of MS4A12 was specific to the colonic apical membrane with strict transcriptional repression in all other tissues, and the increased and maintained expression was associated with colonic cancer ⁽¹⁹⁷⁾. Subsequent functional knockdown of MS4A12 using siRNA in colon cancer cells significantly attenuated cell proliferation, motility and chemotactic tissue infiltration ⁽¹⁹⁷⁾. Furthermore, cells expressing MS4A12 were more reactive to lower concentrations of growth factors than their counterpart cells not expressing MS4A12 ⁽¹⁹⁷⁾. In addition, MS4A1 expression is increased in B cell malignancies, particularly non-Hodgkins B cell lymphomas ⁽¹⁹⁸⁾. Further evidence of a possible role of MS4A

gene family members in cancer has been demonstrated with an increased expression of MS4A8B in small cell lung cancer although no mechanism was described ⁽¹⁸¹⁾.

These observations of possible roles for the MS4A gene family in increased proliferation and neoplasia are of great interest and may be particularly important when considering the success of an anti-MS4A1 antibody (rituximab) for the treatment of B cell lymphomas ⁽¹⁹⁹⁾. However, some MS4A gene family members may reduce cellular proliferation. MS4A3, also known as HTm4, is an MS4A gene family member which is preferentially expressed in the nuclear membrane rather than the cytoplasmic membrane ⁽²⁰⁰⁾. The expression of MS4A3 in the nuclear membrane appears to reduce cell proliferation by binding to KAP, a cyclin-dependent kinase (Cdk) associated phosphatase which dephosphorylates human Cdk2 in the nucleus attenuating cell cycle progression ⁽²⁰⁰⁾. This dephosphorylation of Cdk2 at Thr160 by KAP is facilitated by MS4A3 binding directly to the complex which not only allows KAP greater access to dephosphorylate Thr160 on Cdk2, but also forces the dissociation and exclusion of cyclin A from this complex thus preventing G₁ – S phase transition ⁽²⁰¹⁾.

1.7.2 Project aims

The aim of this study was firstly to identify the MS4A gene family members expressed in both primary human lung mast cells (HLMC) and in the available mast cell lines HMC-1 and LAD-2 cells. In addition, I also aimed to determine the molecular regulation of gene expression and the cellular trafficking of the

expressed gene products. Finally, I aimed to delineate the function of the expressed proteins.

To achieve these goals, I would use a combination of molecular biological techniques to determine the expression profiles, and clone the expressed gene family members in the cell types studied. I would use state-of-the-art real-time QRT-PCR to determine the regulation of gene expression. For cellular localisation, I would use GFP tagged chimeric proteins and confocal microscopy due to the lack of available antibodies. In order to assess protein function, I would have to transfect the cells, which is not possible with the primary HLMC. Therefore, alternative approaches would have to be designed. Such an approach would be to use a new commercially available adenovirus which preliminary data suggests may be an effective method of transducing cDNA into HLMC. Using this technique I plan to both overexpress and functionally knock-down each expressed gene and perform functional assays with these cells to determine their function in activation, mediator release and survival.

CHAPTER 2: MATERIALS AND METHODS

2 MATERIALS AND METHODS

2.1 Cells

2.1.1 Immortalised cell lines

The human mast cell line HMC-1 was a generous gift from Dr. J. Butterfield (Mayo Clinic, Rochester, MN, USA). The cells were cultured, as described previously ⁽²⁰²⁾, in Iscove's medium containing 10% iron-supplemented foetal calf serum and 1.2 mM β -thioglycerol. Cells were split 1:10 every 7 days and resuspended in fresh medium.

LAD-2 cells were obtained from Dr. D Metcalfe (NIH, Bethesda, MD, USA). The cells were cultured, as described previously ⁽²⁰³⁾, in StemPro-34 medium containing supplement, 1% antibiotic/antimycotic solution (all from Sigma-Aldrich, Dorset, UK) and 1% non-essential amino acids (Life technologies, Paisley, UK) with 100ng/ml recombinant human SCF added (R&D, Abingdon, UK). Half of the medium supplemented with SCF was changed every 7 days.

Chinese hamster ovary (CHO) cells were kindly provided by Andrew Chadburn (Dept. Cell Physiology and Pharmacology, University of Leicester, UK). Cells were maintained in HAMS F12 medium containing 10% FBS (Life Technologies, Paisley, UK). Cultures were passaged when confluent, which was typically every 5 days, and split 1:10 for each passage.

2.1.2 Human lung mast cell isolation

All human subjects gave written informed consent and the study was approved by the Leicestershire Research Ethics Committee, UK. Lung tissue (typically 10-20g) was obtained by surgical resection for bronchial carcinoma. Lung tissue was finely chopped and filtered through 100µm gauze (Fisher Scientific, Loughborough, UK) to remove alveolar macrophages and blood cells. Lung tissue was stored overnight at 4°C in Dulbecco's modified Eagles medium (DMEM) 10% FBS (Life Technologies, Paisley, UK) containing 1% antibiotic/antimycotic solution (Sigma-Aldrich, Dorset, UK). Collagenase type 1A (7.5mg/g lung tissue) (Sigma-Aldrich) and hyaluronidase (3.75mg/g lung tissue) (Sigma-Aldrich) were added and incubated for 75 minutes at 37°C with stirring. Dispersed cells were filtered through 50µm gauze to remove connective tissue and washed 3 times by centrifugation at 250 x g for 8 minutes. Lung cells were incubated for 40 minutes in a blocking buffer of HBSS containing 1% BSA (Sigma-Aldrich,), 10% horse serum and 2% FBS (Life Technologies). Mast cells were purified using pan mouse IgG coated magnetic dynabeads[®] (DynaI, Wirral, UK) conjugated with mouse anti-human CD117 (mAb YB5.B8) (Cambridge Bioscience, Cambridge, UK). The final HLMC purity was >98% with cell viability >97% (monitored by exclusion of trypan blue).

Following isolation, HLMC were cultured in DMEM/Glutamax/HEPES containing 10% FBS, 1% MEM nonessential amino acids (all from Life Technologies), 1% antibiotic/antimycotic solution (Sigma-Aldrich), 100 ng/ml recombinant human (rh)SCF, 50 ng/ml rhIL-6 and 10 ng/ml rhIL-10 (R&D, Abingdon, UK) at 37°C in a humidified incubator flushed with 5% CO₂.

TABLE 2.1: Cell line characteristics

Cell Type	Origin	Important characteristics
HLMC	Human lung resections	HLMC best represent airway mast cells in vivo. They have good expression of FcεRI and react well to IgE-dependent stimulation (typically 30-50% histamine release). They contain high levels of histamine which increases with time in culture. They proliferate after 2-3 wks in culture but only very slowly. They require a cocktail of expensive cytokines to survive in culture (particularly SCF). We can successfully transduce cDNA into HLMC with adenoviruses.
HMC-1 cells	Mastocytosis patient	HMC-1 cells are a widely used cell line for mast cell biology. They proliferate rapidly in culture and require no cytokine supplements due to a gain-of-function mutation in cKIT (SCF receptor). They do not express FcεRI and so cannot be activated by IgE-dependent stimulation. They contain very low levels of histamine (>20 x less than HLMC) and do not respond well to stimuli. We can successfully transduce cDNA into HMC-1 cells with adenoviruses and lipid-based transfections work but with poor efficiency.
LAD-2 cells	Mast cell leukaemic patient	LAD-2 cells are used in mast cell biology research, but to a lesser degree than HMC-1 cells. Partly, because they require SCF to survive in culture since they have no gain-of-function mutation in cKIT. They express FcεRI but respond poorly to IgE-dependent stimulation. In addition, they contain very low amounts of histamine (comparable to HMC-1). We cannot successfully transfect LAD-2 with adenoviruses or lipid-based techniques.
CHO cells	Chinese hamster ovary	CHO cells are an electrically “quiet” cell with little endogenous current and so are a common cell type used for electrophysiology. They are very easily transfected with cDNA.

2.2 MS4A GENE EXPRESSION ANALYSIS

2.2.1 Isolation of total RNA from human mast cells

Total RNA was initially isolated using the Wizard SV Total RNA Isolation system from Promega (Promega, Southampton, UK) according to the manufacturer's instructions. However, the quality and quantity of RNA isolated using this system did not reach the standards required for detailed molecular biology. Therefore I changed to the QIAGEN RNEasy kit which was used according to the manufacturer's instructions (QIAGEN, Crawley, U.K.).

2.2.2 RT-PCR

To determine which MS4A gene family members were expressed by human mast cells, RT-PCR was designed to amplify regions which were conserved across splice variants of each family member, but which were distinct from other family members. Thus the transmembrane regions which have very high homology within the gene family were avoided (**Figure 2.1**). Regions around the 5' end of the mRNA which encodes the cytosolic amino terminal of the proteins were selected as they demonstrated the greatest diversity in nucleotide sequence (**Table 2.2**). Primers and the resulting amplicon were all BLAST searched to confirm that regions were sufficiently unique. All regions contained at least one intron.

RT-PCR was carried out using the single tube AccessQuick RT-PCR system (Promega, Southampton, UK). This kit uses a master mix system which

eliminates the requirement to add individual reagents, such as nucleotides, to the PCR reaction. 25µl of the master mix was added to each of the PCR reaction tubes on ice. 20µl of sterile DNase/RNase free water was added to each tube. 1µl of forward primer and 1µl of reverse primer were added to each tube making a final concentration of 2µM of each primer. 1µl of AMV reverse transcriptase was added to each tube, or 1µl of sterile DNase/RNase free water was added to the no reverse transcriptase control. Finally, 2µl of total RNA was added to each reaction. Total RNA was diluted to ensure that 1µg of total RNA was added to each condition.

All tubes were then transferred to the heating block. The protocol for RT-PCR was set as follows. Samples were held at 48°C for 45 minutes to enable reverse transcription of the mRNA using the reverse primer added. This was followed by 5 minutes at 95°C to denature the cDNA and inactivate the reverse transcriptase. Samples were then run at 95°C for 1 minute, 50°C for 1 minute and 68°C for 2 minutes for 40 cycles. A final extension step of 48°C for 7 minutes was performed to ensure complete extension before samples were held at 4°C. Samples were then run on a 1.5% agarose gel containing 0.5µg/ml ethidium bromide for 1 hour before visualisation with an ultraviolet lightbox. Bands were excised from the gel and the gel was purified using the QIAquick Gel Extraction Kit according to the manufacturer's instructions (QIAGEN, Crawley, U.K.). Purified cDNA from the expressed MS4A gene family members was incorporated into the pGEM[®] T Easy Vector System (**Figure 2.2**) according to the manufacturer's instructions (Promega, Southampton, UK). Briefly, 3µl of

cDNA was incubated with 5µl of 2 x reaction buffer, 1µl of pGEM T easy vector, and 1µl of T4 DNA ligase and incubated overnight at 4°C.

50µl of highly competent JM109 *Escherichia coli* cells were thawed on ice for 5 minutes before 3µl of overnight ligation reaction product was added to the cells. JM109 cells were incubated with the ligation products for 20 minutes on ice. Following the incubation, cells were heat shocked for 50 seconds at exactly 42°C and returned to ice for 5 minutes. 950µl of Luria Broth was added to each of the 50µl samples and incubated at 37°C for 90 minutes with rotational agitation at 150 rpm. Agar plates were prepared by autoclaving Luria Broth Agar. Once the agar has cooled sufficiently, 100µg/ml ampicillin was added immediately prior to pouring plates. Plates were then allowed to set upside-down in an incubator set at 37°C.

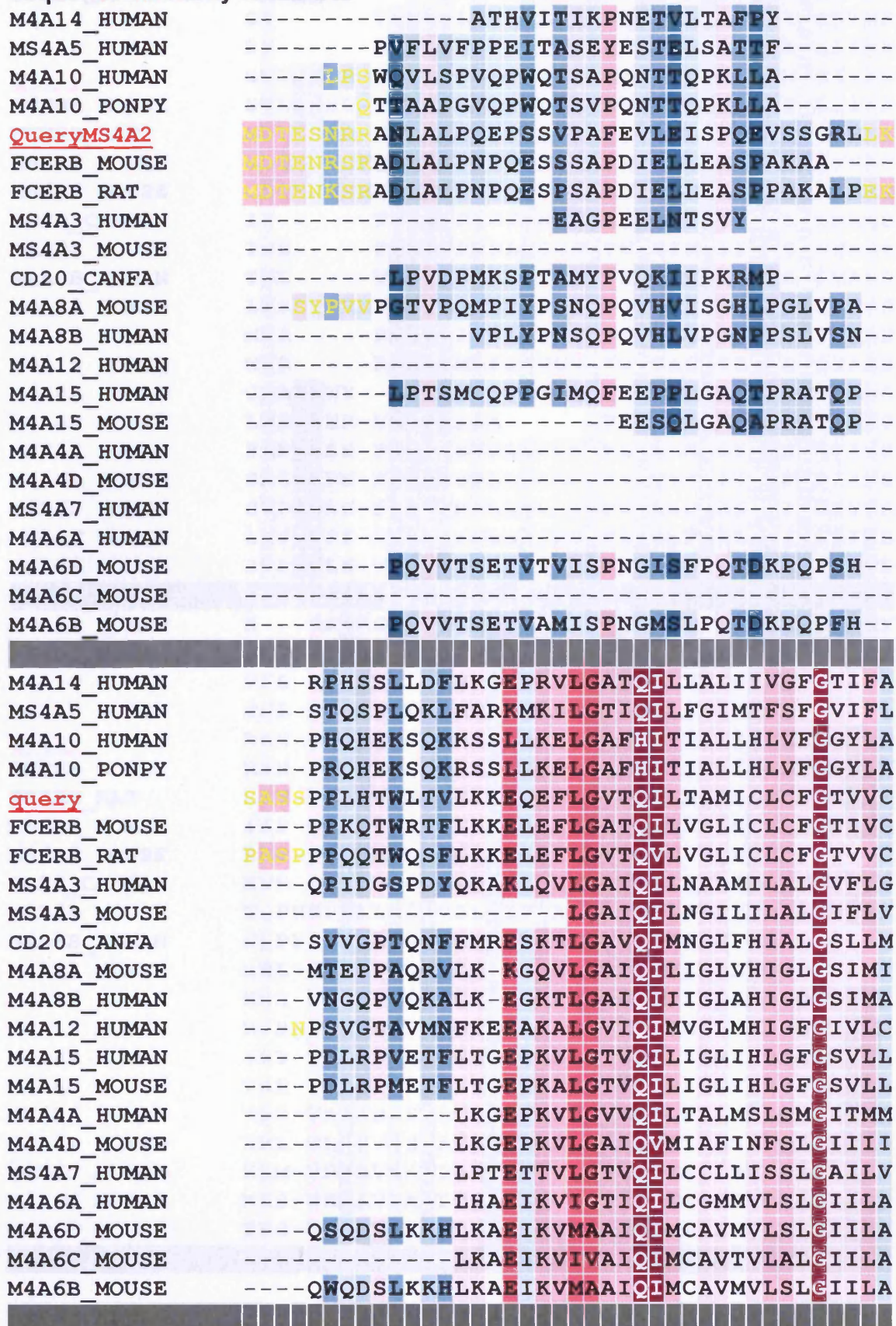
Once the agar plates had set, 100µl of IPTG and 20µl of X-galactose were added to the plates and allowed to dry. Once dry, 200µl of the transformed JM109 cells were added to each plate and spread using a spreader sterilised with ethanol and flaming. The remaining 800µl of suspension was centrifuged at 5000 x g for 5 minutes and resuspended in 200µl of Luria Broth. This was then spread onto another identical plate. Plates were then allowed to dry inverted in an incubator (37°C) with the lids removed for 30 minutes before the lids were replaced and the plates were incubated at 37°C overnight.

The following day, the plates were moved to 4°C for 2 days to develop the colour of the plate. Untransformed colonies will develop a blue colour which is

more evident after incubation at 4°C. Thus, white colonies were subcultured into a broth culture containing 100µg/ml ampicillin and incubated overnight with rotational agitation at 150 rpm. Cultures were then centrifuged at 5000 x g for 5 minutes and the broth was removed by inversion and blotting on a paper towel. Transformed cell pellets were lysed and the cDNA was purified using the Wizard SV Plasmid Purification Kit according to the manufacturer's instructions (Promega).

The pGEM[®] T Easy vector contains EcoRI restriction sites either side of the inserted cDNA in the multiple cloning site of the vector. Therefore, purified cDNA was incubated for 3 hours at 37°C with 10 units of EcoRI in NEB buffer 1 containing 1% BSA (New England Biolabs, Hitchin, U.K.). Following this incubation, samples were run on a 1.5% agarose gel for 1 hour at 80V and cDNA containing the inserts were sent for sequencing (Protein and Nucleic Acids Chemistry Laboratory, University of Leicester) to confirm specificity.

FIGURE 2.1: Multiple sequence alignment of proteins with high amino acid sequence similarity to MS4A2



M4A14_HUMAN LNYIG---FSQRLPLVVLTCGYPFWGCALIFILITGYLTVTDK
MS4A5_HUMAN FTLINPY---FRFPFIFLSCGYPFWGSVLFINSGLIIVK
M4A10_HUMAN SI-----VKNLHLVVLKSWYPFWGAASFLISGILAITMK
M4A10_PONPY ST-----VKSLLHLVVLKSWYPFWGAASFLISGILAITMK
query SVLDISH-IEGDISSFRAGYPFWGAIFFSISGMLSIISE
FCERB_MOUSE SVLYVSD-FDEEVLLLYKLGYPFWGAVLFLVLSGFLSIISE
FCERB_RAT STLQTSDFDDEVLLLYRAGYPFWGAVLFLVLSGFLSIMSE
MS4A3_HUMAN SLQYFYHFQKHFHFFFTFTGYPIWGAVFVFCSSGTLSSVAG
MS4A3_MOUSE CLQHVSHHFRHFFFTFTGYPLWGAVFVFISSGSLTVAAG
CD20_CANFA IH-----TDVCAPICTMWYPLWGGIMFIISGSLAAAD
M4A8A_MOUSE TNL-----FSHYTPVSLGGFPFWGGIWFIIISGSLVAAE
M4A8B_HUMAN TVL-----VGEYLSISFYGGFPFWGGLWFIISGSLVAAE
M4A12_HUMAN LISFSFREVLFPASTAVTGGYPFWGGLSFIISGSLSVSAS
M4A15_HUMAN MVR-----RGHVGIFFIIEGGVPFWGGACFIISGSLVAAE
M4A15_MOUSE MVR-----RGLLGMFLFIIEGGVPFWGGACFIISGSLVAAE
M4A4A_HUMAN CMAENTY---GSNPISVYIGYTIWGSVMFIISGSLSIAAG
M4A4D_MOUSE LNRVSERFMSVLLLA-----PFWGSIMFIFSGSLSIAAG
MS4A7_HUMAN FAPYFSH-FNFAISTTLLMSGYPFLGALCFGITGSLSIISG
M4A6A_HUMAN SASFSPN-FIQVISTLLNSAYPFIGPFFFIISGSLSIATE
M4A6D_MOUSE SVPSNLH-FISVFSILLESGYPFVGALFFAISGILSIVTE
M4A6C_MOUSE SVPEVPI-FNSVFSVLLKSGYPFIGALFFIASGILSIITE
M4A6B_MOUSE SVPSNLH-FISVFSVLLKSGYPFIGALFFIIVSGILSIVTE

M4A14_HUMAN K---SKLLGQGVVTGMNVISSLVAITGITFTILSYRHQDKY
MS4A5_HUMAN RKT-TETLIILSRIMNFLSALGAIAGIILLTFGFILDONY
M4A10_HUMAN TFS-KTYLKMCLMTNLI SLFCVLSGLFVISKDL-----
M4A10_PONPY TFS-KTYLKMCLMTNLVSLFCVLSGLFVISKDL-----
query RRN-ATYLVRGSLGANTASSIAGGTGITILINLKS LAY
FCERB_MOUSE RKN-TLYLVRGSLGANIVSSIAAGTGIAMLILNLTNNFAY
FCERB_RAT RKN-TLYLVRGSLGANIVSSIAAGLGIAILILNLSNNSAY
MS4A3_HUMAN IKP-TRTWIQNSFGMNIASATIALVGTAFSLNIAVNIQS
MS4A3_MOUSE RNP-TRMLMQNSFGINIASTTIAFVGTVFLSVHL-----
CD20_CANFA KNP-RKSLVKGKMIMNSLSLFAAISGIFLIMDIFNITIS
M4A8A_MOUSE TQPNSPOLLNGSVGLNIFSAICSAVGVIMLFITDISISSGY
M4A8B_HUMAN NQPYSYCLLSGSLGLNIVSAICSAVGVILFITDL-----
M4A12_HUMAN KEL-SRCLVKGSLGMNIVSSILAFIGVILLVDM-----
M4A15_HUMAN KNH-TSCLVRSSLGTNILSVMAAFAGTAILLMDFGVTRRD
M4A15_MOUSE RNH-TSCLLKSSLGTNILSAMAFAAGTAILLMDFGVTRWD
M4A4A_HUMAN IRT-TKGLVRGSLGMNITSSVLAASGILINTFSLAFYSFH
M4A4D_MOUSE VKP-TKAMIISL SVNTISSVLAVAASIIGVISVISGVFR
MS4A7_HUMAN KQS-TKPFDLSSLTSNAVSSVTAGAGLFLADSMVALRTA
M4A6A_HUMAN KRL-TKLLVHSSLVGSILSALSALVCFIILSVKQATLNPA
M4A6D_MOUSE KKM-TKPLVHSSLALSILSVLSALTGIAILSVSLAALPA
M4A6C_MOUSE RKS-TKPLVDASLTLNILSVSFAFVGIIIIISVSLAGLPA
M4A6B_MOUSE TKS-TKPLVDSSLTLNILSVSFAFMGIIIIISVSLAGLPA

M4A14_HUMAN -----COMPSFEE

```

MS4A5_HUMAN      -----ICGYS-HQNSQCKAVTVLFL
M4A10_HUMAN      -----
M4A10_PONPY      -----
query           IHIHSC-----QK-FFETK-CFMASFS T
FCERB_MOUSE     --MNNC-----KN-VTEDDGCFVASFT T
FCERB_RAT       --MNYC-----KD-ITEDDGCFVTSEIT
MS4A3_HUMAN     --LRSC-----HSSS-ESPDLCNYMGSISN
MS4A3_MOUSE     -----
CD20_CANFA      -----HFFKMENTL
M4A8A_MOUSE     --IYPS-----YYP-YQE--NLGVRTGV
M4A8B_HUMAN     -----
M4A12_HUMAN     -----
M4A15_HUMAN     -----VDR
M4A15_MOUSE     -----VGR
M4A4A_HUMAN     --HPYC-----NYY-GNSNNCHGTMSILM
M4A4D_MOUSE     --Q-----FRSQPAIA
MS4A7_HUMAN     --SQHCGSEMDYLSSLPYSEYYYP I-YEIKDCCLTSVSLT
M4A6A_HUMAN     --SLQCELDKNNIPTRSYVSYFYHDSLYTTDCYTAKASLA
M4A6D_MOUSE     --LQQCKLAFTQLDTTQDAYHFFSP-EPLNSCFVAKAALT
M4A6C_MOUSE     --SEQCKQSKELSLIEHDYYQPFYN-SDRSECAVTKSILT
M4A6B_MOUSE     --SEQC---LQSKELRPTEYHYHQF-LDRNECFRAAKSVLA
M4A14_HUMAN     ICVFSRTLFIIVLFFL-----
MS4A5_HUMAN     GILITLMTFSIIELFISL PFSILGCHSE-----
M4A10_HUMAN     -----
M4A10_PONPY     -----
query           EIVVMMLFLTILGLGSAVSLTICGAGEELKGNKVPEDRVY
FCERB_MOUSE     ELVLMMLFLTILAFCSAVLFTIYRIGQELESKRVPDDRLY
FCERB_RAT       ELVLMMLFLTILAFCSAVLLIYRIGQEFERSKVPDDRLY
MS4A3_HUMAN     GMV-----
MS4A3_MOUSE     -----
CD20_CANFA      NLIKAPMPYVDIHNC-----
M4A8A_MOUSE     AISSVLLIFCLLELSIASVSS-----
M4A8B_HUMAN     -----
M4A12_HUMAN     -----
M4A15_HUMAN     GYLAVLTIFTVLEFF-----
M4A15_MOUSE     GYLAVLTIFTILEFF-----
M4A4A_HUMAN     GLDGMVLLLSVLEFCIAVSLSAFG-----
M4A4D_MOUSE     SLDVLMTILNMLEFCIAVSVSAFG-----
MS4A7_HUMAN     GVLVVMLIFTVLEL-----
M4A6A_HUMAN     GTLSLMLICTLLEFCI LAV-----
M4A6D_MOUSE     GVFSLMLISSVLELGLAV-----
M4A6C_MOUSE     GALSVMMLIISVLELGLAL-----
M4A6B_MOUSE     GVFSLMLISTMLELGLAV-----

```

```

M4A14_HUMAN -----
MS4A5_HUMAN -----
M4A10_HUMAN -----
M4A10_PONPY -----
query      EELNIYSATYSELEDPGEMSPPIDL
FCERB_MOUSE EELNVYSPIYSELEDKGETSSFVE--
FCERB_RAT   EELHVYSPIYSALEDTRASAPV--
MS4A3_HUMAN -----
MS4A3_MOUSE -----
CD20_CANFA -----
M4A8A_MOUSE -----
M4A8B_HUMAN -----
M4A12_HUMAN -----
M4A15_HUMAN -----
M4A15_MOUSE -----
M4A4A_HUMAN -----
M4A4D_MOUSE -----
MS4A7_HUMAN -----
M4A6A_HUMAN -----
M4A6D_MOUSE -----
M4A6C_MOUSE -----
M4A6B_MOUSE -----

```

Legend:

The conservation scale:

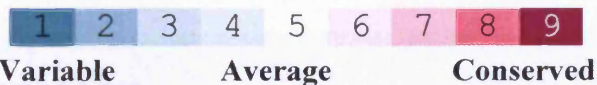


Figure 6: Multiple sequence alignment for proteins with high homology to MS4A2. This sequence alignment demonstrates that there are four conserved regions (red regions) which are interspaced with variable regions (blue regions). These conserved regions represent high sequence homology between proteins which correspond to the four transmembrane regions of the family. The two extracellular loop domains for each protein are the least conserved regions, but vary greatly in length between splice variants. Therefore, the cytoplasmic N-terminal regions (the residues at the start of these sequences) were selected for the design of primers from the nucleotide sequences.

TABLE 2.2: Primers designed for RT-PCR of MS4A family members to confirm expression in human mast cells

MS4A2				Amplicon
Forward Primer 5' -AATCTTGCTCTCCACAGGA-3'	50% G+C	60°C Tm		AATCTTGCTCTCCACAGGAGCCTTCCAG<INTRON>TGTGCCTGCATTTGAAGTCTTGAAATATCTCCCAGGAAGTATCTTCAGGCAGACTATTGAAGTCGGCCTCATCCCACCACTGCA
Reverse Primer 5' -TGTGTTACCCCAGGAAGTC-3'	55% G+C	60°C Tm		TACATGGCTGACAGTTTTGAAAAAAGAGCAGGAGTTCTGGGG<INTRON>GTAACACA
MS4A4A				Amplicon
Forward Primer 5' -GCATGGGAATAACAATGATGTG-3'	41% G+C	60°C Tm		GCATGGGAATAACAATGATGTGTATGGCATCTAATACTTATGGAAGTAACCCTATTTCCGTGTATATCGGGTACACAATTTGGGGGTAGTAA TG<INTRON>TTTATTATTTTTCAGGATCCTTG
Forward Primer 5' -TCCTAGACTACCTCGGACCAG-3'	57% G+C	59°C Tm		TCAATTGCAGCAGGAATTAGAATACTACAAAAGGCCTG<INTRON>GTCCGAGGTAGTCTAGGA
MS4A6A				Amplicon
Forward Primer 5' -GGATCATTGTCATCTGCT-3'	45% G+C	60°C Tm		GGATCATTGTCATCTGCTTCCTTCTCTCCAAATTTTACCCAAGTGACTTCTACACTGTTGAACTCTGCTTACCCATTCATAGGACCCTTTT TT<INTRON>TTTATCATCTCTGGCTCTCTA
Forward Primer 5' -AGGCTGCTATGCACCAAAG-3'	50% G+C	60°C Tm		TCAATCGCCACAGAGAAAAGGTTAACCAAGCTTTTG<INTRON>GTGCATAGCAGCCT
MS4A6E				Amplicon
Forward Primer 5' -GACTGCCATAGAGCCAAAGC-3'	55% G+C	60°C Tm		GACTGCCATAGAGCCAAAGCCAGTCTGGCT<INTRON>GGAAGTCTGTCTCTGATGCTGGTT TCTACTGTGTTGGAGTTCTGCCTAGCTGTGCTCACTGCTGTGCTGCAGTGGAAACAGACTGT
Forward Primer 5' -CCAGCATCATGAGTCGTCTT-3'	50% G+C	59°C Tm		CTGACTTCCCTGG<INTRON>TTACTCATGTCTCAAGACGACTCATGATGCTGG
MS4A7				Amplicon
Forward Primer 5' -CCTGAGGACTGCCTCTCAAC-3'	60% G+C	60°C Tm		CCTGAGGACTGCCTCTCAACATTGTGGCTCA GAAATGGATTATCTATCCTCATTGCCTTATT CCGAGTACTATTATCCAATATATGAAATCAA AGATTGTCTCCTGACCAGTGTGAGTTTAAACA
Forward Primer 5' -CCAGGGTTGTTGGAGTAGA-3'	55% G+C	60°C Tm		<INTRON>GGTGTCTTAGTGGTGATGCTCATCTTCACTGTGCTGGAGCTCTTATTAGCTGCA TACAGTTCTGTCTTTTGGTGGAAACAGCTCT ACTCCAACAACCCTGGG

2.2.3 Quantitative real time RT-PCR

For the quantitative real time RT-PCR (QRT-PCR), primers were designed to specifically amplify each individual splice variant of the MS4A family members expressed by human mast cells. Primers were designed to be 18-22 bp in length with a melting temperature (T_m) within 1-2°C of 60°C (Table 2.3). PCR products were designed to be between 150 and 300 bp which is considered to be optimal for QRT-PCR using SYBR[®] Green as the reporter molecule. All PCR products were designed to contain at least one intron (usually > 1 kb) to eliminate DNA contamination issues. QRT-PCR was designed to be carried out using the Full Velocity SYBR[®] Green RT-PCR single tube system from Stratagene (Amsterdam, The Netherlands). Using a single tube for both reverse transcription and PCR amplification increases specificity, since only the gene of interest (GOI) is reverse transcribed, although sensitivity is lower.

Quantitative RT-PCR was carried out using the FullVelocity[®] SYBR[®] Green QRT-PCR system (Stratagene, Amsterdam, The Netherlands). For the assay, 12.5 µl of 2 x master mix was added to each tube of a 96 well QRT-PCR plate. 8.9375 µl of PCR grade water was added to each well. 1 µl of forward primer and 1 µl of reverse primer were added to make a final concentration of 200 nM of each primer. 0.5 µl of the reference dye ROX was added to each well followed by 0.0625 µl of stratascript reverse transcriptase. Finally, 1 µl of total RNA, totalling 100 ng/reaction tube, was added and the plates were sealed with optically clear tube caps (Stratagene). Plates were then centrifuged at 400 x g for 1 minute to eliminate bubbles which would otherwise interfere with the reading of the plate.

The 96 well plates were then transferred to the Mx3000P quantitative PCR machine (Stratagene) for analysis. The protocol was set to read for both SYBR Green and ROX with ROX set as the reference dye. Assays were performed in triplicate and included a no template control. The temperature protocol was as follows: an initial reverse transcription step of 50°C for 30 minutes was followed by 95°C for 5 minutes to inactivate the reverse transcriptase. Then 50 cycles of 95°C for 20 seconds followed by 60°C for 30 seconds were performed. Fluorescent readings were taken at the end of the 60°C step. After the 50 cycles a SYBR Green melting point was performed by raising the temperature to 95°C for 30 seconds then dropping to 60°C for 1 minute. The temperature was then slowly raised to 95°C with continual fluorescence readings to determine the melting point of the cDNA products. Products were also run on a 1.5% agarose gel to confirm that the products were the expected length. Bands were then excised from the gel and sequenced as described previously (see section **2.2.2 RT-PCR**).

TABLE 2.3: Primers designed for quantitative real time RT-PCR of expressed MS4A family members and splice variants in human mast cells

	G+C	Tm	Size
MS4A2			
Forward Primer 5'-AATCTTGCTCTCCACAGGA-3'	50%	60°C	167bp
Reverse Primer 5'-TGTGTTACCCCCAGGAACTC-3'	55%	60°C	
MS4A2 Novel Variant			
Forward Primer 5'-AATCTTGCTCTCCACAGGA-3'	50%	60°C	167bp
Reverse Primer 5'-ATAGAAAACCCCAGGAACTC-3'	45%	60°C	
MS4A4A Variant 1			
Forward Primer 5'- GCATGGGAATAACAATGATGTG -3'	41%	60°C	170bp
Reverse Primer 5'- TCCTAGACTACCTCGGACCAG -3'	57%	59°C	
MS4A6A Variant 1			
Forward Primer 5'- TGTTCCCAATGAGACCATCA -3'	45%	60°C	262bp
Reverse Primer 5'- GGGTCCTATGAATGGGTAAGC -3'	52%	60°C	
MS4A6A Variant 1 Polymorphism			
Forward Primer 5'- TCACAACCTGTTCCCAATGA -3'	45%	60°C	156bp
Reverse Primer 5'- GCCAGAGATGATAAACCCAAT -3'	43%	58°C	
MS4A6 Novel Variant			
Forward Primer 5'- AAACCCGAACCCACCAAC -3'	55%	60°C	253bp
Reverse Primer 5'- CATCAGAGAGAGAGTTCCACTGC -3'	52%	60°C	
MS4A7 Short Variant			
Forward Primer 5'- TGCTATTACAATCCCAAACCA -3'	38%	58°C	155bp
Reverse Primer 5'- AATGCCAAACCCAAGAACG -3'	47%	60°C	
MS4A7 Long Variant			
Forward Primer 5'- GCTTTACACCAAAGGGCATC -3'	50%	60°C	251bp
Reverse Primer 5'- GCCAAAACACAGAGCTCCTAA -3'	48%	60°C	

2.3 MOLECULAR BIOLOGY

2.3.1 MS4A family cloning

The full open reading frames (ORF) of the expressed MS4A gene family members were amplified using primers designed to incorporate compatible restriction sites at either end of the clone for directional cloning into a variety of vectors (**Table 2.4**). Suitable restriction sites were selected following a search of each ORF using the online restriction site search tool WebCutter 2.0 which is available on the internet (<http://rna.lundberg.gu.se/cutter2/>). A triple guanine motif was added to the 5' end of each primer to increase stability and minimise the effect of 5' degradation by polymerases. Manual checks of the primer sequences were performed to identify any regions which may be self-complementary.

The expressed MS4A genes were cloned using the selected primers and a single tube AccessQuick™ RT-PCR System (Promega, Southampton, UK). The AccessQuick™ RT-PCR System uses a 2x master mix which contains all of the nucleotides (dNTP's), *Tfl* DNA Polymerase, magnesium sulfate and reaction buffer. Thus 25 µl of 2x master mix was added to each PCR reaction tube. 17 µl of PCR grade pure water was added to each tube, before the addition of 1 µl of the forward and reverse primers to make a final concentration of 2 µM of each primer. 1 µg of total RNA was added to each tube in a final volume of 5 µl immediately prior to the addition of 1 µl (5 units) of AMV reverse transcriptase, making a final volume of 50 µl in each tube.

RT-PCR was carried out in a single tube. Reverse transcription was carried out at 48°C for 45 minutes followed by 5 minutes at 95°C. 40 cycles of melting at 95°C for 1 minute, annealing at 60°C for 1 minute followed by extension at 72°C for 2 minutes were performed. A final extension step of 7 minutes at 72°C was performed after the 40 cycles. 10 µl of 6x loading dye was added to each sample and products were run on a 1.5% agarose gel containing 0.5 µg/ml ethidium bromide for 1 hour at 80V. Gels were visualised on an UV emitting light box and bands were excised using a clean scalpel blade. DNA from the excised bands was purified using the QIAquick Gel Extraction Kit (QIAGEN, Crawley, UK) according to the manufacturer's instructions.

TABLE 2.4: Primers designed for cloning of MS4A family members and splice variants in human mast cells

MS4A2	G+C	Restriction Site	Size
Forward Primer 5'- GGG GAATTC ATGGACACAGAAAGTAATAGGAG -3'	44%	EcoRI	750bp
Reverse Primer 5'- GGG GGATCC TTATAAATCAATGGGAGGAGAC -3'	48%	BamHI	
MS4A4 Variant 1			
Forward Primer 5'- GGG GAATTC ATGACAACCATGCAAGGAATGGAAC -3'	47%	EcoRI	680bp
Reverse Primer 5'- GGG GGATCC TCAAACCTCATTAAGTGGTGTGG -3'	54%	BamHI	
MS4A4A Variant 2			
Forward Primer 5'- GGG GAATTC ATGCATCAGACCTACAGCAGAC -3'	52%	EcoRI	740bp
Reverse Primer 5'- GGG GGATCC TCAAACCTCATTAAGTGGTGTGG -3'	54%	BamHI	
MS4A6A Variant 1			
Forward Primer 5'- GGG GAATTC ATGACATCACAACTGTTCCCAATG -3'	47%	EcoRI	750bp
Reverse Primer 5'- GGG GGATCC TTAAGAAGTCAATAGTTCTTC -3'	43%	BamHI	
MS4A6A Variant 2			
Forward Primer 5'- GGG GAATTC ATGACATCACAACTGTTCCCAATG -3'	47%	EcoRI	680bp
Reverse Primer 5'- GGG GGATCC TTAAGTGAAGCCGGCCAGCAC -3'	63%	BamHI	
MS4A6A Variant 3			
Forward Primer 5'- GGG GAATTC ATGACATCACAACTGTTCCCAATG -3'	47%	EcoRI	540bp
Reverse Primer 5'- GGG GGATCC TCAGAGTAAGCCTGTTCCAC -3'	57%	BamHI	
MS4A7			
Forward Primer 5'- GGG GAATTC ATGCTATTACAATCCCAAACCATG -3'	42%	EcoRI	725bp 590bp
Reverse Primer 5'- GGG GGATCC TTATATCCAAGACCGTGAAGAAC -3'	50%	BamHI	

Purified cDNA from the expressed MS4A gene family members was incorporated into the pGEM[®] T Easy Vector System (**Figure 2.2**) (Promega, Southampton, UK). The AccessQuick[™] RT-PCR System using *Tfl* DNA polymerase which adds a single template-independent nucleotide (adenine) onto the 3' end of the amplified DNA ⁽²⁰⁴⁾. This single-nucleotide overhang allows hybridisation with and cloning into T vectors, which have a complementary 3' single thymidine overhang. Thus 3 µl of cDNA was added to 5 µl of 2x ligation buffer, 1 µl of T4 DNA ligase and 1 µl of pGEM[®] T easy vector and left for 16 hours at 4°C. 50 µl of highly competent JM109 *Eschericia coli* cells were thawed on ice for 5 minutes before 3 µl of overnight ligation reaction product was added to the cells. JM109 cells were incubated with the ligation products for 20 minutes on ice. Following the incubation, cells were heat shocked for 50 seconds at exactly 42°C and returned to ice for 5 minutes. 950 µl of Luria Broth was added to each of the 50 µl samples and incubated at 37°C for 90 minutes with rotational agitation at 150 rpm. Agar plates were prepared by autoclaving Luria Broth Agar. Once the agar has cooled sufficiently, 100 µg/ml ampicillin was added immediately prior to pouring plates. The JM109 cells were then plated out and colonies selected as described above (see section **2.2.2 RT-PCR**).

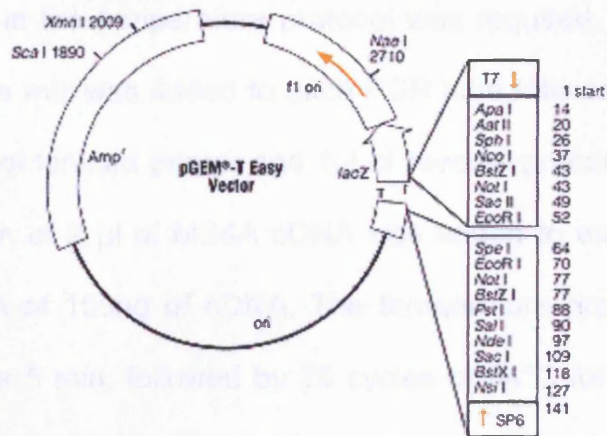


FIGURE 2.2: Map of the pGEM[®]-T Easy Vector.

2.3.2 Generation of green fluorescent protein - MS4A chimeric proteins

MS4A gene family clones were GFP tagged using the pEGFP N1 vector from Clontech (**Figure 2.3**). This vector incorporates GFP cDNA onto the 3' end of the cloned inserts. Therefore, the stop codon on the 3' end of the open reading frame must be removed. Primers were designed to remove the stop codons from the clones (**Table 2.5**) and care was taken in the design of the primers to ensure that the sequence of the clone and that of the GFP tag remained in reading frame after insertion of the insert into the vector. In most cases, it was required to change the restriction sites on the primers for directional cloning into the new vector.

In order to change the restriction sites for GFP tagging and to remove the stop codons, MS4A clones were PCR amplified using the newly designed primers (**Table 2.5**). PCR was performed by using the same AccessQuick[™] RT-PCR System as for the initial RT-PCR. However, for the normal PCR using this kit the addition of reverse transcriptase was omitted. In addition, no reverse

transcription step in the temperature protocol was required. Thus for the PCR 25 μ l of 2 x master mix was added to each PCR tube followed by 21 μ l of PCR grade water. 1 μ l of forward primer and 1 μ l of reverse primer were each added before the addition of 2 μ l of MS4A cDNA was added to each well to make a final concentration of 100ng of cDNA. The temperature protocol used for the PCR was 94°C for 5 min, followed by 25 cycles of 94°C for 1 min, 50°C for 1 min, and 68°C for 2 min, followed by a final extension step of 68°C for 7 min.

Following amplification, the PCR products were run on a 1.5% agarose gel, gel excised and purified as described above (see section **2.2.2 RT-PCR**). The PCR products were then cloned into pGEM[®]-T Easy Vectors as described above (see section **2.2.2 RT-PCR**). Following the cloning, amplification, purification and sequencing of the cDNA, clone inserts were excised using restriction enzymes to cut the incorporated restriction sites and inserted to pEGFPN1 by directional cloning. In brief, pEGFPN1 plasmids and cDNA clones were cut with the same restriction enzymes (10 units) for 3 h at 37°C. Digests were then run on a 1.5% agarose gel before cDNA clones and the linear (cut) plasmid bands were excised and purified. The insert and plasmid were then combined at a molar ratio of 3:1 and T4 ligase was added.

After successful transferral of the clones into the GFP vectors, highly competent JM109 cells were transformed in the same way as described for the cloning. However, it is not possible to chromogenically screen for successful transformation using the pEGFP N1 vector. Thus several colonies were sub-cultured in broth and grown overnight for each clone and screening was

performed on the purified DNA isolated from colonies using restriction enzyme digestion. However, few colonies would grow which were not transformed since the antibiotic resistance gene encoded by the vector is for kanamycin and plates with kanamycin added have very little growth of untransformed cells. DNA which was demonstrated to contain a cDNA insert after restriction enzyme digestion was sequenced to confirm sequence integrity.

2.3.3 Generation of adenoviral constructs

Primary human lung metastatic cells (H1299) are relatively difficult to transfect with

50% relative non-viral method being demonstrated by the use of adenoviral

approaches can only achieve 10% transfection efficiency. However, a recently developed

DPH) effectively transduced H1299 cells with adenoviral vectors. The

were prepared for shipment to Boston, MA. The adenoviral vectors were

generation of their viruses. The adenoviral vectors were prepared for shipment

designed to amplify the DNA of the adenoviral vectors. The adenoviral

restriction sites (Table 2.5) were designed to amplify the DNA of the

restriction sites (Table 2.5) were designed to amplify the DNA of the

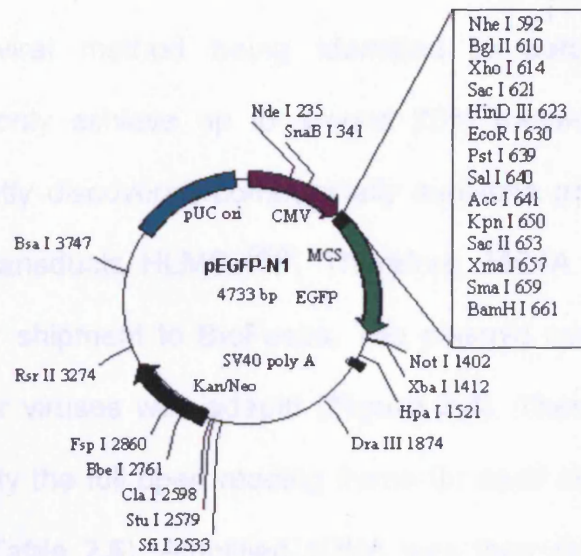


FIGURE 2.3: Map of the pEGFP-N1 Vector.

TABLE 2.5: Primers designed for producing MS4A : eGFP chimeric proteins

MS4A2	Buffer activity	Restriction Site
Forward Primer 5'- GGG GAGCTC ATGGACACAGAAAGTAATAGGAG -3'	100%	SacI
Reverse Primer 5'- GGG CCGCGG TAAATCAATGGGAGGAGACATTC -3'	100%	SacII
MS4A4		
Forward Primer 5'- GGG GAGCTC ATGACAACCATGCAAGGAATGGAAC -3'	100%	SacI
Reverse Primer 5'- GGG CCGCGG AACCTCATTAAGTGGTGTGGGAG -3'	100%	SacII
MS4A6		
Forward Primer 5'- GGG GAGCTC ATGACATCACAACCTGTTCCCAATG -3'	100%	SacI
Reverse Primer 5'- GGG CCGCGG AGAAGTCAATAGTTCTTCATATC -3'	100%	SacII
MS4A7		
Forward Primer 5'- GGG AAGCTT ATGCTATTACAATCCCAAACCATG -3'	100%	HindIII
Reverse Primer 5'- GGG CCGCGG TATCCAAGACCGTGAAGAACTC -3'	75%	SacII

2.3.3 Generation of adenoviral constructs

Primary human lung mast cells (HLMC) are notoriously difficult to transfect with no reliable non-viral method being identified to date. Even adenoviral approaches can only achieve up to around 25% transfection at maximum. However, a recently discovered commercially available adenovirus (BioFocus DPI) effectively transduces HLMC ⁽²⁰⁵⁾. Therefore, MS4A gene family clones were prepared for shipment to BioFocus. The plasmid construct used for the generation of their viruses was adapt6 (**Figure 2.4**). Therefore, primers were designed to amplify the full open reading frame for each clone with compatible restriction sites (**Table 2.6**). Amplified cDNA was then cloned into pGEM[®] T easy vectors as described above. The resulting cDNA was then sequenced to confirm sequence integrity.

Viruses were also constructed containing shRNA for gene silencing. The shRNA constructs were designed and generated by BioFocus DPI.

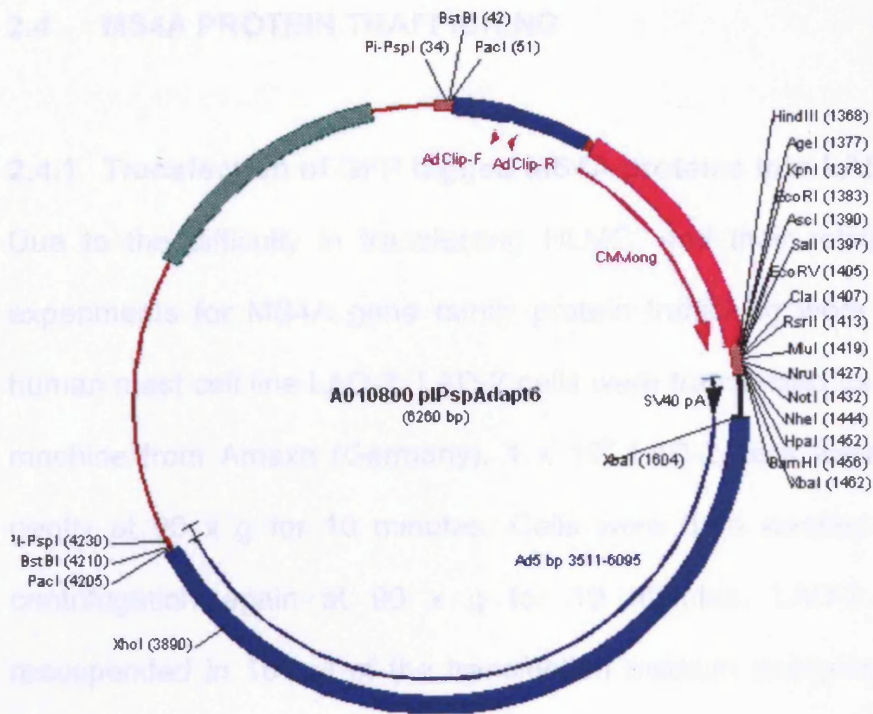


FIGURE 2.4: Map for Adapt6 Vector.

TABLE 2.6: Primers designed for producing MS4A adenoviral constructs

MS4A2	Restriction Site
Forward Primer 5'- GGG GAATTC ATGGACACAGAAAGTAATAGGAG -3'	EcoRI
Reverse Primer 5'- GGG GGATCC TTATAAATCAATGGGAGGAGAC -3'	BamHI
MS4A4	
Forward Primer 5'- GGG AAGCTT ATGACAACCATGCAAGGAATGGAAC -3'	HindIII
Reverse Primer 5'- GGG GTCGAC TCAAACCTCATTAAGTGGTGTGG -3'	Sall
MS4A6	
Forward Primer 5'- GGG GTCGAC ATGACATCACAACCTGTTCCCAATG -3'	Sall
Reverse Primer 5'- GGG GGATCC TTAAGAAGTCAATAGTTCTTC -3'	BamHI
MS4A7	
Forward Primer 5'- GGG AAGCTT ATGCTATTACAATCCCAAACCATG -3'	HindIII
Reverse Primer 5'- GGG GAATTC TTATATCCAAGACCGTGAAGAAC -3'	EcoRI

2.4 MS4A PROTEIN TRAFFICKING

2.4.1 Transfection of GFP tagged MS4A proteins into LAD-2 cells

Due to the difficulty in transfecting HLMC, and their relative paucity, initial experiments for MS4A gene family protein trafficking were performed in the human mast cell line LAD-2. LAD-2 cells were transfected using the Nucleofor[®] machine from Amaxa (Germany). 1×10^6 LAD-2 cells were centrifuged very gently at 90 x g for 10 minutes. Cells were then washed once in PBS by centrifugation again at 90 x g for 10 minutes. LAD-2 cells were then resuspended in 100 μ l of the transfection medium designed for use with the Amaxa system containing 2 μ g of the appropriate cloned cDNA. The kit used was the basic nucleofector kit for primary mammalian epithelial cells. The mixture was then placed into cuvettes supplied with the kit and inserted into the nucleofector machine. The programme for aortic smooth muscle was selected and run. Cells were then plated out in 35 mm glass bottom dishes with 2 ml of normal LAD-2 growth medium with 100 ng/ml of SCF added, and left overnight at 37°C in a humidified incubator for confocal analysis the following day.

2.4.2 Transfection of GFP tagged MS4A proteins into HMC-1 cells

For the transfection of HMC-1 cells, it was possible to achieve modest transfection efficiency using lipid based technologies due to the rapid replication of the HMC-1 cells. Thus for the HMC-1 cells, transfection was achieved using FuGENE HD reagent (Roche). 1×10^5 HMC-1 cells were plated out into 1 ml of HAM F12 medium containing 10% FBS and 1% non essential amino acids (Invitrogen) into a 24 well culture plate (it is essential that there is no antibiotic

added to the media). The cells were then allowed to rest in a humidified incubator set at 37°C and flushed with 5% CO₂. Meanwhile, the MS4A cDNA and the FuGENE HD reagent were brought to room temperature. Then 500ng of MS4A cDNA in pEGFP N1 (usually ~2 µl) was added to 50 µl of DMEM with no added supplements. 2 µl of FuGENE HD reagent was also added to a separate tube containing 50 µl of DMEM with no added supplements. After 5 min the tube containing the cDNA in DMEM was added to the tube containing the FuGENE HD reagent and gently mixed before incubation for 20 min to form the cDNA:lipid complexes. Following the incubation, the mixture was added drop-wise to the cells and mixed. Analysis was then performed 24-48 h after transfection.

2.4.3 Transduction of MS4A gene family members into HLMC

Transfection of gene product cDNA into HLMC had not previously been achievable. However, a commercially available adenovirus can successfully transduce cDNA into HLMC ⁽²⁰⁵⁾. There are 2 adenoviruses available from BioFocus DPI (Leiden, The Netherlands) which will transduce HLMC. Therefore, I performed optimisation experiments using both viruses to establish the optimal method for transduction. The viruses available were the Ad5C01Att01 and Ad5C20Att01 adenoviruses which are replication deficient Ad5 adenoviruses with different genetic backbones ⁽²⁰⁶⁾.

2.4.3.1 Transduction of HLMC using Ad5C01Att01 adenovirus

HLMC were first transduced using the Ad5C01Att01 adenovirus. The virus was dispatched at viral titres of 7.16×10^9 virus particles (VP) / ml on average with a

range from 1.1×10^9 to 1.7×10^{10} VP / ml. The eGFP control virus (Batch ID 12730) was used to optimise transduction and was dispatched at a titre of 9.4×10^9 VP / ml. A range of 500 – 5000 VP / HLMC was used (giving a multiplicity of infection (MOI) of 500 – 5000) to obtain the optimum transduction efficiency with the minimum cytotoxicity. Appropriate amounts of virus were then added to DMEM with 10% FBS, 1% non-essential amino acids and 1% antibiotic/antimycotic to ensure that 500 μ l of the diluted virus equated to the appropriate MOI for each condition. 1×10^5 HLMC were plated out in 500 μ l of DMEM with 10% FBS, 1% non-essential amino acids, 1% antibiotic/antimycotic, and 2 x final concentration of SCF (final concentration of 100ng/ml), IL-6 (final concentration of 50 ng/ml) and IL-10 (final concentration of 10 ng/ml). 500 μ l of diluted virus was then added immediately to each well and incubated at 37°C in an humidified incubator flushed with 5% CO₂ for the indicated amount of time from 24-72 h. Transduction efficiency was monitored by fluorescence microscopy during the time-points. Due to the relatively poor transduction efficiency with this virus, the efficiency was deduced more accurately by flow cytometry.

2.4.3.2 Transduction of HLMC using Ad5C20Att01 adenovirus

HLMC were next transduced using the Ad5C20Att01 adenovirus. This virus was dispatched at viral titres of 7.41×10^7 infective units (IU) / ml on average with a range from 1.05×10^7 to 8.95×10^9 IU / ml. The Ad5C20Att01 virus was dispatched with the new unit of IU rather than VP to improve reproducibility of results between batches. The IU is the amount of actively infective virus as apposed to the total virus particles and in the batches that I use equates to 1 IU

being roughly equal to 100 VP. The eGFP control virus (Batch ID 12538) was used to optimise transduction and was dispatched at a titre of 2.11×10^8 IU / ml. For the optimisation, an MOI of 1 to 50 IU / HLMC was used. Optimisation determined that a multiplicity of infection (MOI) of 10 infective units (IU) of the virus per HLMC was sufficient for ~100% transduction efficiency after 48 h with minimal toxicity. No special culturing conditions were required for the viruses so they were simply added to the cells at an MOI of 10 IU / HLMC.

2.4.4 Immunofluorescence of MS4A gene products in HLMC

Where possible, immunofluorescence of MS4A gene family members was carried out on HLMC. There was no way of transfecting HLMC with GFP-tagged MS4A gene family members without incorporating the GFP tagged cDNA into the Ad5C20Att01 adenoviruses (Biofocus DPI) in addition to the adenoviruses already purchased. Although this was possible, it was prohibitively expensive for this project. However, antibodies which were not available in the earlier stages of this project had become available during the latter stages. Thus for the gene family members which had an available antibody, immunofluorescence was attempted.

For the immunofluorescence, 2×10^5 HLMC were plated out into 500 μ l of normal mast cell growth medium (DMEM with 10% FBS, 1% non-essential amino acids, 1% antibiotic/antimycotic, 100 ng/ml SCF, 50 ng/ml IL-6 and 10 ng/ml IL-10). An appropriate amount of Ad5C20Att01 adenovirus to make an MOI of 10 was then added to the cells in 500 μ l of the same mast cell growth medium to make a total of 1 ml of culture medium. The cells were then

incubated for 48 h. Following the incubation with the viruses, the cells were stained for flow cytometry (see section **2.8.1 Flow cytometry** below). Cells which were left after flow cytometry were cytopun onto Silane coated microscope slides and coverslipped using fluorescence mounting medium (Sigma) and examined using confocal microscopy.

2.4.5 Confocal microscopy

Confocal microscopy was carried out on the Olympus FV1000 microscope within the advanced microscopy suite in the Department of Biochemistry, University of Leicester, Leicester, U.K. Images were either taken with live cells in 35 mm dishes kept at 37°C, or specimens were fixed and mounted, as indicated, using a fluorescence mounting medium (QIAGEN). Images were acquired under oil immersion and analysed using Fluoview FV10-ASW 1.6 and ImageJ 1.37v software.

2.5 MEDIATOR RELEASE ASSAYS

2.5.1 Mast cell challenge experiments

Mast cell challenge experiments were carried out on HLMC. 2×10^5 HLMC were plated out in 24 well tissue culture plates in 500 μ l of HLMC culture medium supplemented with 2 x final concentration of cytokines (see section 2.1.3). 2×10^6 infective units (IU) of Ad5C20Att01 adenovirus in 500 μ l of HLMC growth medium was added to the appropriate wells giving a final multiplicity of infection (MOI) of 10 IU / mast cell. Cells were incubated for 48 h or 7 days prior to release assays.

For mast cell challenge, cells plus medium from each well of the 24 well plates were harvested and placed into 1.5 ml eppendorf tubes. Tubes were then centrifuged for 5 minutes at 5000 rpm in an eppendorf microcentrifuge. The supernatants were removed and the pellets were resuspended in 200 μ l of DMEM (without supplements) before 5 μ l was taken for cell counts. 190 μ l of DMEM (without supplements) was added to each eppendorf followed by 10 μ l of human myeloma IgE (Calbiochem). The cells were then incubated for 45 min at 37°C. Following the incubation, eppendorfs were centrifuged for 5 min at 5000 rpm in an eppendorf microcentrifuge. The supernatant was removed and the cells were resuspended in DMEM (without supplements) at a concentration of 2×10^5 cells / ml. 50 μ l of cells were added to each well of a V bottom 96 well plate before the addition of 50 μ l of either DMEM alone for the control, or 50 μ l of 2 x final concentration of goat anti-human-IgE (Sigma-Aldrich). The plates were then incubated at 37°C in a humidified incubator flushed with 5% CO₂ for 45 min. The plates were then centrifuged at 250 g for 5 min. Supernatants were removed and stored for histamine and LTC₄ measurement. Cell pellets for control wells were lysed in 200 μ l of ultrapure water and frozen for measurement of total histamine content.

2.5.2 Histamine radioenzymatic assay

Histamine release was measured by radioenzymatic assay. Samples were obtained from the challenge experiments. Samples were defrosted and 75 μ l of each sample was added to each well of a 96 well deep well cluster plate. 75 μ l of standard samples were added to the standard curve wells. The deep well

plates were then centrifuged at 500 g for 30 s to bring the entire sample to the base of the well and eliminate cross contamination of samples. Histamine methyl transferase (HMT) and ^3H S adenosyl methionine (^3H SAM) were both added to DMEM (with no supplements) at a ratio of 5 ml of DMEM to 500 μl of HMT with 0.5 MBq of ^3H SAM for each plate. Then 50 μl of this mixture was added to each well of the 96 well plates. The plates were then mixed by mild agitation and centrifuged at 500 g for 30 s. The plates were then incubated at 37°C for 45 min. Following the incubation, the reaction was stopped by adding 50 μl of 10 M NaOH to each well and the wells were mixed with mild agitation. 400 μl of toluene:isoamyl alcohol (4:1) solution was then added to each well and the wells were sealed with strip caps. The plates were then vigorously shaken to allow the ^3H enzymatically transferred histamine to dissolve into the solvent phase. The plates were then centrifuged at 500 g for 1 min to separate the phases and 75 μl of the top organic phase was transferred to corresponding wells on a solid scintillant, shallow well Lumiplate (Packard Bell). The organic solvent was then evaporated using warm air flow leaving precipitated tritiated sample behind. Plates were then sealed using Topcount TopSeal (Packard Bell) and read on the Topcount scintillation plate reader (Company). Data was corrected for efficiency as disintegrations per minute (DPM). All data had background radiation removed and were calculated as pg / ml histamine from the standard curve. This data was then converted to % histamine (of total) by calculated total histamine content from the lysed cell pellets.

2.6 ELECTROPHYSIOLOGY

2.6.1 Single cell patch clamping

The whole-cell variant of the patch-clamp technique was used ^(112;207). Patch pipettes were made from borosilicate fibre-containing glass (Clark Electromedical Instruments, Reading, UK), and their tips were heat polished, typically resulting in resistances of 4–6 M Ω . For recording, mast cells were placed in 35-mm dishes containing standard external solution. Whole-cell currents were recorded using an Axoclamp 200A amplifier (Axon Instruments, Foster City, CA, USA), and currents were evoked by applying voltage commands to a range of potentials in 10 mV steps from a holding potential of –20 mV. The currents were digitized (sampled at a frequency of 10 kHz), stored on computer, and subsequently analyzed using pClamp software (Axon Instruments). Capacitance transients were minimized using the capacitance neutralization circuits on the amplifier. Correction for series resistance was not routinely applied. Experiments were performed at 27°C, and the temperature controlled by a Peltier device. Experiments were performed with a perfusion system (Automate Scientific, San Francisco, CA) to allow solution changes, although drugs were added directly to the recording chamber.

2.6.1.1 Patch clamping solutions

The standard pipette solution contained: KCl, 140 mM; MgCl₂, 2 mM; HEPES, 10 mM; Na⁺-ATP, 2 mM; GTP, 0.1 mM (pH 7.3).

The standard external solution contained: NaCl, 140 mM; KCl, 5 mM, CaCl₂, 2 mM; MgCl₂, 1 mM; HEPES, 10 mM (pH 7.3).

The NMDG external solution contained: NMDG Cl, 140 mM; KCl, 5 mM, CaCl₂, 2 mM; MgCl₂, 1 mM; HEPES, 10 mM (pH 7.3).

The sodium methane sulphonate external solution contained: sodium methane sulphonate, 140 mM; KCl, 5 mM, CaCl₂, 2 mM; MgCl₂, 1 mM; HEPES, 10 mM (pH 7.3).

2.7 CELL SURVIVAL/PROLIFERATION AND CELL CYCLE ASSAYS

2.7.1 Trypan blue method

HLMC were plated out at 5×10^4 cells per well, and HMC-1 cells were plated out at 2.5×10^4 cells per well in 24 well plates in duplicate. HLMC were plated in 1ml (final volume) of DMEM 10% FBS containing 1% antibiotic/antimycotic, 1% non-essential amino acids and 100 ng/ml of SCF. HMC-1 cells were plated in 1ml (final volume) of Iscove's medium containing 10% iron-supplemented foetal calf serum and 1.2 mM β -thioglycerol. The appropriate virus was added to each condition at a multiplicity of infection (MOI) of 10 infective units (IU) per cell. This is the equivalent of about 1000 virus particles (VP) per cell. The cells were incubated at 37°C in a humidified incubator flushed with 5% CO₂ for the indicated time. At the end of the incubation, cells were removed and centrifuged at 250 g for 5 minutes. The cells were resuspended in 20 μ l of DMEM and 20 μ l

of trypan blue solution was added. Cells were then counted and viability was assayed by exclusion of trypan blue dye using a haemocytometer.

2.7.2 Apoptosis assays

Apoptosis was assayed using propidium iodide (PI) and annexin V staining. HLMC and HMC-1 cells were plated out at 2×10^5 cells per well in 1ml (final volume) of appropriate medium in duplicate in a 24 well plate. HLMC were plated in DMEM 10% FBS containing 1% antibiotic/antimycotic, 1% non-essential amino acids and 100 ng/ml of SCF. HMC-1 cells were plated in Iscove's medium containing 10% iron-supplemented foetal calf serum and 1.2 mM β -thioglycerol. The appropriate adenovirus was added to each condition at an MOI of 10 IU per cell. Cells were incubated for 24 or 48 h at 37°C in a humidified incubator flushed with 5% CO₂. After the incubation, the duplicate wells were combined and the cells were centrifuged at 250 g for 5 minutes. The supernatant was removed and the cell pellets were washed in 2 ml of cold PBS and split into 4 FACS tubes (500 μ l per tube). The tubes were then centrifuged again at 250 g for 5 min. The cell pellets were then resuspended in 195 μ l of either annexin binding buffer (ABB) or HEPES buffer without calcium (essentially ABB but without calcium). 1 μ l of FITC conjugated annexin V was added to the annexin control (tube 1 – the HEPES buffer without calcium), the annexin in ABB (tube 2) and the annexin plus PI (Tube 4) conditions. The tubes were then incubated at room temperature for 15 min. Samples were then analysed using 2 colour flow cytometry FACS. For the conditions containing PI, 2 μ l of PI was added to the tube immediately prior to loading into the FACScan.

Tube conditions for apoptosis assays

Tube	ABB or Hepes (w/o cal)	Condition	Annexin	PI
1	Hepes (10mM) 195 μ l (wo calcium)	Annexin control	1 μ l	-
2	ABB 195 μ l	Annexin	1 μ l	-
3	ABB (10mM) 195 μ l	PI	-	2 μ l
4	ABB 195 μ l	Annexin + PI	1 μ l	2 μ l

2.7.3 Proliferation assays – ³H-thymidine uptake

For the ³H-thymidine uptake proliferation assays, 100 μ l of HMC-1 media (see **section 2.1.2**) or HLMC culture media supplemented with 2x final concentration of cytokines (see **section 2.1.3**) containing 8×10^3 HLMC and 4×10^3 HMC-1 cells, respectively, were plated out into a V bottom 96 well plate in triplicate. 100 μ l of either HMC-1 media or HLMC culture media was then added to the control wells. 8×10^4 and 4×10^4 infective units (IU) of Ad5C20Att01 adenovirus (BioFocus DPI, Galapagos, Leiden, The Netherlands) were diluted into 100 μ l of HLMC culture medium and HMC-1 culture medium, respectively, and added to the appropriate cells. Thus the final multiplicity of infection (MOI) was 10 IU / mast cell of either the GFP cDNA control virus (Batch #12538) or the custom made MS4A2 novel truncation cDNA virus (Batch #15451). A low control containing either HLMC in culture media without the addition of cytokines, or HMC-1 cells in HMC-1 media without FBS were also included.

Cells were then incubated for 80 h with the viruses at 37°C in a humidified incubator flushed with 5% CO₂. After 80 h, the cells were centrifuged at 250 x g for 5 minutes and the supernatants removed. The cell pellets were then resuspended in 200 μ l of either HMC-1 media or HLMC culture media

supplemented with cytokines containing 1 μl / ml of ^3H -thymidine (Amersham) to make a final concentration of 37 kBq per well. The cells were then incubated for 16 h at 37°C in a humidified incubator flushed with 5% CO_2 . Following the incubation, the plates were then centrifuged at 400 x g for 5 min and the supernatant was removed and discarded. The cells pellets were washed 2 x with 200 μl of PBS by centrifugation (400 x g for 5 min each). Cell pellets were then resuspended in 5 % TCA and incubated for 1 hour at 4°C. The cells were again centrifuged at 400 x g for 5 min and the supernatant discarded. 50 μl of absolute ethanol was added to each well and left overnight to evaporate. The following day, 200 μl of 1% SDS was added to each well and mixed thoroughly. This was then added to 10 ml of liquid scintillant and read in a scintillation counter. Data was retrieved as counts per minute and calculated by removing the background counts (using 200 μl of 1% SDS in 10 ml of scintillant).

2.7.4 Cell cycle analysis

For the analysis of the cell cycle I used flow cytometry and propidium iodide (PI) after incubation with RNase A. The same cells were used as for the apoptosis assays (**section 2.7.2**). The remaining cells after the apoptosis assays were fixed overnight in 70% ethanol at 4°C, centrifuged at 250 g for 8 min and resuspended in PBS 0.1% BSA and stored at 4°C until analysis. Prior to analysis, cells were washed 2 x in PBS and resuspended in 100 μl of PBS. Cells were then incubated for 30 min with 100 $\mu\text{g}/\text{ml}$ RNase A at room temperature, stained with 3 $\mu\text{g}/\text{ml}$ PI for 30 min and analyzed on the BD FACSCanto flow cytometer. Data was acquired on forward scatter (FCS) against light side scatter (SSC) and a secondary gate was placed around the single cell

population on a pulse area versus pulse width dot plot and analyzed for cell cycle analysis.

2.8 PROTEIN EXPRESSION ASSAYS

2.8.1 Flow cytometry

For the analysis of protein expression, and for the regulation of FcεRI expression, I used single colour flow cytometry. Flow cytometry was performed on either live cells, for surface expression, or fixed and permeabilised cells, for intracellular staining. Where adenoviruses were used, 2×10^5 HLMC or HMC-1 cells were plated out into a 24 well culture dish and incubated with Ad5C20Att01 adenoviruses at an MOI of 10 IU / cell in a final volume of 1 ml. For flow cytometry, cells were incubated with the virus for either 24 or 48 h prior to analysis.

2.8.1.1 Intracellular staining for flow cytometry

For the intracellular staining, HLMC or HMC-1 cells were removed from culture and centrifuged at $250 \times g$ for 8 minutes. The cells were resuspended in PBS containing 0.5% BSA at 1×10^5 cells / ml. 1 ml of cells in PBS 0.5% BSA was added to each FACS tube and the cell were again centrifuged at $300 \times g$ for 5 min. The supernatant was discarded by inversion and blotting on a paper towel before the supernatant was resuspended in 1 ml of PBS 4% paraformaldehyde and incubated on ice for 15 min to fix the cells. The cells were then centrifuged at $300 \times g$ for 5 min and the supernatant discarded by inversion. The cells were then resuspended in 1 ml PBS 0.5% BSA + 0.1% saponin and centrifuged

again at 300 x g for 5 min. The supernatant was again discarded and the cell pellet was resuspended in 100 µl of primary antibody (concentrations given for each application in results section) and incubated on ice for 45 min. 1 ml of PBS 0.5% BSA + 0.1% saponin was added to each tube and the tubes were centrifuged at 300 x g for 5 min. The supernatant was discarded and 100 µl of FITC labelled secondary antibody (DAKO) was added to each cell pellet at a dilution of 1:10 with PBS 0.5% BSA + 0.1% saponin and incubated for 45 min on ice and protected from light. 1 ml of PBS 0.5% BSA + 0.1% saponin was added to each tube and centrifuged at 300 x g for 5 min. The supernatant was discarded and the cell pellets were resuspended in 300 µl of PBS 0.5% BSA + 0.1% saponin ready for analysis using the FACScan machine.

2.8.1.2 Extracellular staining for flow cytometry

For extracellular staining, the cells were removed from culture and centrifuged at 250 x g for 8 min. The supernatant was removed by inversion and blotting on a paper towel and then the cells were resuspended in PBS 0.5% BSA at a concentration of 1×10^5 cells / ml. 1 ml of cells was added to each FACS tube and centrifuged at 300 x g for 5 min. The supernatant was discarded and the cell pellet was resuspended in 100 µl of primary antibody (concentrations given for each application in results section) and incubated on ice for 45 min. 1 ml of PBS 0.5% BSA was added to each tube and the tubes were centrifuged at 300 x g for 5 min. The supernatant was discarded and 100 µl of FITC labelled secondary antibody (DAKO) was added to each cell pellet at a dilution of 1:10 with PBS 0.5% BSA and incubated for 45 min on ice and protected from light. 1 ml of PBS 0.5% BSA was added to each tube and centrifuged at 300 x g for 5

min. The supernatant was discarded and the cell pellets were resuspended in 300 µl of PBS 0.5% BSA ready for analysis using the FACScan machine.

2.8.2 Western blotting

HLMC and HMC-1 cells (4×10^6) from the indicated conditions were washed with cold PBS and resuspended in ice-cold RIPA lysis buffer containing protease inhibitors. The insoluble debris was removed by centrifugation at 10,000 g for 10 min. Proteins were then mixed with 2 x SDS loading buffer and heated at 100°C for 10 min. Proteins were then loaded into a 12 % NuPAGE Novex gel (Invitrogen) and run for 1 h at 200V. For protein lysate staining, the gel was then stained using SimplyBlue™ SafeStain (Invitrogen) for 1 h to visualize overexpression. For western blotting, the proteins were blotted onto a nitrocellulose membrane after the electrophoresis. The membranes were blocked in 5% non-fat milk in PBS 0.1% Tween20 for 3 hours at 4°C. Membranes were then incubated with primary antibodies (concentrations given for each application in results section) in 0.5% non-fat milk in PBS 0.1% Tween20 overnight at 4°C. The following day, membranes were washed 3 times in PBS 0.1% Tween20. Horse radish peroxidase conjugated secondary antibodies were added according to manufacturer's specifications (Dako) and incubated for 1 h at room temperature. Membranes were washed 3 times in PBS 0.1% Tween20. Bands were visualised ECL reagent (Amersham) and exposed to photographic film.

TABLE 2.7: Antibodies used

Antibody	Supplier	Method used	Dilution
Anti CD117 (mouse anti-human) (monoclonal)	BD Biosciences	HLMC isolation	N/A
MS4A2 N-terminal (N-17) (Goat anti-human) (polyclonal)	Santa Cruz Biotechnology	Western Blotting	1:400
MS4A2 extracellular loop (S-17) (Goat anti-human) (polyclonal)	Santa Cruz Biotechnology	Western Blotting / IF	1:400 / 1:20
MS4A2 C-terminal (C-18) (Goat anti-human) (polyclonal)	Santa Cruz Biotechnology	Western Blotting / IF	1:400 / 1:20
Cdk2 phospho T160 (ab47330) (Rabbit anti-human) (polyclonal)	AbCam	Western Blotting	1:1000
Cdk1 (ab6537) (Rabbit anti-human) (polyclonal)	AbCam	Western Blotting	1:1000
Cdk1 phospho Y15 (ab47594) (Rabbit anti-human) (polyclonal)	AbCam	Western Blotting	1:1000
FcεRI alpha (clone 3G6) (Mouse anti-human) (monoclonal)	Upstate Biotechnology	FACS	1:10

CHAPTER 3: RESULTS

3 RESULTS

3.1 RT-PCR

3.1.1 MS4A gene family expression in human mast cells

In order to identify the expression of the MS4A gene family in human mast cells, I first needed to identify the family members expressed without the added complication of splice variants. Therefore, I performed RT-PCR with regions of mRNA which are homologous between splice variants. Thus with this approach I found that MS4A2 was expressed in the human lung mast cells (HLMC), the HMC-1 cells and the LAD-2 cells (**Figure 3.1**). The expression of MS4A4, however, was less obvious. There was a strong band in the LAD-2 cells, but this was much less obvious in both the HLMC and HMC-1 cells (**Figure 3.1**). Similarly, with both MS4A6 and MS4A7 there were clear bands with the LAD-2 cells RNA (**Figure 3.1**), but again with the HMC-1 cells and the HLMC these bands were less apparent. The bands from the LAD-2 cells were gel excised and cloned into pGEM T easy vectors prior to DNA sequencing which confirmed the specificity of the reaction.

The fact that the primers all worked with the LAD-2 cells demonstrates that the primers will amplify the products. However, the expression of these gene family members still needed to be confirmed in HMC-1 and HLMC. Reasons for this could be the quality and quantity of RNA obtained from the primary cells. Indeed, **Figure 3.1** suggests that the amount of integral RNA in the HLMC samples was less than that obtained from the LAD-2 cells since the intensity of the band for MS4A2 was less than that in both the HMC-1 cells and the LAD-2 cells. This is counterintuitive since MS4A2 is a component of the IgE receptor

which is more highly expressed in HLMC than either the LAD-2 or the HMC-1 cells. Therefore, the method for RNA isolation was subsequently changed (see Materials and Methods).

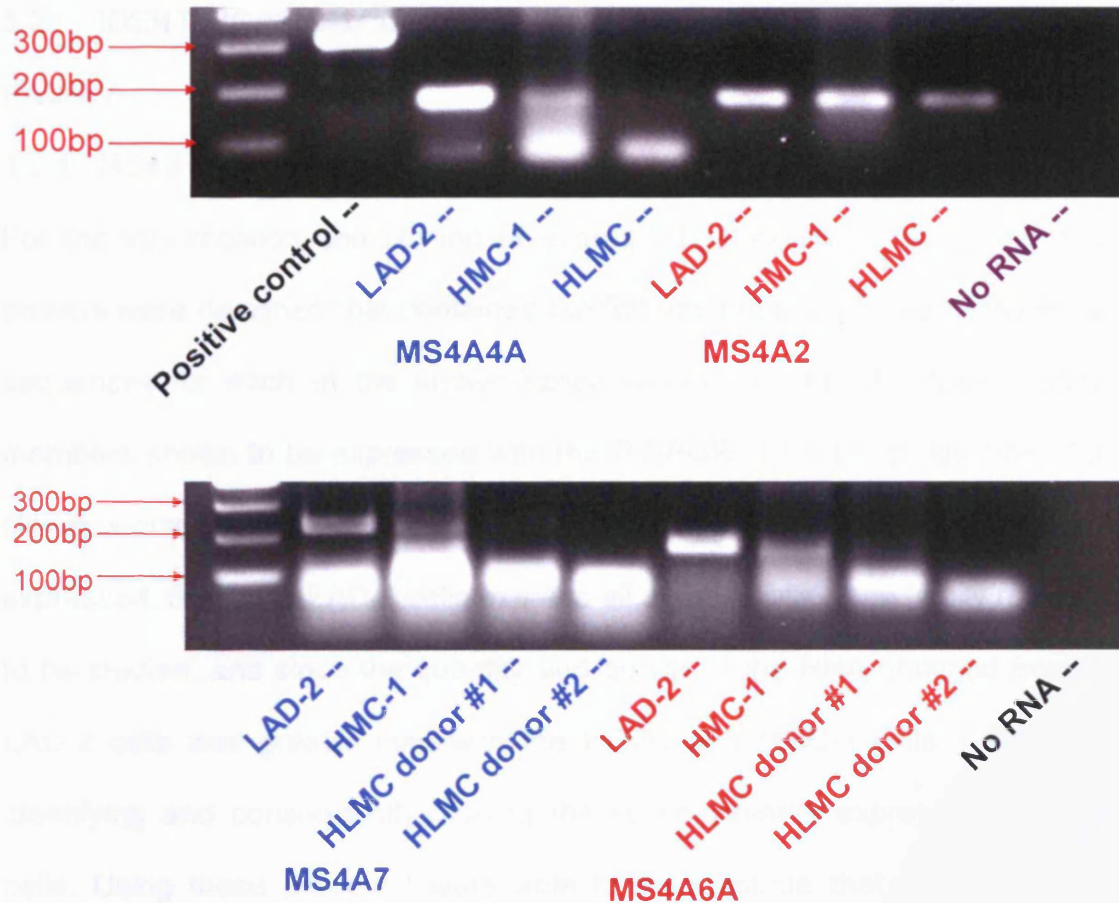


Figure 3.1: RT-PCR for MS4A gene expression in human mast cells.

Figure showing the RT-PCR products run through an agar gel demonstrating that LAD-2 cells express all 4 of the genes studied. HMC-1 cells and HLMC both express MS4A2, but the expression of the other family members could not be confirmed using this approach. Confirmation of the expression profiles in these cell types is given later in this chapter.

3.2 IDENTIFICATION, CLONING AND SEQUENCING OF MS4A GENE FAMILY

3.2.1 MS4A gene family cloning

For the identification and cloning of expressed MS4A gene family members, primers were designed that contained the full open reading frame of the known sequences for each of the known splice variants of the MS4A gene family members shown to be expressed with the RT-PCR. Thus the production of the clones would also serve as a method of identification for the splice variants expressed. Since the LAD-2 cells express all of the MS4A gene family members to be studied, and since the quantity and quality of the RNA obtained from the LAD-2 cells was greater than with the HLMC and HMC-1 cells, I started by identifying and consequently cloning the splice variants expressed in LAD-2 cells. Using these primers I were able to demonstrate that the LAD-2 cells expressed the full length open reading frames for MS4A2, MS4A6 variant 1 and both the long and short variants for MS4A7 (**Figure 3.2A**). Disappointingly, the primers for MS4A4 did not work using this protocol. However, subsequent changes in the RT-PCR protocol resolved this issue and the MS4A4 primers worked which demonstrated that the LAD-2 cells express variant 1 of MS4A4 (**Figure 3.2B**).

However, whilst cloning and sequencing the expected products I also cloned the unexpected products from the gel (**Figure 3.2A**), which when sequenced were identified as both known and novel splice variants. These splice variants consisted of truncations of the known variants where either an exon was removed, or had been replaced with a different exon. This is not uncommon with the MS4A gene family since both the long and short variants of

MS4A7 have identical sequences except for a truncation in the shorter variant which is missing exon 2 (**Figures 3.12 & 3.13**). This is the case for the novel splice variant of MS4A2 which I identified as the shorter, but distinct, band visible in the MS4A2 lane of the gel (**Figure 3.2A**). This novel variant is missing exon 3 which results in a truncation, the consequence of which, is the loss of two of the membrane spanning domains (described in detail later on). Similarly, the multiple bands evident in the MS4A6 lane were splice variants that were present rather than non-specific amplification. This was discovered after isolating several colonies of *E. coli* which had been transformed with the MS4A6 clones. After isolating the cDNA from the bacteria and incubating with the incorporated restriction enzymes, digests of the cDNA had products which differed in size (**Figure 3.3**). Subsequent sequencing identified them as a novel variant and a known polymorphism truncation of MS4A6 variant 1.

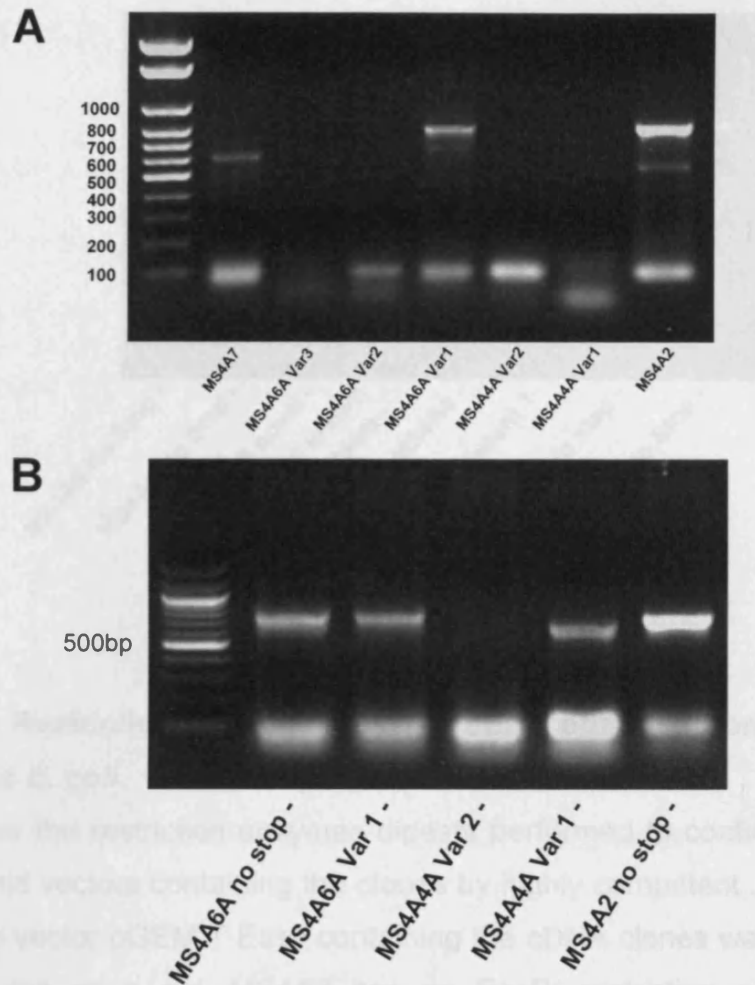


Figure 3.2: RT-PCR cloning of the full length open reading frame of MS4A gene family members and their splice variants in LAD-2 cells.

A) RT-PCR products from the LAD-2 RNA. Important to note that the lane on the far right which used the primers for MS4A2 had 2 distinct bands. The larger band (735 bp) was indeed MS4A2, but the shorter band (597 bp) was a novel truncation of MS4A2 which was missing exon 3. For MS4A6, there appeared to be several bands and after sequencing several colonies there were at least 3 variants of MS4A6 expressed. MS4A7 appeared to have a single band which corresponded more to the short variant (588 bp) rather than the long variant (723 bp). However, both variants were present in different colonies when sequenced which may account for the smeared appearance of the band. B) Changing the PCR conditions enabled the successful cloning of MS4A4 variant 1 which did not work in the initial cloning protocol. MS4A6 variant 1 was re-cloned due to a single point mutation in the original clone.

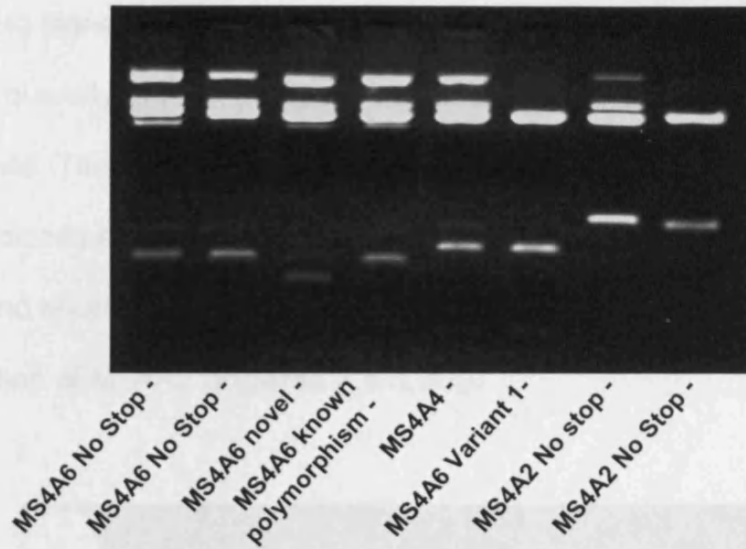


Figure 3.3: Restriction enzyme digests of cDNA obtained from transformed *E. coli*.

Figure shows the restriction enzymes digests performed to confirm the uptake of the plasmid vectors containing the clones by highly competent JM109 *E. coli*. cDNA of the vector pGEM T Easy containing the cDNA clones was treated with EcoRI and ran on a gel. MS4A2 has no EcoRI restriction sites within its sequence and so appears as the full length cDNA. MS4A4 and MS4A6 however, both contain an EcoRI site within their open reading frame and so are cleaved into two pieces which appear smaller and can be seen as a double band. It is still evident that MS4A6 has got bands of different sizes from the different colonies which turned out to be unexpected splice variants after sequencing. The 2 left columns which were thought to be MS4A6 variant 1 turned out to be the known polymorphism of MS4A6 variant 1 which had the stop codon removed for GFP tagging.

I next began to clone the MS4A gene family members expressed in HLMC. The integrity and quantity of RNA available from these cells was not as good as with the LAD-2 cells. Therefore, with disappointing yields, I was unable to isolate as many of the clones as with the LAD-2 cells. I was, however, able to isolate both of the long and short variants of MS4A7 and both the known variant and the novel truncation of MS4A2 (Figures 3.4 & 3.5).

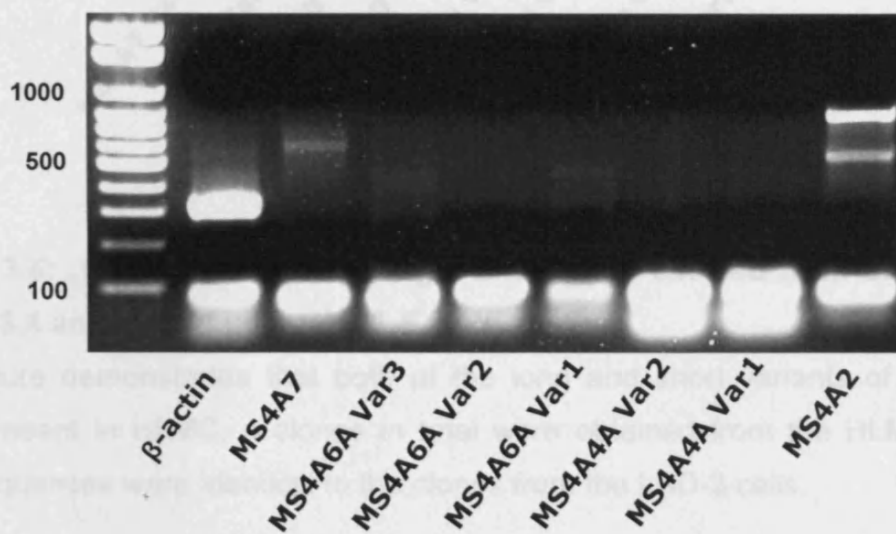


Figure 3.4: RT-PCR cloning of the full length open reading frame of MS4A gene family members and their splice variants in HLMC.

RT-PCR cloning was carried out on HLMC RNA pooled from 4 donors. The same double band could be seen with the MS4A2 primers in the HLMC as was evident with the LAD-2 cells, but interestingly, the smaller band for the novel variant appears stronger in the HLMC than in the LAD-2 cells. In addition, the band present in the MS4A7 lane was comparable to the LAD-2 cells and also showed that both variants were present when sequenced. The MS4A4 lanes were negative, but this was using the old RT-PCR protocol which also did not work in the LAD-2 cells. MS4A6 variant 1 had a band which was smaller than expected, but given the number of splice variants present in the LAD-2 cells, this band was excised, cloned and sequenced, but turned out to be non-specific amplification.

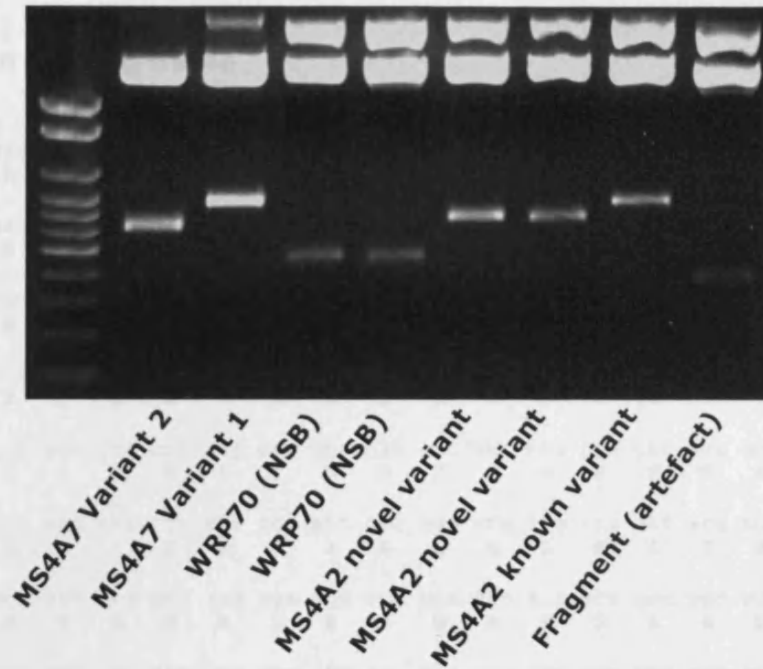


Figure 3.5: Restriction enzyme digests of cDNA excised from the gel of Figure 3.4 and cloned into JM109 *E. coli*.

This figure demonstrates that both of the long and short variants of MS4A7 were present in HLMC. 4 clones in total were obtained from the HLMC, and their sequences were identical to the clones from the LAD-2 cells.

Figure 3.6: The full open reading of MS4A2.

3.2.2 Cloned sequences of the MS4A gene family

The cloning process revealed that there were 8 MS4A gene family members expressed in the LAD-2 cells, and that at least 4 of these were also expressed in the HLMC. The gene family members expressed were MS4A2, a novel truncation of MS4A2 (MS4A2_{trunc}), MS4A4 variant 1, MS4A6 variant 1, MS4A6 variant 1 polymorphism, MS4A6 novel variant, MS4A7 variant 1 and MS4A7 variant 2.

MS4A2 open reading frame

```

atg gac aca gaa agt aat agg aga gca aat ctt gct ctc cca cag gag cct tcc agt gtg
M D T E S N R R A N L A L P Q E P S S V
cct gca ttt gaa gtc ttg gaa ata tct ccc cag gaa gta tct tca ggc aga cta ttg aag
P A F E V L E I S P Q E V S S G R L L K
tcg gcc tca tcc cca cca ctg cat aca tgg ctg aca gtt ttg aaa aaa gag cag gag ttc
S A S S P P L H T W L T V L K K E Q E F
ctg ggg gta aca caa att ctg act gct atg ata tgc ctt tgt ttt gga aca gtt gtc tgc
L G V T Q I L T A M I C L C F G T V V C
tct gta ctt gat att tca cac att gag gga gac att ttt tca tca ttt aaa gca ggt tat
S V L D I S H I E G D I F S S F K A G Y
cca ttc tgg gga gcc ata ttt ttt tct att tct gga atg ttg tca att ata tct gaa agg
P F W G A I F F S I S G M L S I I S E R
aga aat gca aca tat ctg gtg aga gga agc ctg gga gca aac act gcc agc agc ata gct
R N A T Y L V R G S L G A N T A S S I A
ggg gga acg gga att acc atc ctg atc atc aac ctg aag aag agc ttg gcc tat atc cac
G G T G I T I L I I N L K K S L A Y I H
atc cac agt tgc cag aaa ttt ttt gag acc aag tgc ttt atg gct tcc ttt tcc act gaa
I H S C Q K F F E T K C F M A S F S T E
att gta gtg atg atg ctg ttt ctc acc att ctg gga ctt ggt agt gct gtg tca ctc aca
I V V M M L F L T I L G L G S A V S L T
atc tgt gga gct ggg gaa gaa ctc aaa gga aac aag gtt cca gag gat cgt gtt tat gaa
I C G A G E E L K G N K V P E D R V Y E
gaa tta aac ata tat tca gct act tac agt gag ttg gaa gac cca ggg gaa atg tct cct
E L N I Y S A T Y S E L E D P G E M S P
ccc att gat tta taa
P I D L -

```

Figure 3.6: The full open reading of MS4A2.

The sequence of MS4A2 with the nucleic acid sequence in lower case and the proposed amino acid sequence in capitals. The section highlighted in red corresponds to exon 3 which is missing in the novel variant.

MS4A2_{trunc} open reading frame

```
atg gac aca gaa agt aat agg aga gca aat ctt gct ctc cca cag gag cct tcc agt gtg
M D T E S N R R A N L A L P Q E P S S V
cct gca ttt gaa gtc ttg gaa ata tct ccc cag gaa gta tct tca ggc aga cta ttg aag
P A F E V L E I S P Q E V S S G R L L K
tcg gcc tca tcc cca cca ctg cat aca tgg ctg aca gtt ttg aaa aaa gag cag gag ttc
S A S S P P L H T W L T V L K K E Q E F
ctg ggg ttt tct att tct gga atg ttg tca att ata tct gaa agg aga aat gca aca tat
L G F S I S G M L S I I S E R R N A T Y
ctg gtg aga gga agc ctg gga gca aac act gcc agc agc ata gct ggg gga acg gga att
L V R G S L G A N T A S S I A G G T G I
acc atc ctg atc atc aac ctg aag aag agc ttg gcc tat atc cac atc cac agt tgc cag
T I L I I N L K K S L A Y I H I H S C Q
aaa ttt ttt gag acc aag tgc ttt atg gct tcc ttt tcc act gaa att gta gtg atg atg
K F F E T K C F M A S F S T E I V V M M
ctg ttt ctc acc att ctg gga ctt ggt agt gct gtg tca ctc aca atc tgt gga gct ggg
L F L T I L G L G S A V S L T I C G A G
gaa gaa ctc aaa gga aac aag gtt cca gag gat cgt gtt tat gaa gaa tta aac ata tat
E E L K G N K V P E D R V Y E E L N I Y
tca gct act tac agt gag ttg gaa gac cca ggg gaa atg tct cct ccc att gat tta taa
S A T Y S E L E D P G E M S P P I D L -
```

Figure 3.7: The full open reading of MS4A2_{trunc} variant.

The sequence of MS4A2_{trunc} with the nucleic acid sequence in lower case and the proposed amino acid sequence in capitals.

MS4A4A Variant 1 open reading frame

```

atg aca acc atg caa gga atg gaa cag gcc atg cca ggg gct ggc cct ggt gtg ccc cag
M T T M Q G M E Q A M P G A G P G V P Q
ctg gga aac atg gct gtc ata cat tca cat ctg tgg aaa gga ttg caa gag aag ttc ttg
L G N M A V I H S H L W K G L Q E K F L
aag gga gaa ccc aaa gtc ctt ggg gtt gtg cag att ctg act gcc ctg atg agc ctt agc
K G E P K V L G V V Q I L T A L M S L S
atg gga ata aca atg atg tgt atg gca tct aat act tat gga agt aac cct att tcc gtg
M G I T M M C M A S N T Y G S N P I S V
tat atc ggg tac aca att tgg ggg tca gta atg ttt att att tca gga ttc ttg tca att
Y I G Y T I W G S V M F I I S G S L S I
gca gca gga att aga act aca aaa ggc ctg gtc cga ggt agt cta gga atg aat atc acc
A A G I R T T K G L V R G S L G M N I T
agc tct gta ctg gct gca tca ggg atc tta atc aac aca ttt agc ttg gcg ttt tat tca
S S V L A A S G I L I N T F S L A F Y S
ttc cat cac cct tac tgt aac tac tat ggc aac tca aat aat tgt cat ggg act atg tcc
F H H P Y C N Y Y G N S N N C H G T M S
atc tta atg ggt ctg gat ggc atg gtg ctc ctc tta agt gtg ctg gaa ttc tgc att gct
I L M G L D G M V L L L S V L E F C I A
gtg tcc ctc tct gcc ttt gga tgt aaa gtg ctc tgt tgt acc cct ggt ggg gtt gtg tta
V S L S A F G C K V L C C T P G G V V L
att ctg cca tca cat tct cac atg gca gaa aca gca tct ccc aca cca ctt aat gag gtt
I L P S H S H M A E T A S P T P L N E V
tga
-

```

Figure 3.8: The full open reading of MS4A4 variant 1.

The sequence of MS4A4 variant 1 with the nucleic acid sequence in lower case and the proposed amino acid sequence in capitals.

and the proposed amino acid sequence in capitals.

MS4A6A Variant 1 open reading frame

```
atg aca tca caa cct gtt ccc aat gag acc atc ata gtg ctc cca tca aat gtc atc aac
M T S Q P V P N E T I I V L P S N V I N
ttc tcc caa gca gag aaa ccc gaa ccc acc aac cag ggg cag gat agc ctg aag aaa cat
F S Q A E K P E P T N Q G Q D S L K K H
cta cac gca gaa atc aaa gtt att ggg act atc cag atc ttg tgt ggc atg atg gta ttg
L H A E I K V I G T I Q I L C G M M V L
agc ttg ggg atc att ttg gca tct gct tcc ttc tct cca aat ttt acc caa gtg act tct
S L G I I L A S A S F S P N F T Q V T S
aca ctg ttg aac tct gct tac cca ttc ata gga ccc ttt ttt ttt atc atc tct ggc tct
T L L N S A Y P F I G P F F F I I S G S
cta tca atc gcc aca gag aaa agg tta acc aag ctt ttg gtg cat agc agc ctg gtt gga
L S I A T E K R L T K L L V H S S L V G
agc att ctg agt gct ctg tct gcc ctg gtg ggt ttc att atc ctg tct gtc aaa cag gcc
S I L S A L S A L V G F I I L S V K Q A
acc tta aat cct gcc tca ctg cag tgt gag ttg gac aaa aat aat ata cca aca aga agt
T L N P A S L Q C E L D K N N I P T R S
tat gtt tct tac ttt tat cat gat tca ctt tat acc acg gac tgc tat aca gcc aaa gcc
Y V S Y F Y H D S L Y T T D C Y T A K A
agt ctg gct gga act ctc tct ctg atg ctg att tgc act ctg ctg gaa ttc tgc cta gct
S L A G T L S L M L I C T L L E F C L A
gtg ctc act gct gtg ctg cgg tgg aaa cag gct tac tct gac ttc cct ggg agt gta ctt
V L T A V L R W K Q A Y S D F P G S V L
ttc ctg cct cac agt tac att ggt aat tct ggc atg tcc tca aaa atg act cat gac tgt
F L P H S Y I G N S G M S S K M T H D C
gga tat gaa gaa cta ttg act tct taa
G Y E E L L T S -
```

Figure 3.9: The full open reading of MS4A6 variant 1.

The sequence of MS4A6 variant 1 with the nucleic acid sequence in lower case and the proposed amino acid sequence in capitals.

MS4A6A Variant 1 polymorphism open reading frame

```
atg aca tca caa cct gtt ccc aat gag acc atc ata gtg ctc cca tca aat gtc atc aac
M T S Q P V P N E T I I V L P S N V I N
ttc tcc caa gca gag aaa ccc gaa ccc acc aac cag ggg cag gat agc ctg aag aaa cat
F S Q A E K P E P T N Q G Q D S L K K H
cta cac gca gaa atc aaa gtt att ggg ttt atc atc tct ggc tct cta tca atc gcc aca
L H A E I K V I G F I I S G S L S I A T
gag aaa agg tta acc aag ctt ttg gtg cat agc agc ctg gtt gga agc att ctg agt gct
E K R L T K L L V H S S L V G S I L S A
ctg tct gcc ctg gtg ggt ttc att atc ctg tct gtc aaa cag gcc acc tta aat cct gcc
L S A L V G F I I L S V K Q A T L N P A
tca ctg cag tgt gag ttg gac aaa aat aat ata cca aca aga agt tat gtt tct tac ttt
S L Q C E L D K N N I P T R S Y V S Y F
tat cat gat tca ctt tat acc acg gac tgc tat aca gcc aaa gcc agt ctg gct gga act
Y H D S L Y T T D C Y T A K A S L A G T
ctc tct ctg atg ctg att tgc act ctg ctg gaa ttc tgc cta gct gtg ctc act gct gtg
L S L M L I C T L L E F C L A V L T A V
EcoRI
ctg cgg tgg aaa cag gct tac tct gac ttc cct ggg agt gta ctt ttc ctg cct cac agt
L R W K Q A Y S D F P G S V L F L P H S
tac att ggt aat tct ggc atg tcc tca aaa atg act cat gac tgt gga tat gaa gaa cta
Y I G N S G M S S K M T H D C G Y E E L
ttg act tct taa
L T S -
```

Figure 3.10: The full open reading of MS4A6 variant 1 polymorphism.

The sequence of MS4A6 variant 1 polymorphism with the nucleic acid sequence in lower case and the proposed amino acid sequence in capitals.

MS4A6A novel variant open reading frame

```
atg aca tca caa cct gtt ccc aat gag acc atc ata gtg ctc cca tca aat gtc atc aac
M T S Q P V P N E T I I V L P S N V I N
ttc tcc caa gca gag aaa ccc gaa ccc acc aac cag ggg cag gat agc ctg aag aaa cat
F S Q A E K P E P T N Q G Q D S L K K H
cta cac gca gaa atc aaa gtt att ggg ttt atc atc tct ggc tct cta tca atc gcc aca
L H A E I K V I G F I I S G S L S I A T
gag aaa agg tta acc aag ctt ttg gtg cat agc agc ctg gtt gga agc att ctg agt gct
E K R L T K L L V H S S L V G S I L S A
ctg tct gcc ctg gtg ggt ttc att atc ctg tct gtc aaa cag gcc acc tta aat cct gcc
L S A L V G F I I L S V K Q A T L N P A
cca ctg cag tgg aac tct ctc tct gat gct gat ttg cac tct gct gga att ctg cct agc
P L Q W N S L S D A D L H S A G I L P S
tgt gct cac tgc tgt gct gcg gtg gaa aca ggc tta ctc tga
C A H C C A A V E T G L L -
```

Figure 3.11: The full open reading of MS4A6 novel variant.

The sequence of MS4A6 novel variant with the nucleic acid sequence in lower case and the proposed amino acid sequence in capitals.

MS4A7 long variant (variant 1) open reading frame

```
atg cta tta caa tcc caa acc atg ggg gtt tct cac agc ttt aca cca aag ggc atc act
M L L Q S Q T M G V S H S F T P K G I T

atc cct caa aga gag aaa cct gga cac atg tac caa aac gaa gat tac ctg cag aac ggg
I P Q R E K P G H M Y Q N E D Y L Q N G

ctg cca aca gaa acc acc gtt ctt ggg act gtc cag atc ctg tgt tgc ctg ttg att tca
L P T E T T V L G T V Q I L C C L L I S

agt ctg ggg gcc atc ttg gtt ttt gct ccc tac ccc tcc cac ttc aat cca gca att tcc
S L G A I L V F A P Y P S H F N P A I S
BamHI
acc act ttg atg tct ggg tac cca ttt tta gga gct ctg tgt ttt ggc att act gga tcc
T T L M S G Y P F L G A L C F G I T G S

ctc tca att atc tct gga aaa caa tca act aag ccc ttt gac ctg agc agc ttg acc tca
L S I I S G K Q S T K P F D L S S L T S

aat gca gtg agt tct gtt act gca gga gca ggc ctc ttc ctc ctt gct gac agc atg gta
N A V S S V T A G A G L F L L A D S M V

gcc ctg agg act gcc tct caa cat tgt ggc tca gaa atg gat tat cta tcc tca ttg cct
A L R T A S Q H C G S E M D Y L S S L P

tat tcg gag tac tat tat cca ata tat gaa atc aaa gat tgt ctc ctg acc agt gtc agt
Y S E Y Y Y P I Y E I K D C L L T S V S

tta aca ggt gtc cta gtg gtg atg ctc atc ttc act gtg ctg gag ctc tta tta gct gca
L T G V L V V M L I F T V L E L L L A A

tac agt tct gtc ttt tgg tgg aaa cag ctc tac tcc aac aac cct ggg agt tca ttt tcc
Y S S V F W W K Q L Y S N N P G S S F S

tcg acc cag tca caa gat cat atc caa cag gtc aaa aag agt tct tca cgg tct tgg ata
S T Q S Q D H I Q Q V K K S S S R S W I

taa
-
```

Figure 3.12: The full open reading of MS4A7 variant 1.

The sequence of MS4A7 variant 1 with the nucleic acid sequence in lower case and the proposed amino acid sequence in capitals.

MS4A7 short variant (variant 2) open reading frame

REGULATION

```
atg cta tta caa tcc caa acc atg ggg gtt tct cac agc ttt aca cca aag ggc atc act
M L L Q S Q T M G V S H S F T P K G I T

atc cct caa aga gag aaa cct gga cac atg tac caa aac gaa gat tac ctg cag aac ggg
I P Q R E K P G H M Y Q N E D Y L Q N G

ctg cca aca gaa acc acc gtt ctt ggg ttt ggc att act gga tcc ctc tca att atc tct
L P T E T T V L G F G I T G S L S I I S

gga aaa caa tca act aag ccc ttt gac ctg agc agc ttg acc tca aat gca gtg agt tct
G K Q S T K P F D L S S L T S N A V S S

gtt act gca gga gca ggc ctc ttc ctc ctt gct gac agc atg gta gcc ctg agg act gcc
V T A G A G L F L L A D S M V A L R T A

tct caa cat tgt ggc tca gaa atg gat tat cta tcc tca ttg cct tat tcg gag tac tat
S Q H C G S E M D Y L S S L P Y S E Y Y

tat cca ata tat gaa atc aaa gat tgt ctc ctg acc agt gtc agt tta aca ggt gtc cta
Y P I Y E I K D C L L T S V S L T G V L

gtg gtg atg ctc atc ttc act gtg ctg gag ctc tta tta gct gca tac agt tct gtc ttt
V V M L I F T V L E L L L A A Y S S V F

tgg tgg aaa cag ctc tac tcc aac aac cct ggg agt tca ttt tcc tcg acc cag tca caa
W W K Q L Y S N N P G S S F S S T Q S Q

gat cat atc caa cag gtc aaa aag agt tct tca cgg tct tgg ata taa
D H I Q Q V K K S S S R S W I -
```

Figure 3.13: The full open reading of MS4A7 variant 2.

The sequence of MS4A7 variant 2 with the nucleic acid sequence in lower case and the proposed amino acid sequence in capitals.

3.3 QUALITATIVE AND QUANTITATIVE REAL TIME PCR AND GENE REGULATION

3.3.1 Qualitative real time RT-PCR for gene expression

Before performing quantitative real time RT-PCR, I first needed to confirm the expression of the identified MS4A gene family members and splice variants in the HLMC and HMC-1 cells. I achieved this through designing and optimising the conditions for quantitative PCR. Thus I began with the LAD-2 cells since I had already confirmed their expression in these cells.

3.3.1.1 Qualitative MS4A gene expression in LAD-2 cells

Using this approach, I was able to confirm that there was good expression of MS4A2 in the LAD-2 cells (**Figure 3.14**). However, with the novel variant of MS4A2 I could see that expression of this truncation was only induced with stimulation of the cells with either IgE alone or with IgE plus antigen (**Figure 3.14**). This is interesting as it suggests an important role in cell function following stimulation. I was also able to confirm the expression of MS4A4 variant 1 (**Figure 3.14**). Importantly, there were bands present in the no template controls which had a similar product size to the bands for both MS4A2 and MS4A2 novel. However, using dissociation melting curves at the end of the PCR reaction can distinguish between the expected melting temperature (T_m) of the products and the production of primer-dimer complexes and non-specific amplification in these cases (**Figure 3.20**). The T_m of the primer-dimers varied and usually had more than one peak, but was consistently different to the T_m of

the sample products (**Figure 3.20**). In addition, the products were sequenced to confirm specificity.

I next examined the expression of the MS4A6 and MS4A7 variants. Interestingly, all of these variants were expressed at very low levels in the resting cells. However, like the novel variant of MS4A2, they were all much more highly expressed after stimulation with IgE (**Figure 3.15**). The only exception was the novel variant of MS4A6. There were multiple bands when using these primers and all of the bands were stronger in the stimulated cells. This could be due to the primers binding to other MS4A6 variants which have identical sequences within them which are themselves upregulated following stimulation. This is highly plausible given the number of variants of MS4A6 and their high similarity. However, further study of all the possible expressed known and novel variants was beyond the scope of this study.

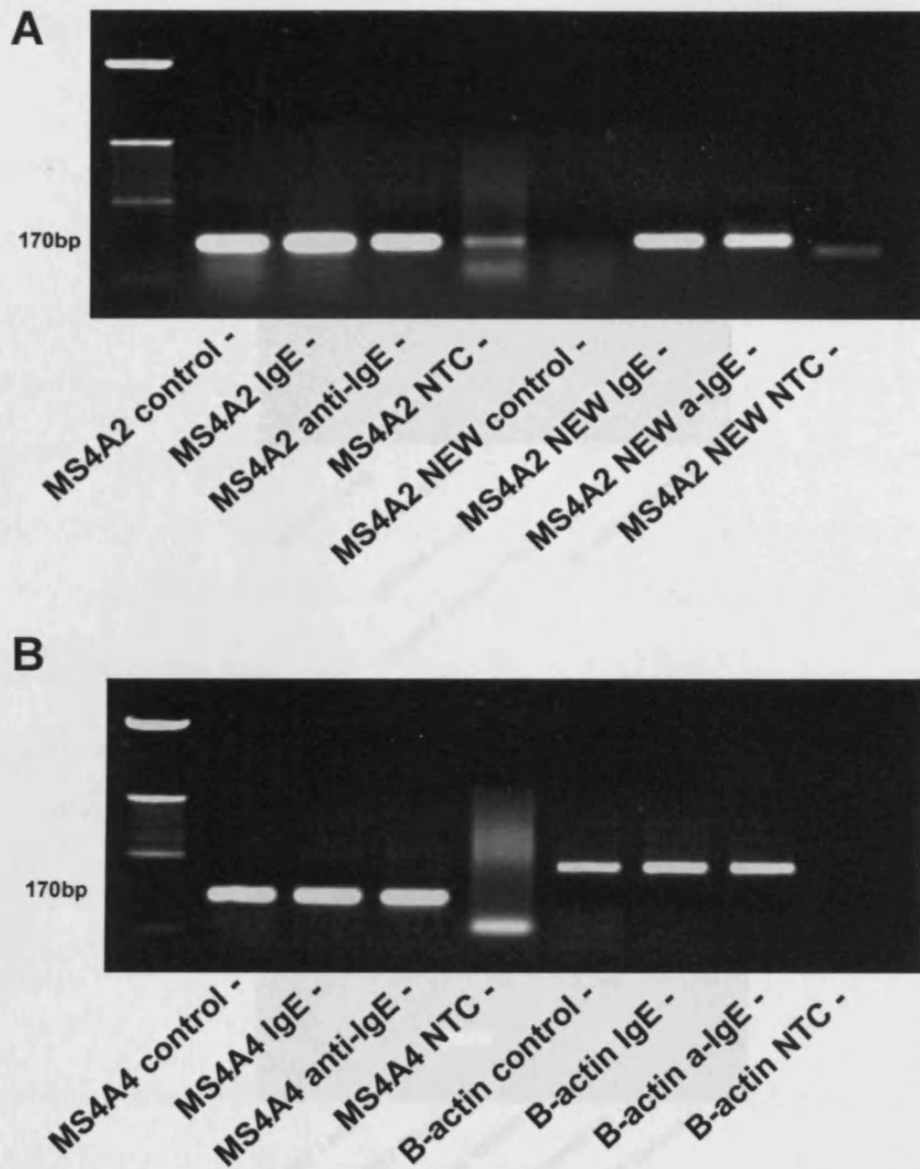


Figure 3.14: LAD-2 products using qualitative real time RT-PCR.

A) MS4A2 was present in all conditions. However, the novel variant of MS4A2 was only detectable after stimulation with either IgE alone, or with IgE/anti-IgE.

B) MS4A4 was also present in all conditions. Beta-actin was used as an internal control, and reactions without any template (NTC) were used as controls for primer-dimerisation. There was evidence of primer-dimers occurring in the reactions which necessitated the use of dissociation curves to validate the data.

MS4A2 appears to be the dominant variant expressed in LAD-2 cells

3.3.4.2 Qualitative MS4A gene expression in HMC-1 cells

Since the methodology for the real time RT-PCR worked consistently well with the LAD-2 cells, I next looked at the expression of the MS4A gene family in the HMC-1 cells. At baseline, the HMC-1 cells do not express any of the MS4A gene family at baseline (Figure 3.15A). However, following stimulation with IgE, the HMC-1 cells express MS4A4 or the novel variant of MS4A6 (Figure 3.15B). The cycle threshold for amplification of MS4A4 was 28.5 and for MS4A6 was 29.5. Both of these genes were amplifying in HMC-1 cells. In addition, the cycle threshold for amplification of MS4A7 was 30.5. This suggests that they were primer-dimers. In addition, the cycle threshold for amplification of MS4A6 Variant 1 was 31.5. This suggests that it was a primer-dimer. The cycle threshold for amplification of MS4A6 Variant 1 Polymorphism was 32.5. This suggests that it was a primer-dimer.

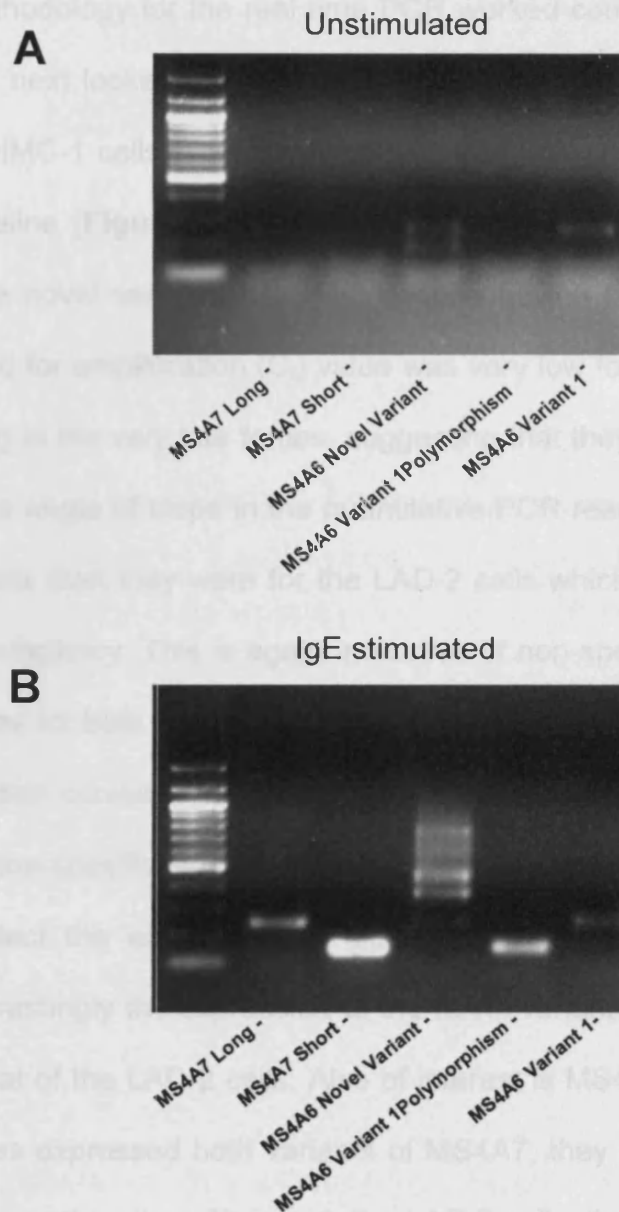


Figure 3.15: LAD-2 products using qualitative real time RT-PCR.

The top panel shows that there was very little expression of either the MS4A6 variants or the MS4A7 variants at baseline. However, following stimulation with IgE, there was good expression of all of the variants with the exception of the novel variant of MS4A6, which was only minimally expressed and the primers were amplifying more than one product. In addition, the short variant of MS4A7 appears to be the dominant variant expressed in LAD-2 cells.

3.3.1.2 Qualitative MS4A gene expression in HMC-1 cells

Since the methodology for the real time PCR worked consistently well with the LAD-2 cells, I next looked to confirm the expression profile of the MS4A gene family in the HMC-1 cells. The HMC-1 cells expressed most of the MS4A gene family at baseline (**Figure 3.16**). The HMC-1 cells did not, however, express MS4A4 or the novel variant of MS4A2 despite having bands in the gel. The cycle threshold for amplification (C_t) value was very low for both of these genes only appearing in the very late forties, suggesting that they were primer-dimers. In addition, the angle of slope in the quantitative PCR reaction was different for the HMC-1 cells than they were for the LAD-2 cells which suggests a different amplification efficiency. This is again indicative of non-specific binding. Thirdly, the product size for both of these genes was the wrong size. Finally, the melting point dissociation curves were not distinct peaks which is also very compelling evidence of non-specific amplification. Therefore, I can conclude that I was unable to detect the expression of either of these genes in HMC-1 cells. However, interestingly the expression of the novel variant of MS4A6 was much higher than that of the LAD-2 cells. Also of interest is MS4A7. Although both of these cell types expressed both variants of MS4A7, they seem to express one preferentially over the other. Thus with the LAD-2 cells, there was clearly higher expression of the short variant of MS4A7 (**Figure 3.15**). Conversely, the HMC-1 cells seemed to preferentially express the long variant of MS4A7 (**Figure 3.16**).

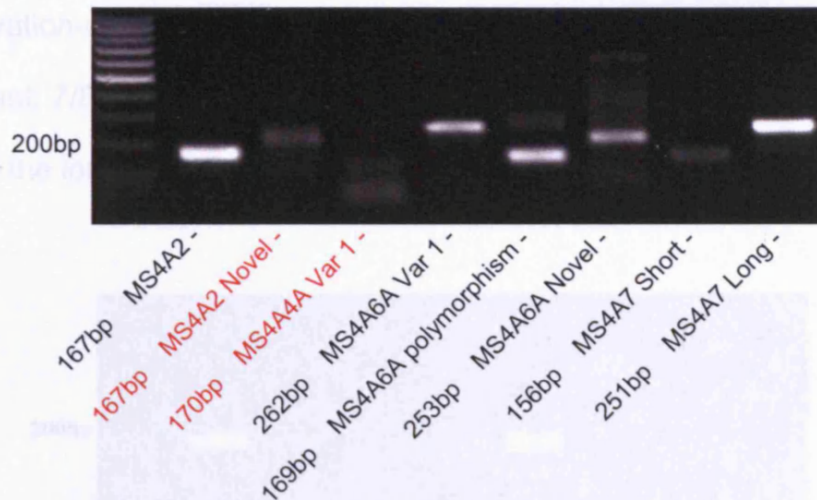


Figure 3.16: HMC-1 products using qualitative real time PCR.

This figure shows that HMC-1 cells express all of the studied MS4A gene family members except for the novel variant of MS4A2 and MS4A4. The band present in the novel MS4A2 lane was non-specific since it was too large and had a dissociation curve with several random peaks which is indicative of primer-dimer formation. Similarly, the band in the MS4A4 lane was too small with a melting curve that had several small peaks. Interestingly, the HMC-1 cells appear to express the novel variant of MS4A6 more highly than the LAD-2 cells. In contrast to LAD-2 cells, the dominant MS4A7 variant expressed in HMC-1 cells was the long variant.

3.3.1.3 Qualitative MS4A gene expression in HLMC

HLMC expressed the majority of the MS4A gene family splice variants examined. However, there was a degree of variability in expression between donors, but this is typical of primary cells. HLMC consistently expressed MS4A2. Thus 8/8 donors expressed MS4A2; 5/8 donors expressed the novel variant of MS4A2 which was usually activation-dependent; 7/8 donors expressed MS4A4 variant 1; 6/8 donors expressed MS4A6 variant 1; 7/8 donors expressed MS4A6 polymorphism, although the expression of this variant was

often activation-dependent (**Figure 3.18**); 0/8 donors expressed the MS4A6 novel variant; 7/8 donors expressed the short variant of MS4A7; and 5/8 donors expressed the long variant of MS4A7.

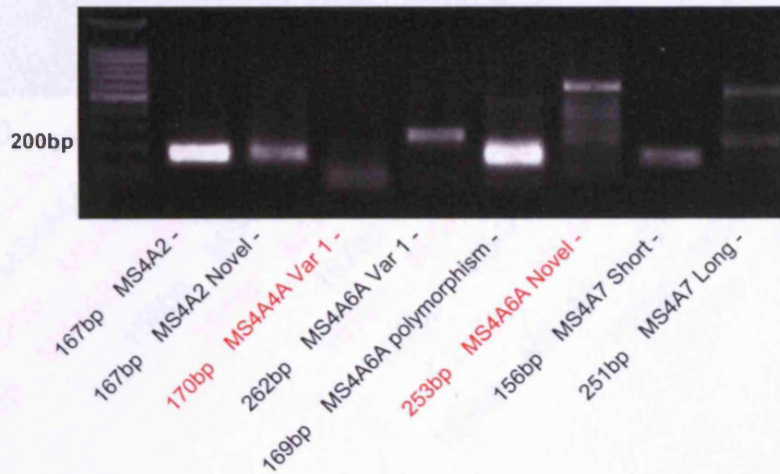


Figure 3.17: HLHC products using qualitative real time PCR.

This figure shows the expression profile of a single HLHC donor at baseline. This donor did not express MS4A4 or MS4A6 novel variant at baseline. There was good expression of the other variants. The long variant of MS4A7 was expressed but there was also amplification of a larger band (~500bp). This band was evident in some donors, but not others. The presence of the band was easily deciphered from the melting curve and quantitative data from donors that had this larger band was not used.

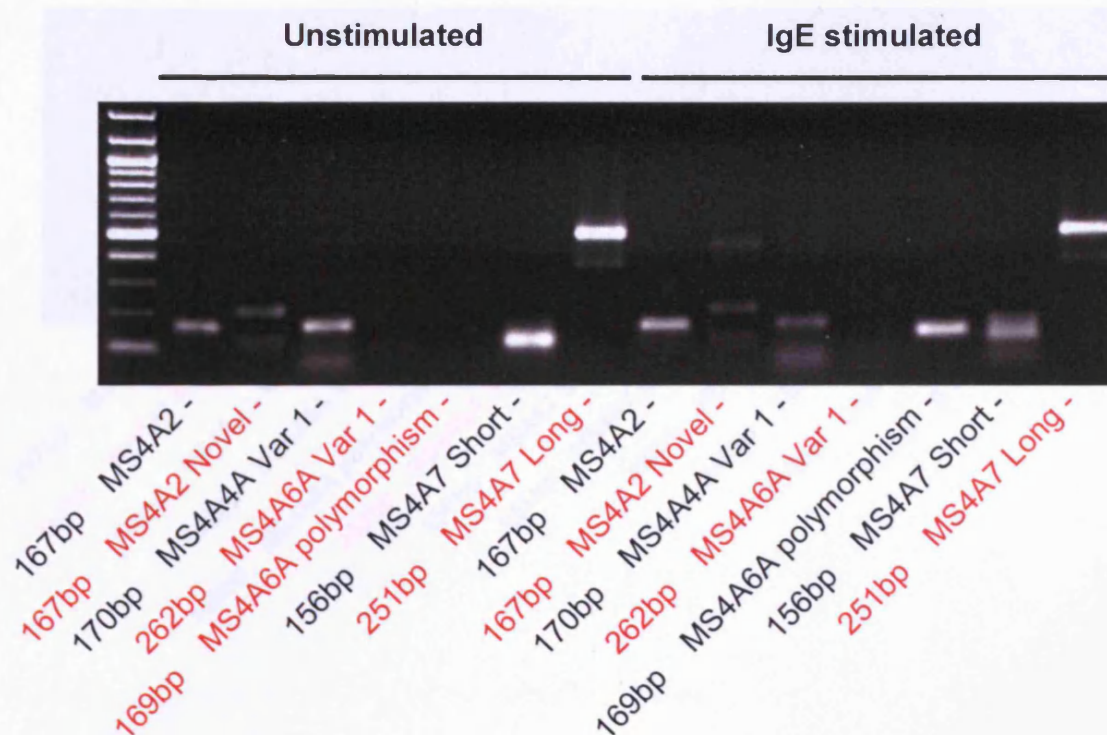


Figure 3.18: Fibrocyte products using real time PCR

Figure 3.18: HLMC products before and after IgE stimulation.

This figure shows the expression profile of a different HLMC donor both at rest and following stimulation with IgE. This donor did not express the novel variant of MS4A2 which shows a double band with 1 band larger and 1 band smaller than the expected size. This pattern, in conjunction with the melting curves, was typical of non-specific amplification of primer-dimer complexes. This donor also did not express MS4A6 variant 1. The long variant of MS4A7 was also not expressed. Interestingly, the expression of the MS4A6 polymorphism was not evident at rest, but was expressed after sensitisation with IgE.

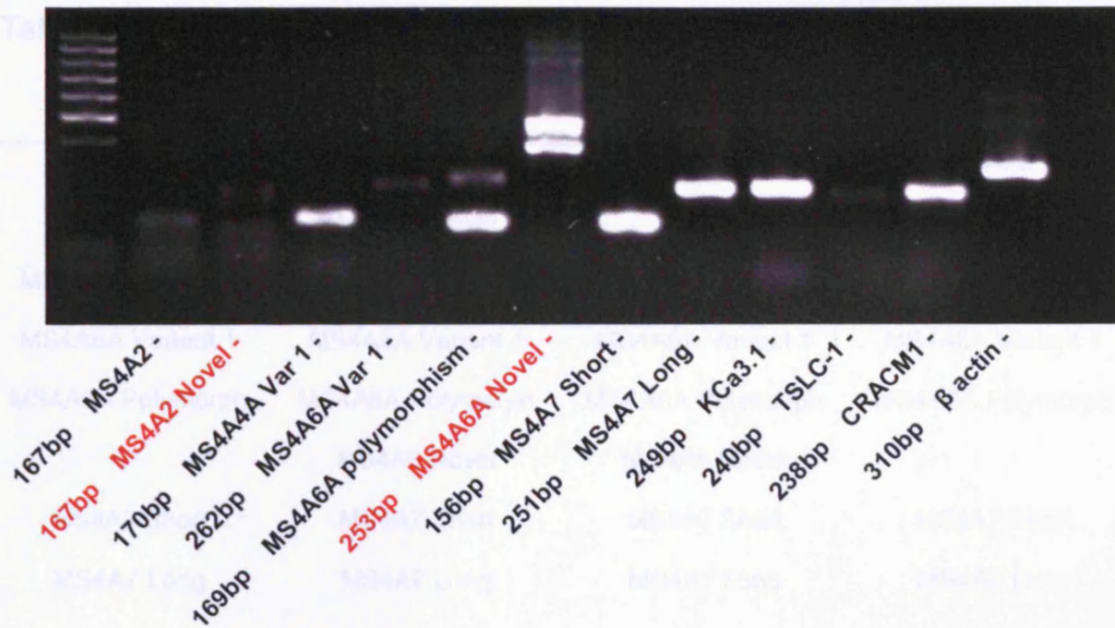


Table 3.1: Interestingly, the novel variants of MS4A2 are only expressed in the cells which have the high affinity I_{Ca} receptor. In addition, the novel variants of MS4A6A are only expressed in the cells which originate from the heart.

Figure 3.19: Fibrocyte products using real time PCR.

This figure shows the expression profile of the MS4A gene family in peripheral blood-derived fibrocytes. This gel is representative of 4 donors. Human primary fibrocytes express MS4A2, MS4A4 variant 1, MS4A6 variant 1, MS4A6 polymorphism and both variants of MS4A7.

3.3.2 Quantitative real time RT-PCR

3.3.2.1 Confirming specificity of QPCR amplification

In order to trust the quantity of RT-PCR data, it was important to ensure that the PCR reaction for each experiment was specific and that there was no amplification of products other than the one of interest. This can be achieved in several ways. However, for QRT-PCR using SYBR Green as the detection molecule, the convention is to use a dissociation melting curve for each reaction at the end of the experiment. Melting points should be close to the calculated melting point for the sequence expected to be amplified. Thus the

Table 3.1: Summary of MS4A gene family expression

HLMC	LAD-2	HMC-1	Fibrocytes
MS4A2	MS4A2	MS4A2	MS4A2
MS4A2 Novel	MS4A2 Novel		
MS4A4A Variant 1	MS4A4A Variant 1		MS4A4A Variant 1
MS4A6A Variant 1	MS4A6A Variant 1	MS4A6A Variant 1	MS4A6A Variant 1
MS4A6A Polymorph	MS4A6A Polymorph	MS4A6A Polymorph	MS4A6A Polymorph
	MS4A6 Novel	MS4A6 Novel	
MS4A7 Short	MS4A7 Short	MS4A7 Short	MS4A7 Short
MS4A7 Long	MS4A7 Long	MS4A7 Long	MS4A7 Long

Table 3.1: Interestingly, the novel variant of MS4A2 was only expressed in the cells which have the high affinity IgE receptor. In addition, the novel variant of MS4A6 was only expressed in the immortalised cell lines which originate from patients with mast cell leukaemia / mastocytosis. These observations raise questions. Could the novel variant of MS4A2 be a critical component of IgE receptor signalling? Could the novel variant of MS4A6 be involved in uncontrolled cell proliferation?

3.3.2 Quantitative real time RT-PCR

3.3.2.1 Confirming specificity of QPCR amplification

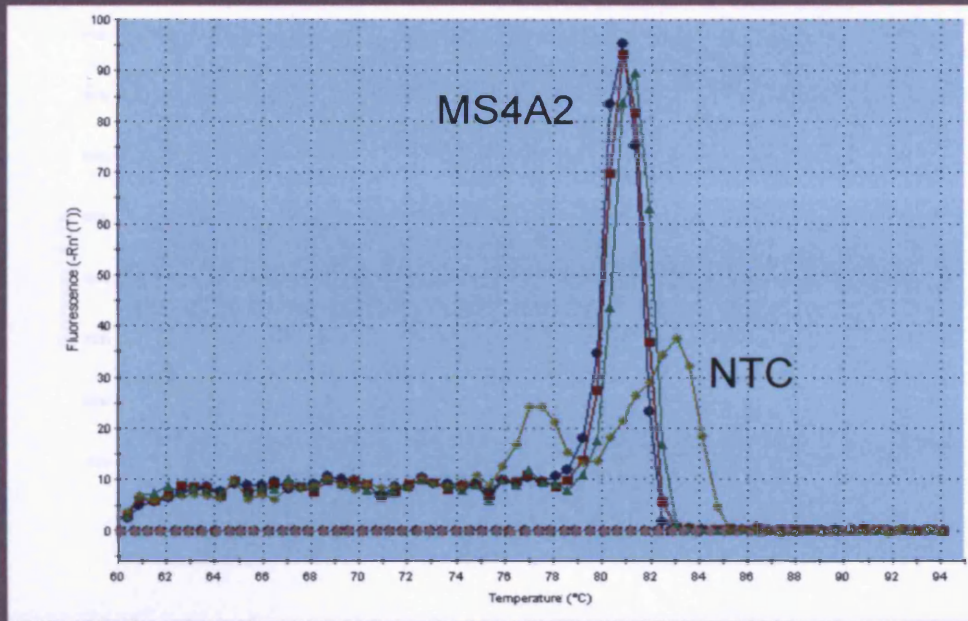
In order to trust the quantitative RT-PCR data, it was necessary to ensure that the PCR reaction for each experiment was specific and that there was no amplification of products other than the gene of interest (GOI). This can be achieved in several ways. However, for QRT-PCR using SYBR Green as the detection molecule, the convention is to use a dissociation (melting) curve for each reaction at the end of the experiment. Melting points should be close to the calculated melting point for the sequence expected to be amplified. Thus the

proposed melting point was calculated for each of the amplicon products using the Oligo Calc (<http://www.basic.northwestern.edu/biotools/oligocalc.html>) algorithm. The actual melting point could then be directly compared to the proposed melting point for each product. It is also important to scrutinise the characteristics of each melting curve as this can give important information as to the quality and reliability of the data. Melting curves containing multiple peaks (an example can be seen in **Figure 3.20A** in the no template control (NTC)), humps adjoining the main peak (an example can be seen in **Figure 3.23A** in the NTC), and even single peaks which have a wide temperature range throughout the peak (an example of this type of peak can be seen in **Figure 3.23B** in the NTC) must be treated with extreme caution and should usually be omitted.

Using the data from the melting curves allows for the full optimisation of the reactions to gain maximum data with minimum non-specific amplification. Thus optimisation was achieved using 200nM final concentration of primers for each GOI. 250nM of primers also worked well, but there was a higher preponderance for non-specific amplification on conditions with lower expression. Thus using 200nM primer concentration, consistent good quality melting curves were seen in all conditions (typical examples of the melting curves are given in **Figures 3.20-3.24**).

Figure 3.20: Dissociation curves for MS4A2 and US4A2 ...
Using gradual increments in temperature the point at which the DNA duplexes is depicted as a peak. The NTC control usually has a different melting temperature to the products and usually has a double peak.

Dissociation Curve



Dissociation Curve

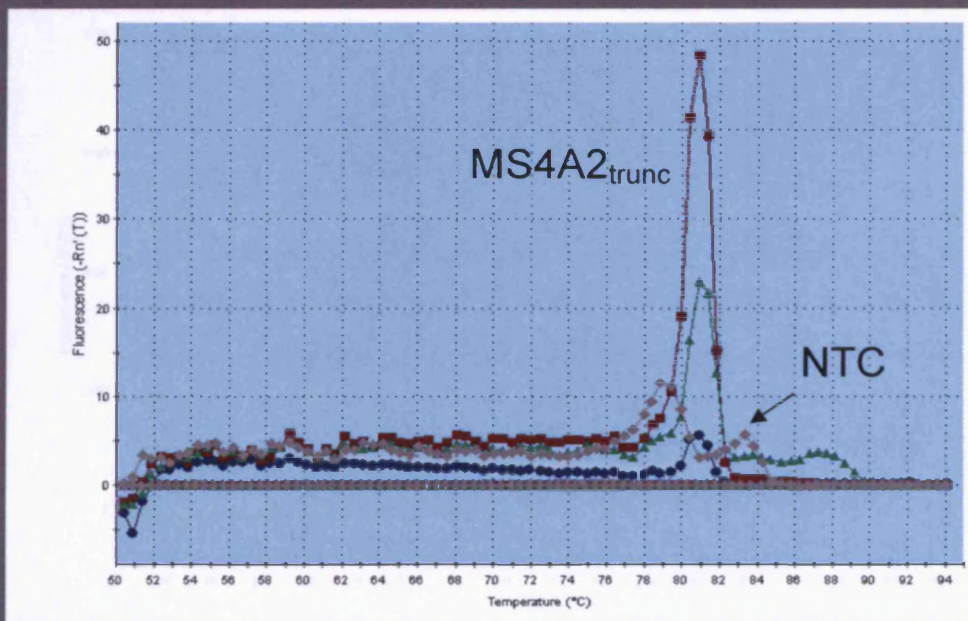


Figure 3.20: Dissociation curves for MS4A2 and MS4A2_{trunc}.

Using gradual increments in temperature the point at which the cDNA dissociates is depicted as a peak. The NTC consistently had a different melting temperature to the products and usually had a double peak.

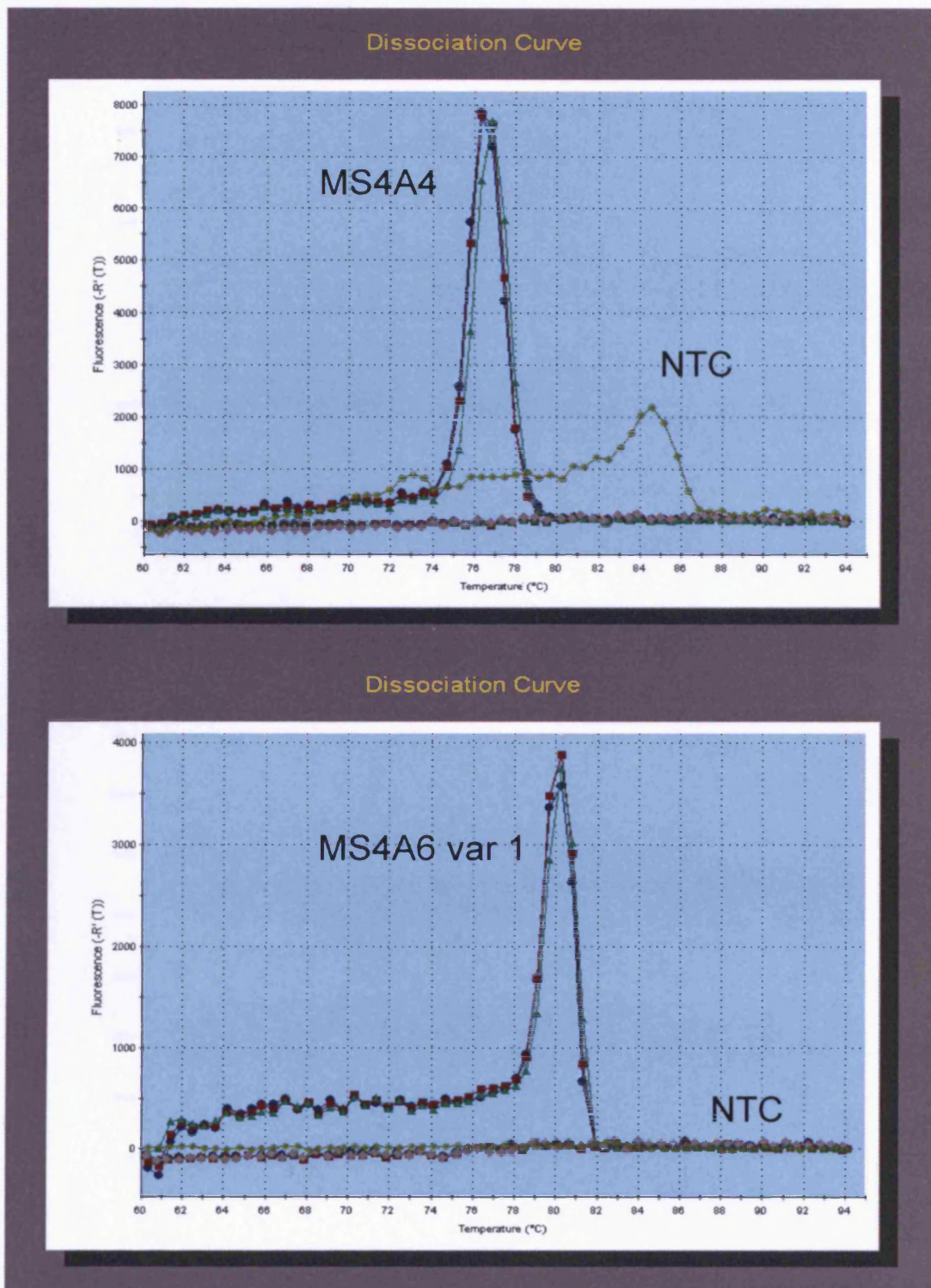
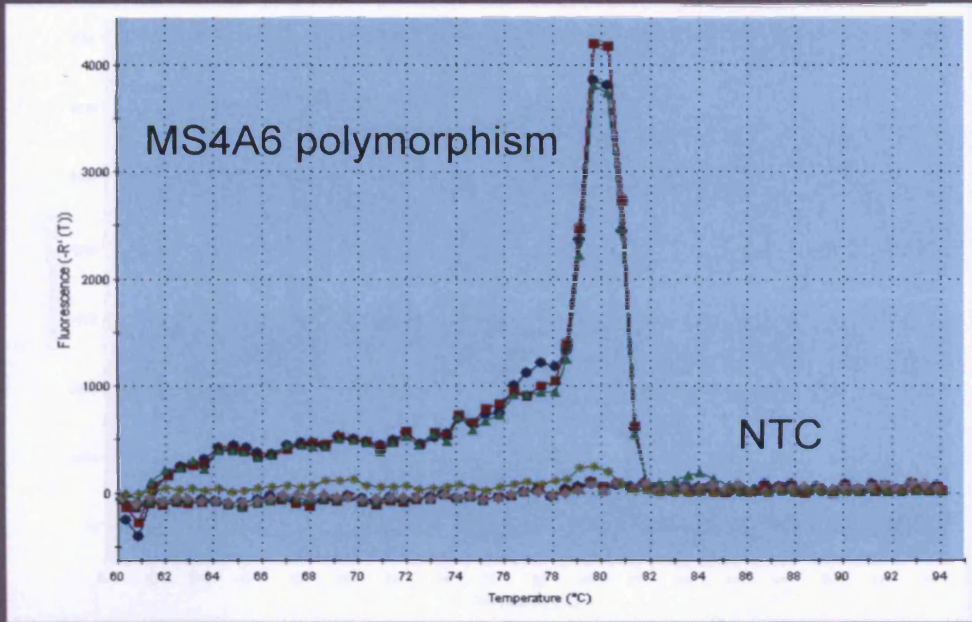


Figure 3.21: Dissociation curves for MS4A4 and MS4A6 Variant 1. MS4A4 and MS4A6 melting curves. There were consistently peaks in the NTC for MS4A4, but these peaks were always easily distinguishable from the MS4A4 product. MS4A6 variant 1 primers yielded no NSB even after 50 cycles.

Dissociation Curve



Dissociation Curve

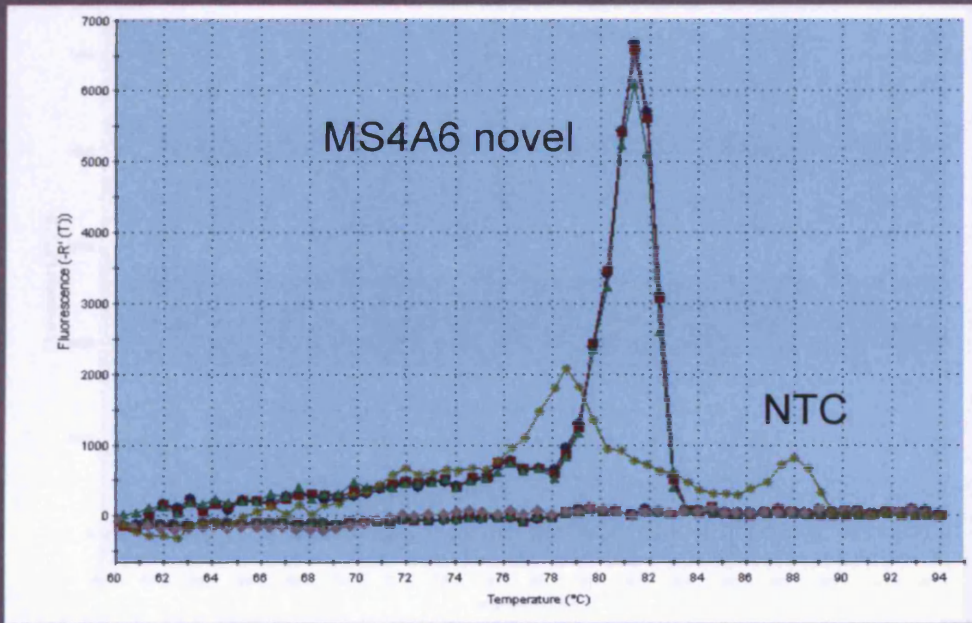
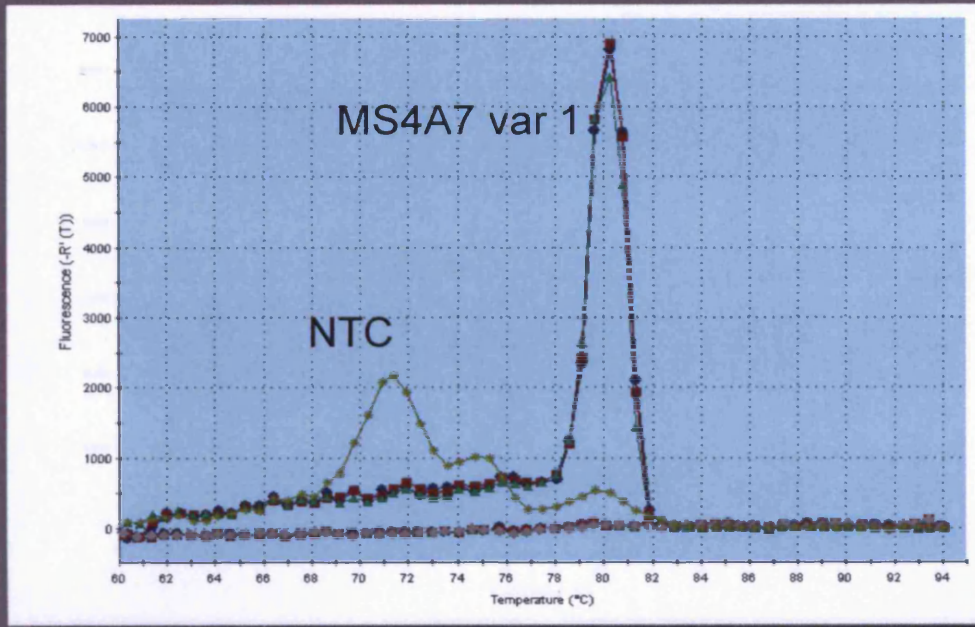


Figure 3.22: Dissociation curves for MS4A6 polymorphism and MS4A6 novel variant.

Dissociation Curve



Dissociation Curve

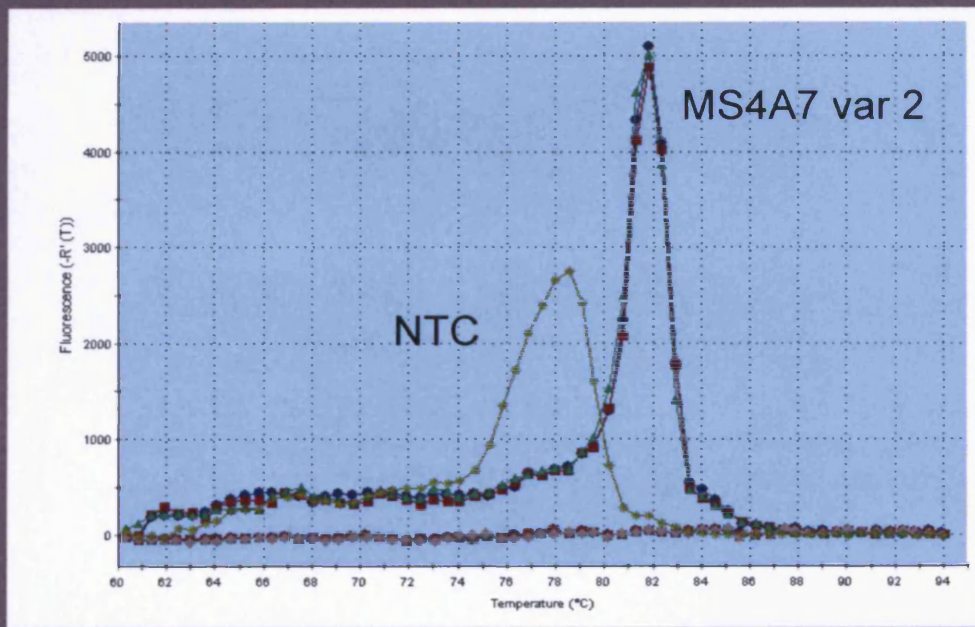


Figure 3.23: Dissociation curves for MS4A7 variants.

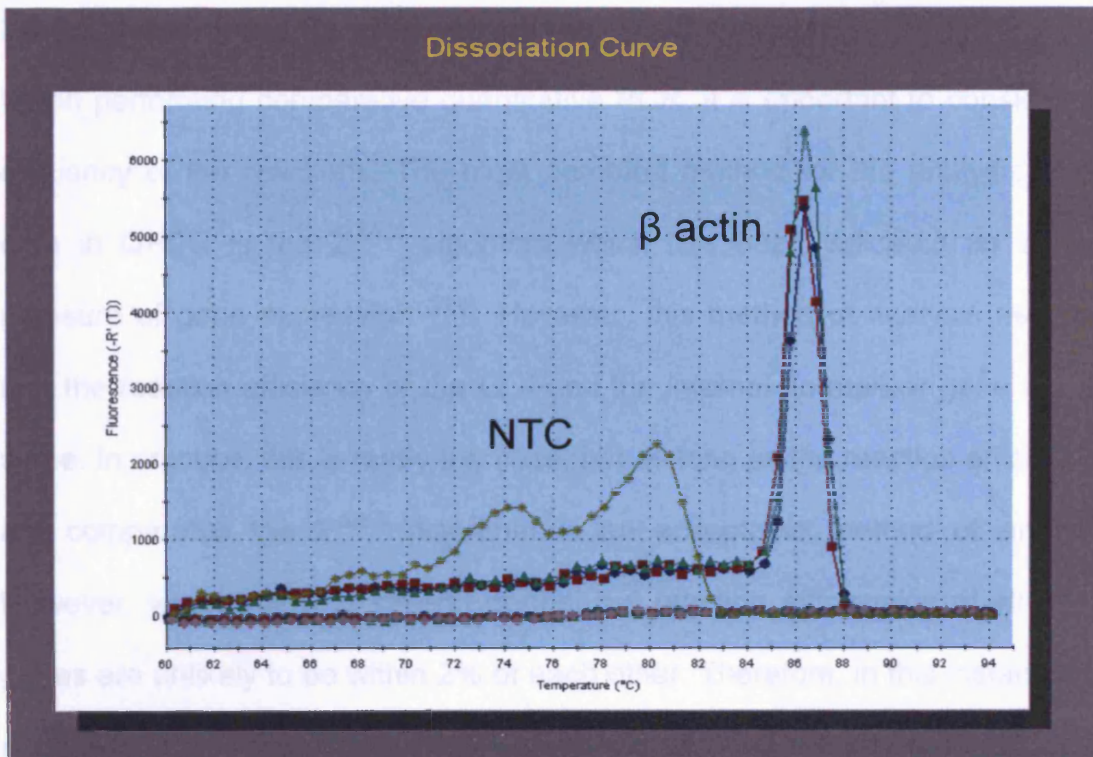


Figure 3.24: Dissociation curves for β -actin.

3.3.2.2 Determining the efficiency of the QPCR reaction

When performing comparative quantitative PCR, it is important to consider the efficiency of the reactions. The most common method for the analysis of the data in QPCR is the $2^{-\Delta\Delta Ct}$ algorithm which has been validated as a good measure of gene expression ⁽²⁰⁸⁾. However, this method of analysis assumes that the reaction efficiency of the GOI and the internal normaliser gene are the same. In practice, this is rarely the case, but as long as the reaction efficiencies are comparable the $2^{-\Delta\Delta Ct}$ algorithm is an acceptable method of analysis. However, when studying several genes, the reaction efficiencies of all of the genes are unlikely to be within 2% of each other. Therefore, in this instance it is important to take the different efficiencies into account and add a correction for efficiency into the algorithm. Since the efficiency of each reaction for each GOI ranged from 72.7% to 101.7% (**Figures 3.25-3.32**) the data was corrected for efficiency.

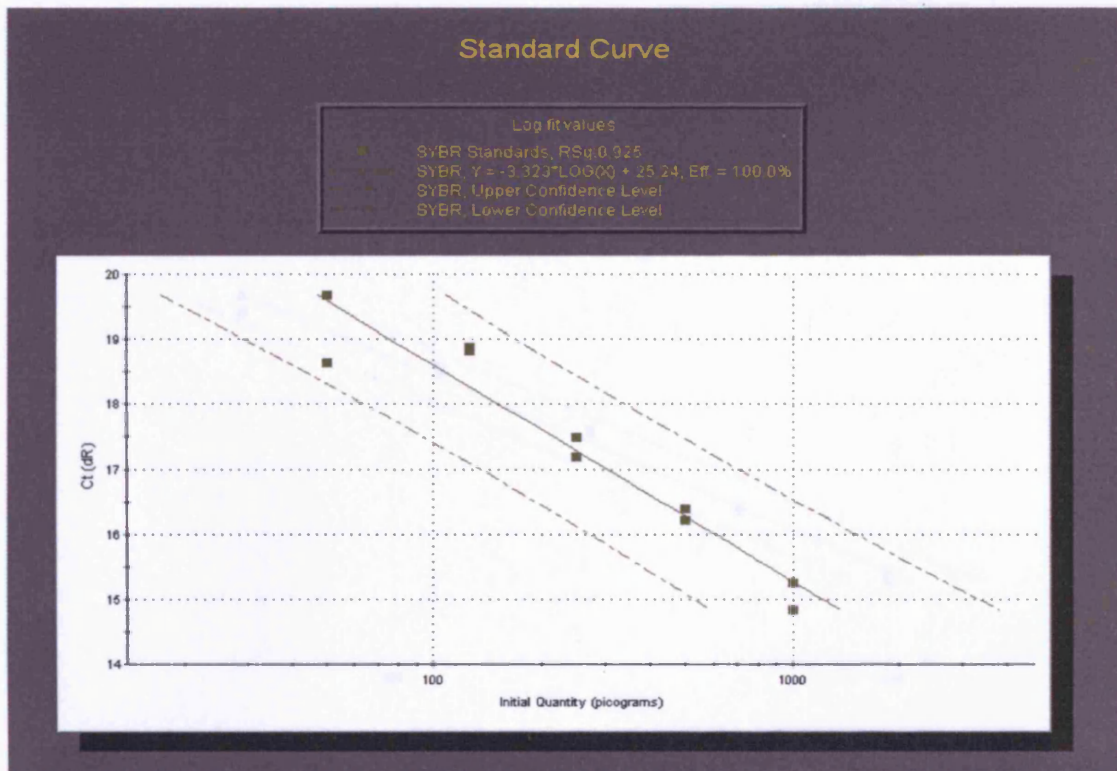


Figure 3.25: Efficiency of MS4A2 QPCR reaction.

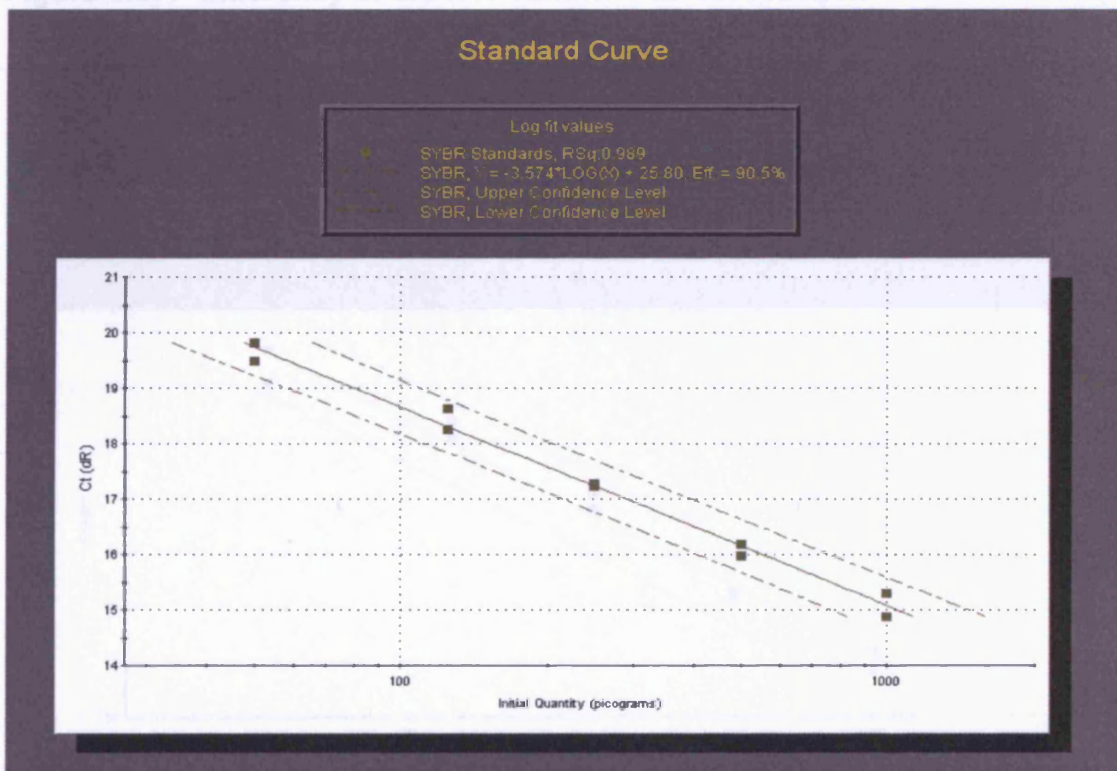


Figure 3.26: Efficiency of MS4A2_{trunc} QPCR reaction.

Figure 3.28: Efficiency of MS4A2 variant 1 QPCR reaction.

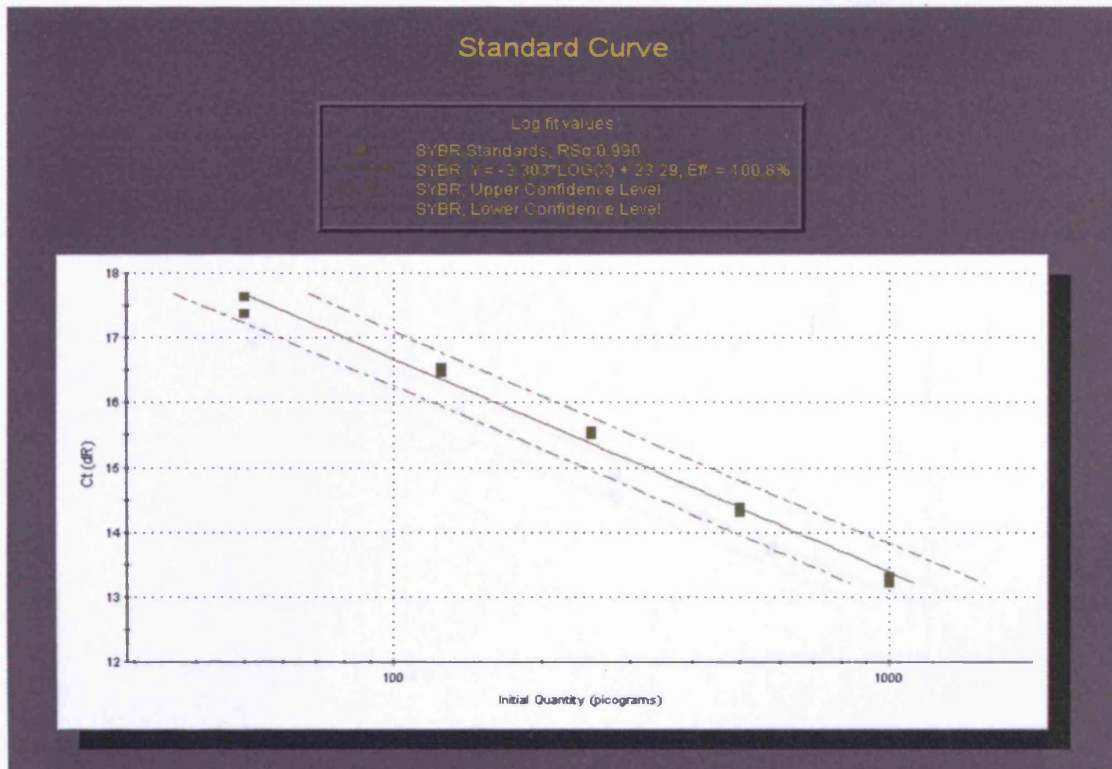


Figure 3.27: Efficiency of MS4A4 variant 1 QPCR reaction

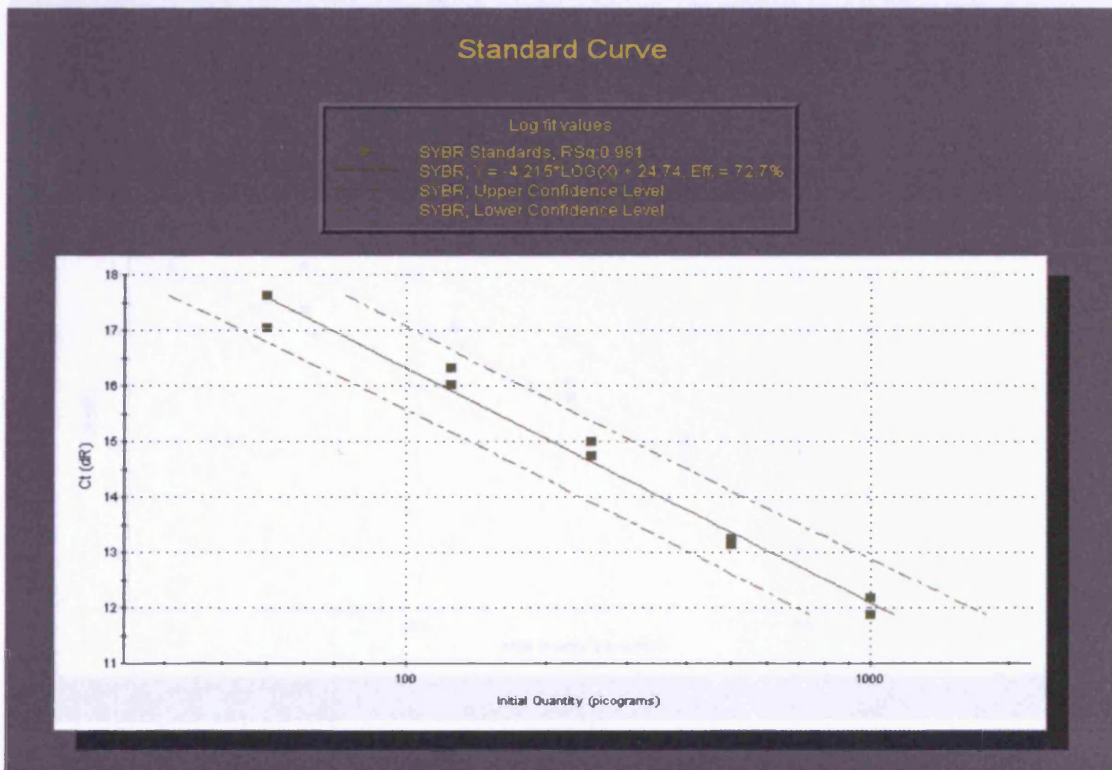


Figure 3.28: Efficiency of MS4A6 variant 1 QPCR reaction

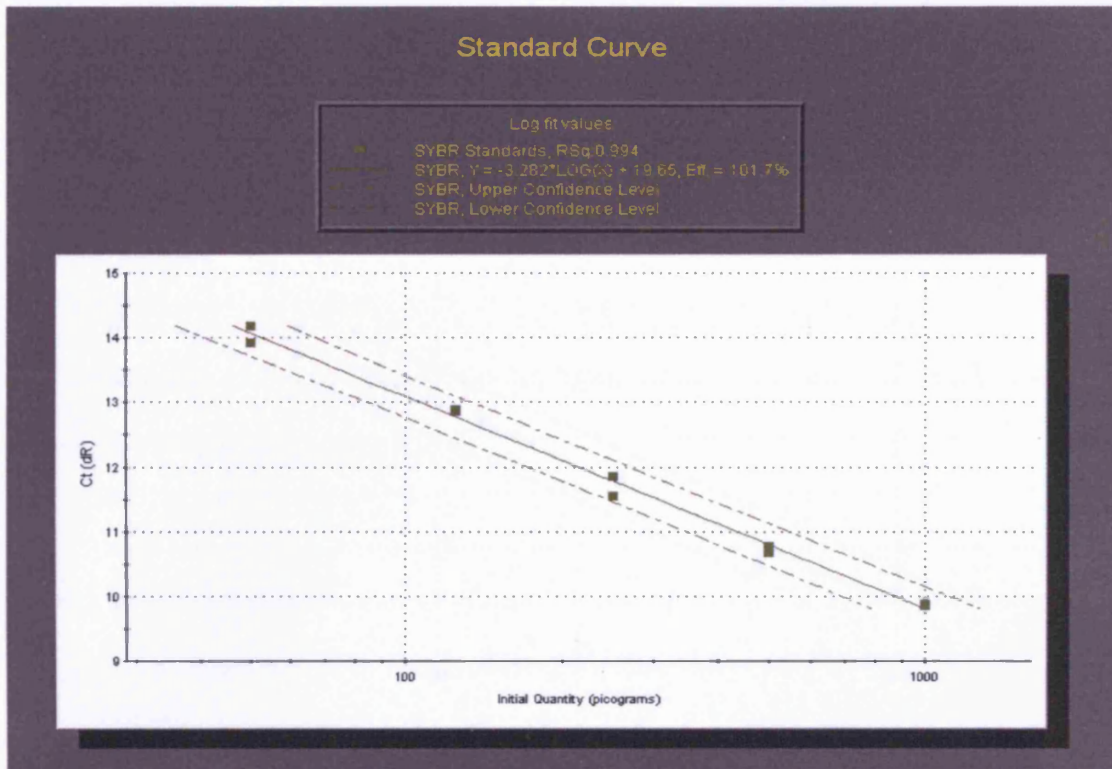


Figure 3.29: Efficiency of MS4A6 polymorphism QPCR reaction

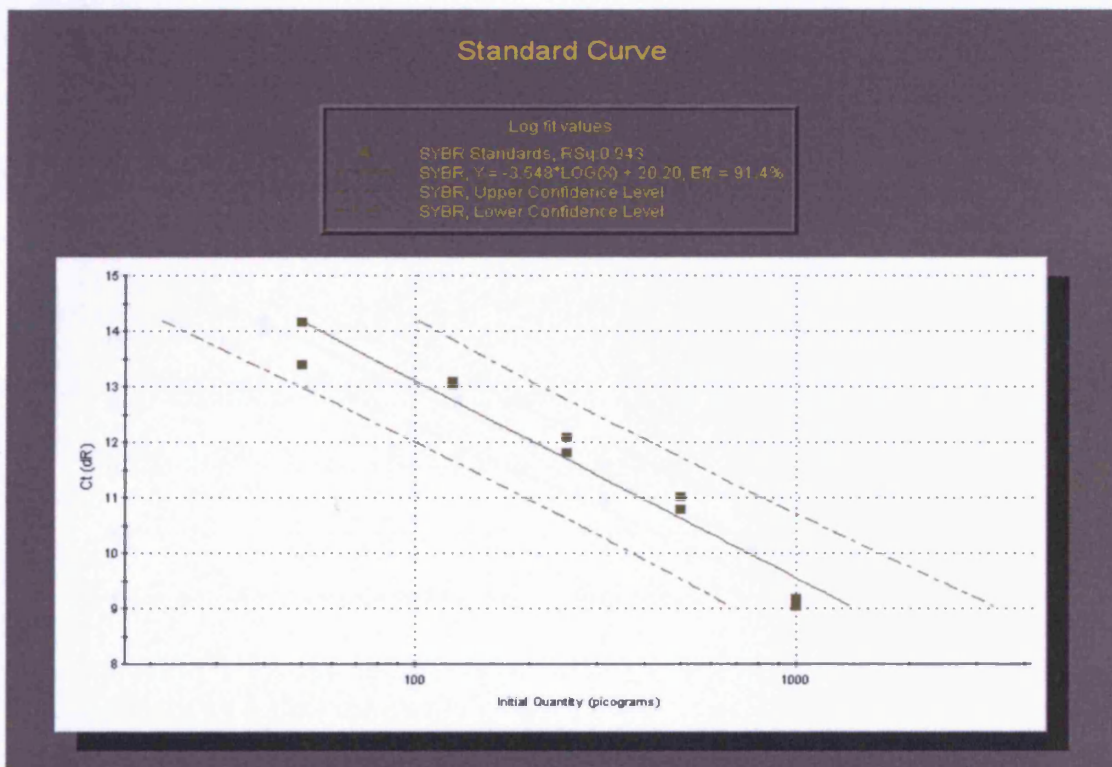


Figure 3.30: Efficiency of MS4A6 novel variant QPCR reaction

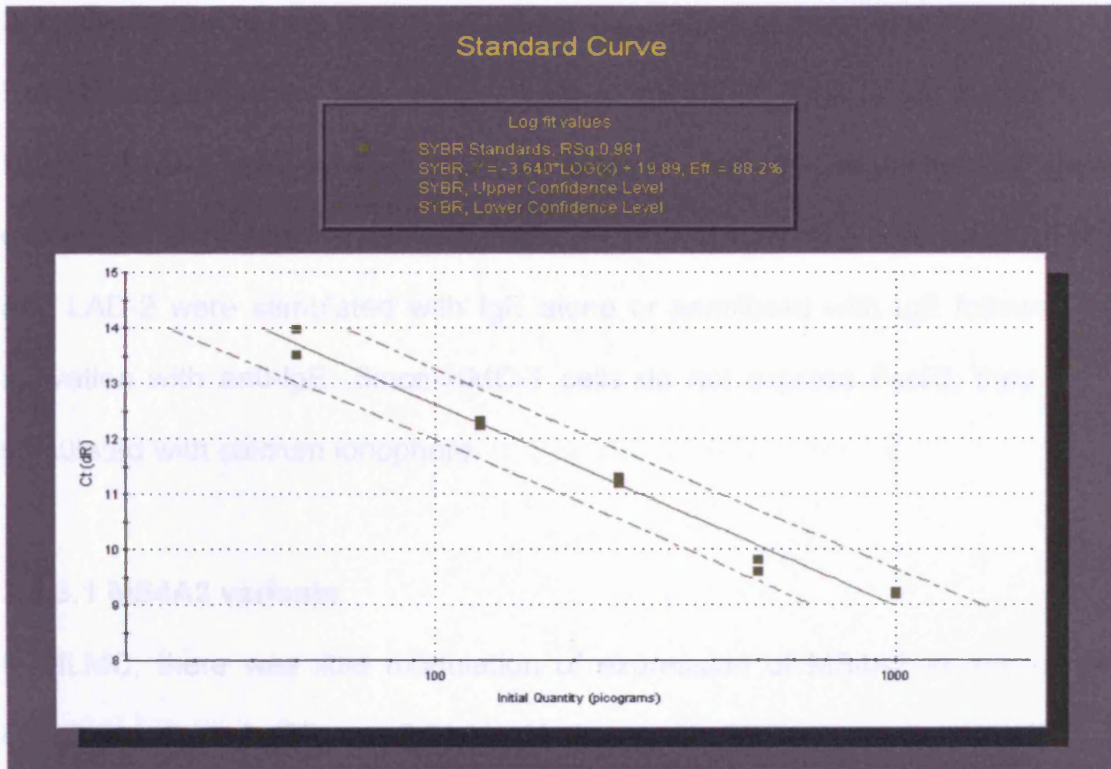


Figure 3.31: Efficiency of MS4A7 short variant QPCR reaction

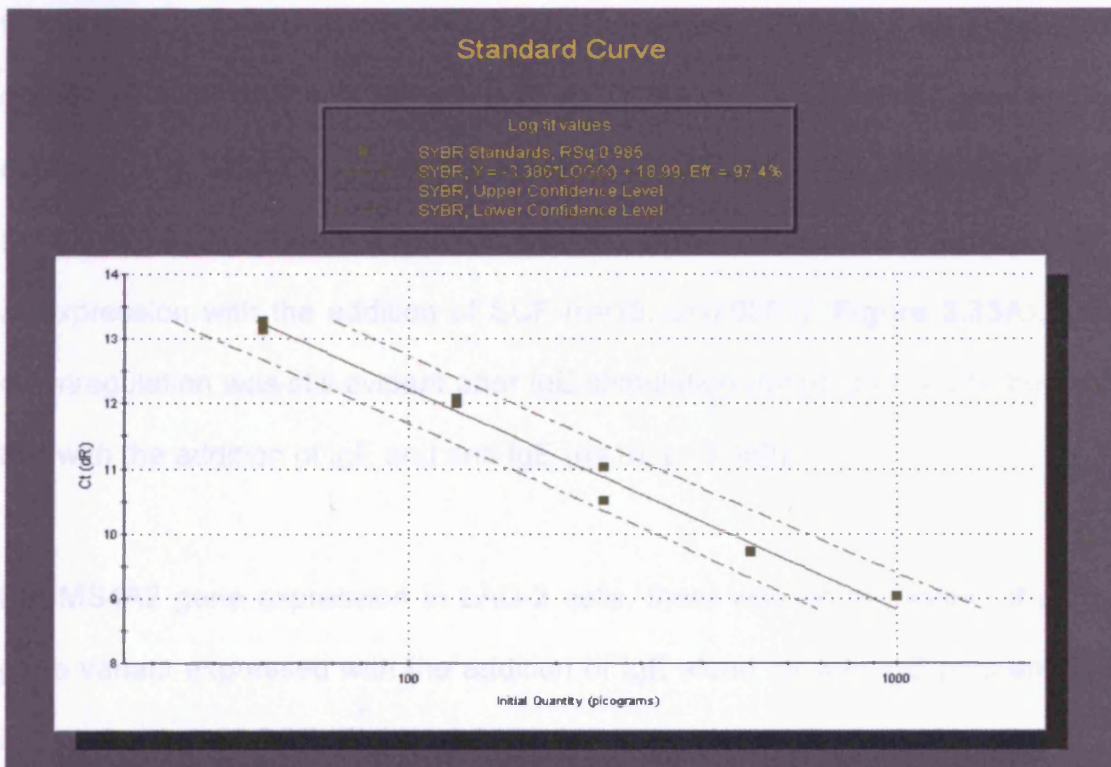


Figure 3.32: Efficiency of MS4A7 long variant QPCR reaction

3.3.3 Quantitative real time RT-PCR for regulation of gene expression

Having established the expression profile of the MS4A gene family members in HLMC, LAD-2 and HMC-1 cells, I next studied the regulation of gene expression using the standard dogmatic method of activating mast cells. HLMC and LAD-2 were stimulated with IgE alone or sensitised with IgE followed by activation with anti-IgE. Since HMC-1 cells do not express FcεRI, they were stimulated with calcium ionophore.

3.3.3.1 MS4A2 variants

In HLMC, there was little modulation of expression of MS4A2 in any of the conditions tested (**Figure 3.33A**). However, there was a very small, but significant decrease in expression of MS4A2 with the addition of SCF compared to the no SCF control (n=10, p=0.0158). Conversely, MS4A2_{trunc} was regulated greatly by SCF and anti-IgE stimulation. There was a significant increase in expression of MS4A2_{trunc} with the addition of anti-IgE in the absence of SCF (n=10, p=0.0469) (**Figure 3.33A**). In addition, there was marked downregulation of expression with the addition of SCF (n=10, p<0.0001) (**Figure 3.33A**). This downregulation was still evident after IgE stimulation (n=10, p<0.0001), but was lost with the addition of IgE and anti-IgE (n=10, p=0.360).

For MS4A2 gene expression in LAD-2 cells, there was no regulation of either gene variant expressed with the addition of IgE alone, or with IgE plus anti-IgE in the absence of SCF (**Figure 3.33B**). However, the addition of 100ng/ml SCF induced modest downregulation of MS4A2 (n=7, p<0.0001) and marked downregulation of MS4A2_{trunc} (n=7, p<0.0001) (**Figure 3.33B**). This

downregulation of gene expression with the addition of SCF was inhibited by activating the cells with both IgE alone, and with IgE plus anti-IgE (**Figure 3.33B**).

Since HMC-1 cells do not express MS4A2_{trunc}, there was only regulation of MS4A2 in these cells. Activation of the cells using calcium ionophore induced a trend suggesting upregulation, but this did not reach significance (n=6, p=0.190) (**Figure 3.33C**).

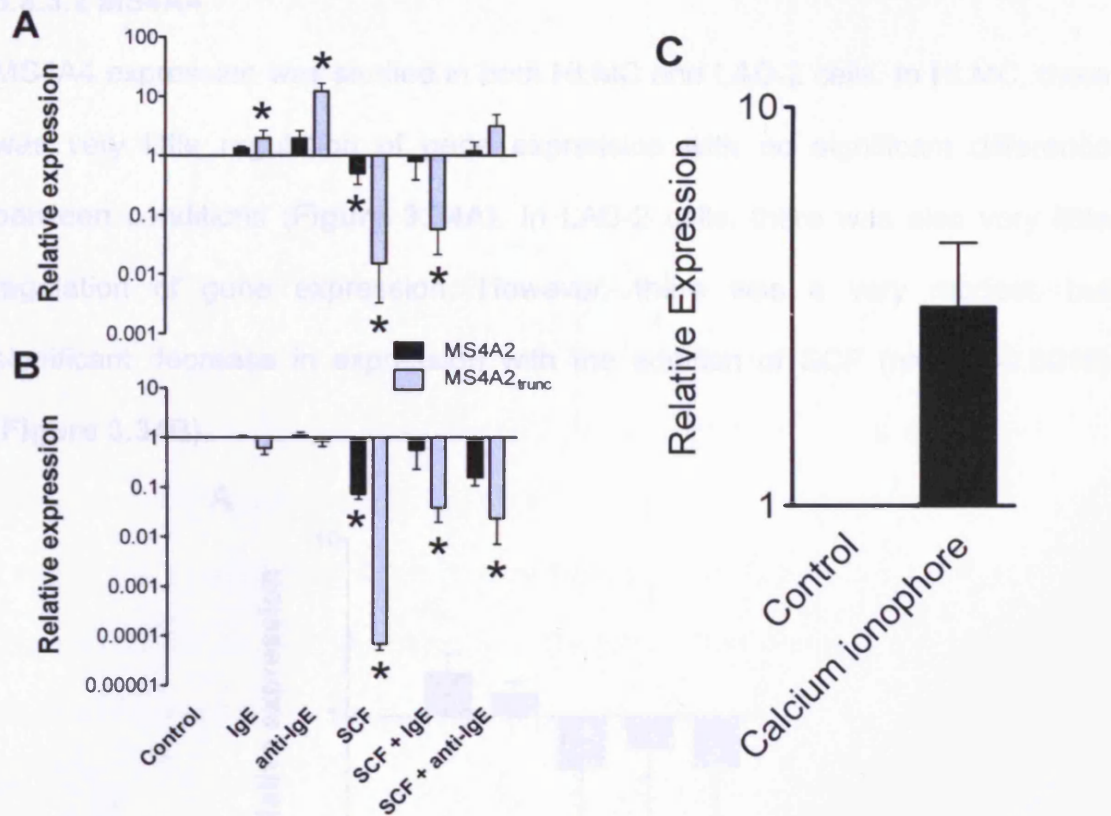


Figure 3.33: SCF down-regulates the expression of MS4A2_{trunc}.

A) Quantitative real-time RT-PCR of MS4A2 and MS4A2_{trunc} expression in HLMC cells. MS4A2_{trunc} was upregulated with both IgE and IgE/anti-IgE stimulation in the absence of SCF in HLMC. This upregulation by IgE and IgE/anti-IgE was still evident in the presence of SCF when compared to the non-stimulated cells. However, the expression was profoundly down-regulated with the addition of SCF. Data presented as the mean \pm SEM of 10 experiments from 5 separate donors. **B)** In LAD-2 cells, there was little regulation of either MS4A2 or MS4A2_{trunc} by IgE and IgE/anti-IgE in the absence of SCF. In keeping with HLMC, the addition of SCF profoundly down-regulated the expression of MS4A2_{trunc} in LAD-2 cells. Data is the mean \pm SEM from 7 experiments. **C)** In HMC-1 cells, there was a trend for the upregulation of MS4A2 with calcium ionophore stimulation but this did not reach significance. Data is the mean \pm SEM from 6 experiments. * $p < 0.05$.

3.3.3.2 MS4A4

MS4A4 expression was studied in both HLMC and LAD-2 cells. In HLMC, there was very little regulation of gene expression with no significant difference between conditions (Figure 3.34A). In LAD-2 cells, there was also very little regulation of gene expression. However, there was a very modest, but significant decrease in expression with the addition of SCF (n=7, p=0.0018) (Figure 3.34B).

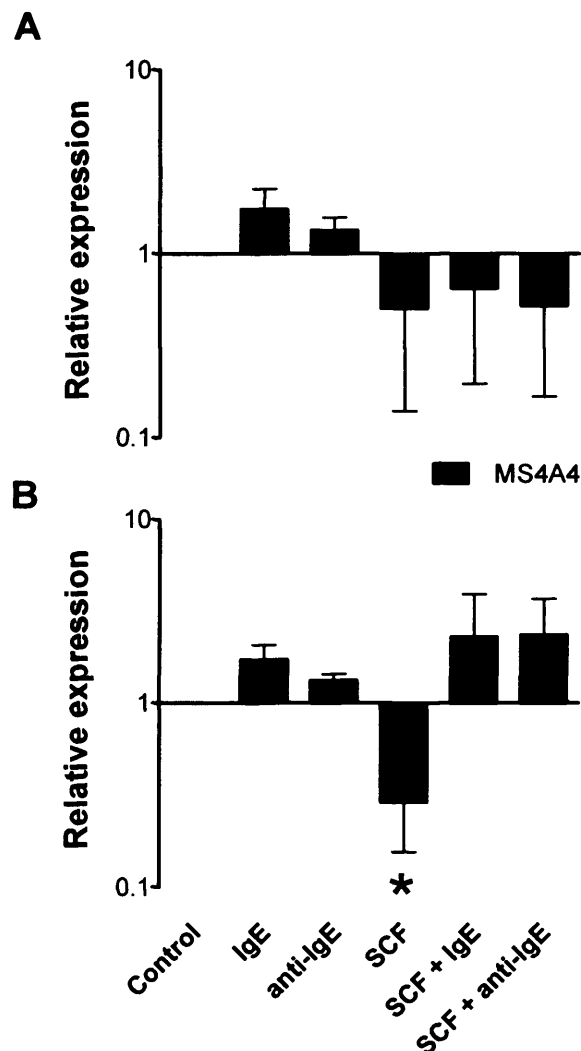


Figure 3.34: Regulation of expression of MS4A4 variant 1.

A) Quantitative real-time RT-PCR of MS4A4 expression in HLMC cells. **B)** Quantitative real-time RT-PCR of MS4A4 expression in LAD-2 cells. * p<0.05.

3.3.3.3 MS4A6 variants

MS4A6 variant expression varied between the cell types. MS4A6 variant 1 and the truncated polymorphism of MS4A6 were expressed in all of the mast cells examined. However, the novel variant of MS4A6 was only reliably expressed in the LAD-2 cells. HLMC do not express the novel variant of MS4A6. The HMC-1 cells do express the novel variant of MS4A6 as shown earlier (**Figure 3.16**). However, the melting curve for the QRT-PCR in HMC-1 cells had a wide peak which was not the exact predicted melting temperature of the product. Although running the products on a gel demonstrated expression, the quantification of this expression should be treated with caution as there must have been some degree of non-specific priming occurring in the reaction.

In the HLMC, there was good and consistent expression of MS4A6 variant 1 in all donors used for QRT-PCR. In some donors there was roughly equal expression of MS4A6 polymorphism at baseline. However, in other donors the expression of the polymorphism was very low. In almost all donors, IgE-dependent activation of the cells induced upregulation of MS4A6 variant 1 expression particularly with anti-IgE activated cells ($n=10$, $p=0.0404$) (**Figure 3.35A**). There was marked downregulation of gene expression with the addition of SCF ($n=10$, $p<0.0001$ for each). MS4A6 polymorphism expression was downregulated with the addition of SCF in the majority of donors. However, one donor in particular showed marked upregulation with the addition of SCF which increased with activation. Therefore, due to the variability in regulation, there was no significant difference in expression between any of the conditions. However, cross-reactivity with other MS4A6 gene family members cannot be

entirely ruled out since there are several other variants of MS4A6 which may be expressed in mast cells. There were several bands present in the LAD-2 cells after cloning MS4A6 and it is very likely that other MS4A6 variants were there which were not cloned. It will therefore be difficult to delineate the role of each splice variant in mast cell function. Furthermore, in LAD-2 cells there appears to be differential regulation of expression for each of the variants detected (**Figure 3.35B**). However, these data are difficult to interpret without knowing the function of each gene product. Although it does appear that SCF may be a key determinant of gene function as gene regulation was much more marked in the presence of SCF.

In HMC-1 cells there was upregulation of all of the expressed variants of MS4A6 with activation with calcium ionophore. Thus with the addition of 5 μ M calcium ionophore MS4A6 variant 1, MS4A6 polymorphism and MS4A6 novel were upregulated by 52.2 ± 3.6 , 20.1 ± 3.2 and 3.2 ± 0.2 fold, respectively, compared to the calibrator ($n=3$, $p=0.0098$, 0.0493 and 0.0119 respectively) (**Figure 3.35C**).

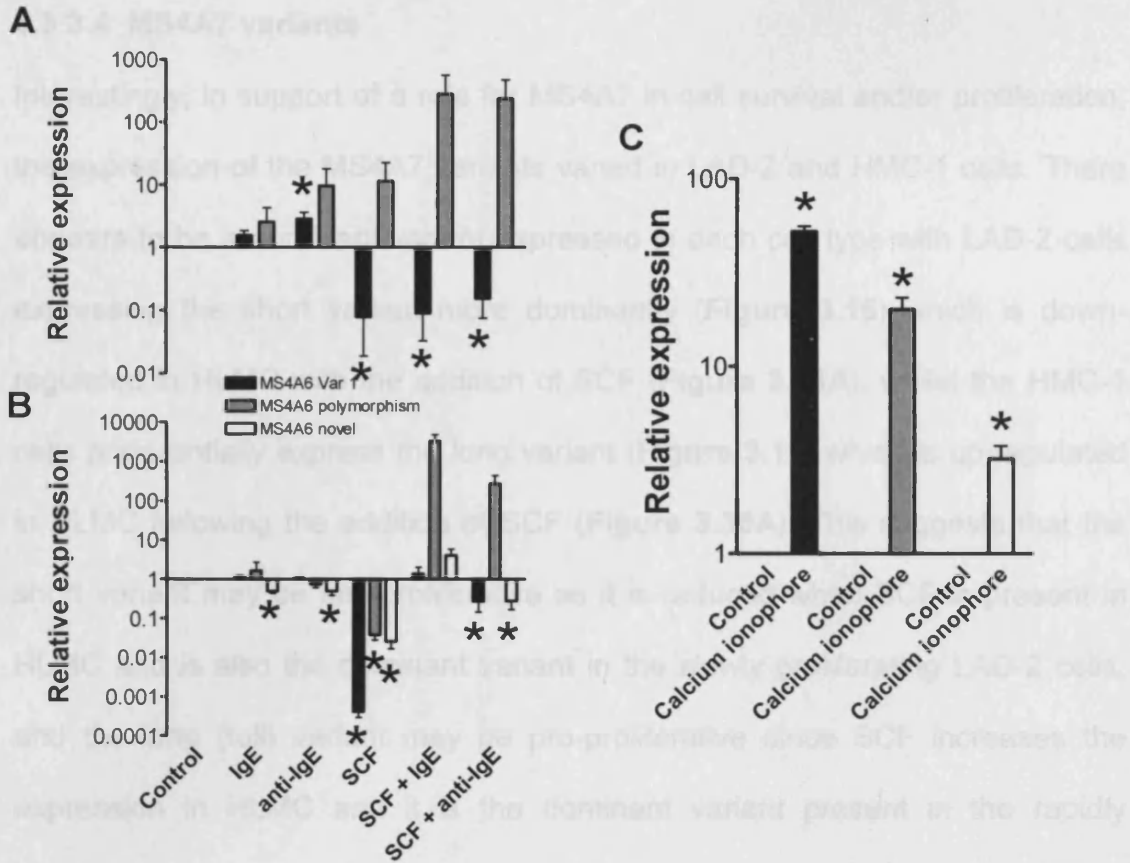


Figure 3.35: Regulation of MS4A6 gene variants in mast cells.

A) Regulation of MS4A6 variants expressed in HLMC. Activation with anti-IgE induces the upregulation of MS4A6 variant 1. SCF markedly downregulates expression of MS4A6 variant 1. MS4A6 polymorphism was too variably expressed in HLMC to achieve statistically significant data. **B)** In LAD-2 cells there was significant downregulation of each MS4A6 variant with the addition of SCF. SCF also induced a greater reactivity to IgE and IgE/anti-IgE, particularly for MS4A6 polymorphism. However, this was accompanied by a greater degree of variability which resulted in the data not reaching significance. **C)** In HMC-1 cells all of the expressed MS4A6 variants were upregulated with the addition of calcium ionophore. * $p < 0.05$.

3.3.3.4 MS4A7 variants

Interestingly, in support of a role for MS4A7 in cell survival and/or proliferation, the expression of the MS4A7 variants varied in LAD-2 and HMC-1 cells. There appears to be a dominant variant expressed in each cell type with LAD-2 cells expressing the short variant more dominantly (**Figure 3.15**) which is down-regulated in HLMC with the addition of SCF (**Figure 3.36A**), whilst the HMC-1 cells preferentially express the long variant (**Figure 3.16**) which is up-regulated in HLMC following the addition of SCF (**Figure 3.36A**). This suggests that the short variant may be anti-proliferative as it is reduced when SCF is present in HLMC and is also the dominant variant in the slowly proliferating LAD-2 cells, and the long (full) variant may be pro-proliferative since SCF increases the expression in HLMC and it is the dominant variant present in the rapidly proliferating HMC-1 cells.

However, the role of MS4A7 variants in cell proliferation may not be as clear as these data suggest. In LAD-2 cells, there is still opposing regulation with SCF. Thus with the addition of SCF, the expression of the short variant of MS4A7 increases and the expression of the long variant decreases (**Figure 3.36B**). This is the reverse of that seen in HLMC. Both variants were also consistently expressed in LAD-2 cells, whereas in the HLMC there was often no expression of the long variant of MS4A7. Therefore, the role of these gene variants in proliferation will need to be further explored.

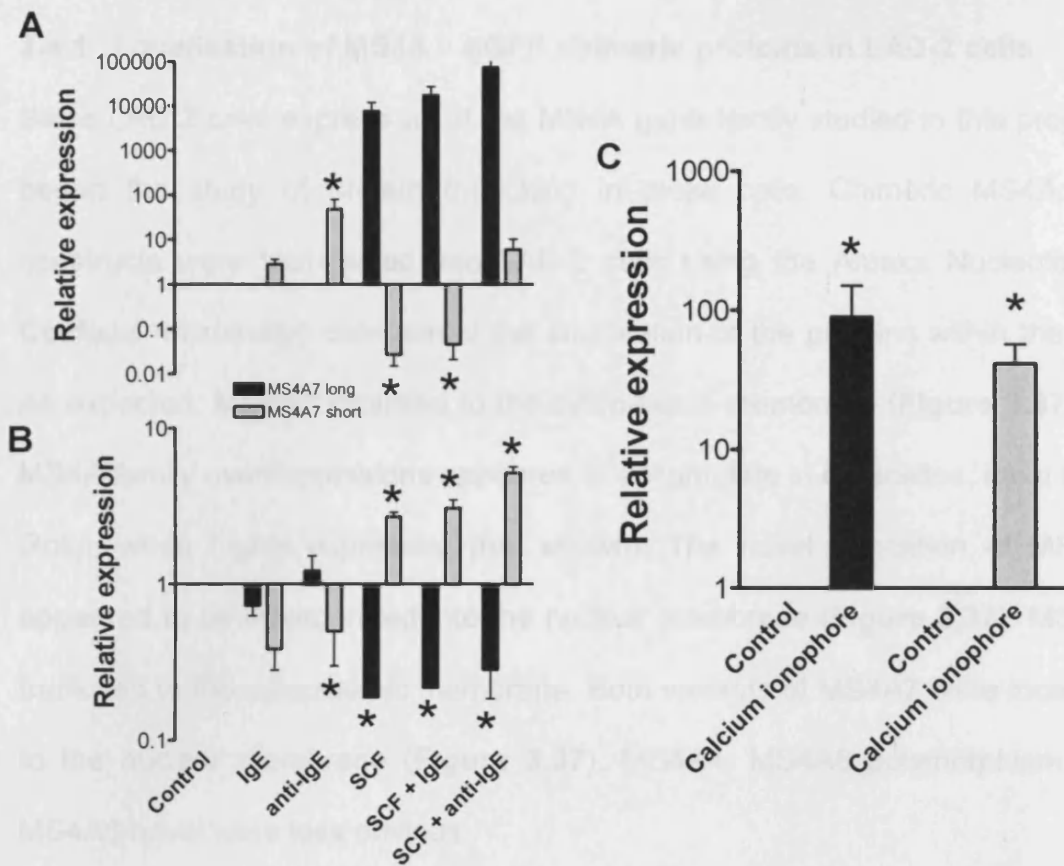


Figure 3.36: Regulation of MS4A7 gene variants in mast cells.

A) Regulation of MS4A7 variants in HLMC. The short variant of MS4A7 was consistently expressed in all donors and was significantly downregulated with the addition of SCF. The long variant of MS4A7 was rarely expressed. However, the addition of SCF occasionally induced expression. Therefore, the relative expression was huge when compared to no expression and as a result of the variability, did not reach significance. **B)** The expression of both MS4A7 variants was always observed with the LAD-2 and HMC-1 (**C**) cells. However, the regulation of expression in the LAD-2 cells was the opposite of that observed in HLMC. Thus SCF reduced the expression of the long variant of MS4A7 and increased the expression of the short variant. **C)** Both of the expressed MS4A7 variants were upregulated with the addition of 5 μ M calcium ionophore in HMC-1 cells. * $p < 0.05$.

3.4 PROTEIN TRAFFICKING AND SUB-CELLULAR LOCALISATION

3.4.1 Localisation of MS4A – eGFP chimeric proteins in LAD-2 cells

Since LAD-2 cells express all of the MS4A gene family studied in this project I began the study of protein trafficking in these cells. Chimeric MS4A:GFP constructs were transfected into LAD-2 cells using the Amaxa Nucleofector. Confocal microscopy determined the localisation of the proteins within the cell. As expected, MS4A2 localised to the cytoplasmic membrane (**Figure 3.37**). All MS4A family overexpressions appeared to accumulate in organelles, most likely Golgi, when highly expressed (not shown). The novel truncation of MS4A2 appeared to be incorporated into the nuclear membrane (**Figure 3.37**). MS4A6 trafficked to the cytoplasmic membrane. Both variants of MS4A7 were localised to the nuclear membrane (**Figure 3.37**). MS4A4, MS4A6 polymorphism and MS4A6 novel were less obvious.

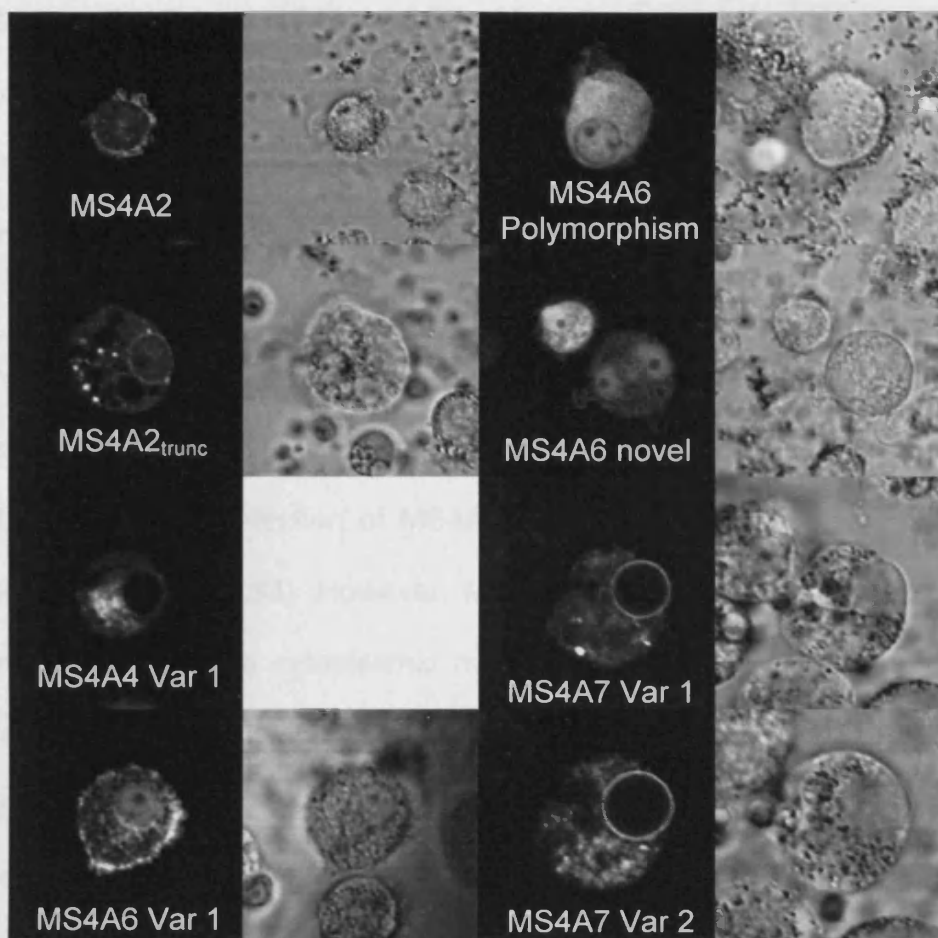


Figure 3.37: MS4A family localisation in LAD-2 cells using nucleofection.

Most of the MS4A family trafficked to membranes. MS4A2 was clearly associated with the cytoplasmic membrane. MS4A2_{trunc} seemed to accumulate in intracellular granules, most likely for storage of excess protein, but was also associated with the nuclear membrane. MS4A4 always demonstrated strong staining of what was most likely the Golgi apparatus, but also seemed to associate with the nuclear membrane. MS4A6 Var 1 had a staining pattern which seemed to show intracellular structural staining, as well as strong cytoplasmic membrane staining. MS4A6 polymorphism stained strongly everywhere in the cell except for nucleoli. MS4A6 novel had intranuclear staining which was excluded from nucleoli. Both variants of MS4A7 had very similar staining to MS4A2_{trunc}, in that there was nuclear membrane staining as well as storage of excess protein in granular structures.

3.4.2 Localisation of MS4A – eGFP chimeric proteins in HMC-1 cells

In order to confirm the trafficking data from the LAD-2 cells, confocal microscopy was performed on HMC-1 cells transfected with GFP tagged MS4A family transfected with FuGENE HD. The nucleofection was harsh on the LAD-2 cells and cell viability was greatly affected by the process. Thus the less harsh method of transfection, lipofection, was used for HMC-1 cells since modest transfection efficiency (~20%) was possible with these cells. In agreement with the LAD-2 cells, transfection of MS4A2 demonstrated cytoplasmic membrane localisation (**Figure 3.38**). However, MS4A2 is known to chaperone the alpha chain of FcεRI to the cytoplasmic membrane ⁽²⁰⁹⁾, but HMC-1 cells do not express the alpha chain of FcεRI ⁽²¹⁰⁾ which means that MS4A2 does not require the alpha chain to be expressed at the cell surface. MS4A2_{trunc} still demonstrated nuclear membrane localisation (**Figure 3.38**). MS4A4 was trafficked to the cytoplasmic membrane (**Figure 3.38**) which was not evident in the LAD-2 cells (**Figure 3.37**). However, the nucleofection of the MS4A4 variant into LAD-2 cells negatively affected cell viability in these conditions and viable MS4A4 transfected LAD-2 cells were scarce. This was not due to the MS4A4 protein as all other methods of transfection/transduction with MS4A4 have failed to show any cytotoxicity. MS4A6 variants show different localisation as MS4A6 var 1 was evident in the cytoplasmic membrane, whereas the other 2 variants studied seemed to be ubiquitous throughout the cell (**Figure 3.38**). In agreement with the LAD-2 cells, both MS4A7 variants were localised to the nuclear membrane (**Figure 3.38**).

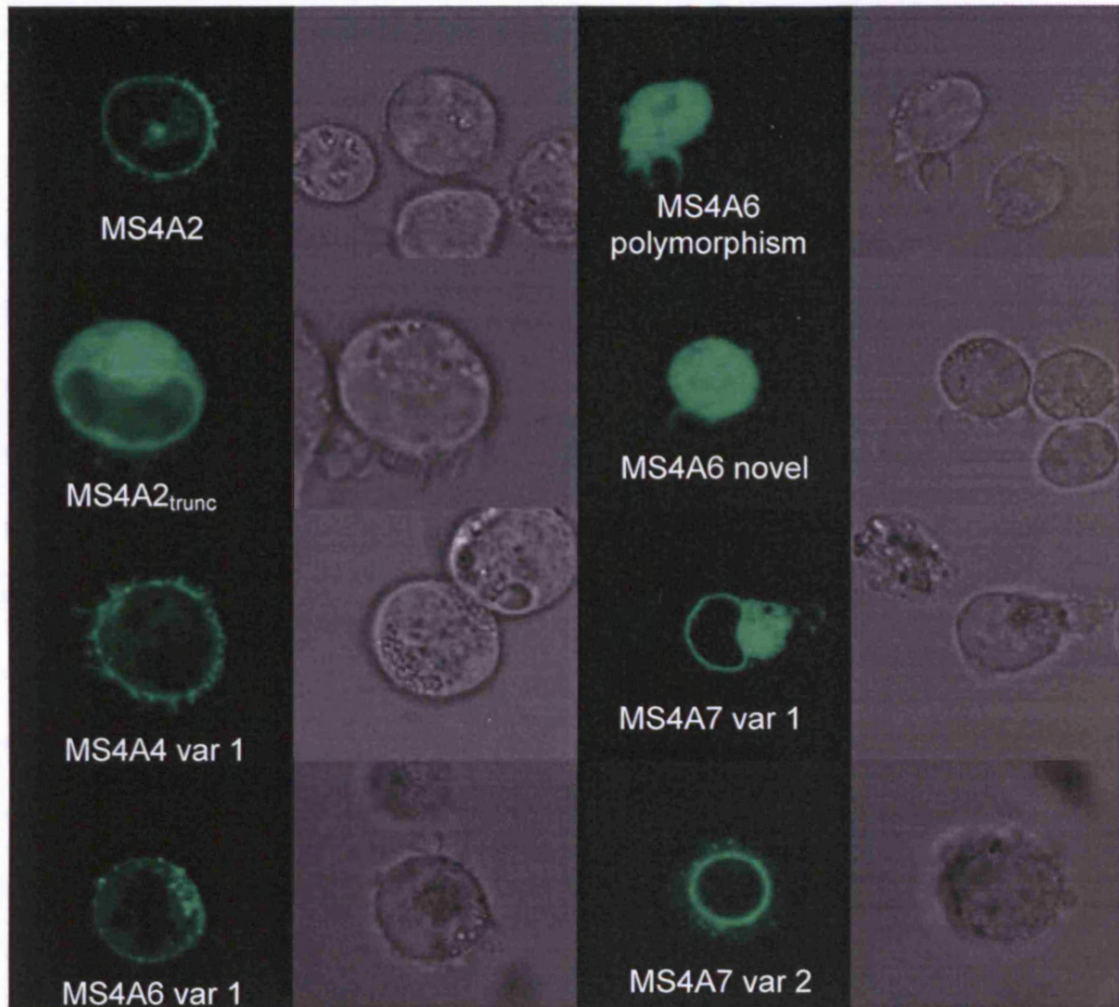


Figure 3.38: MS4A family localisation in HMC-1 cells using lipofection.

These confocal micrographs demonstrate that MS4A2, MS4A4 var 1 and MS4A6 var 1 traffic to the cytoplasmic membrane. MS4A2_{trunc}, and both variants of MS4A7 traffic to the nuclear membrane. Whilst there is cytoplasmic staining of MS4A2_{trunc}, there is clearly nuclear membrane staining. However, MS4A6 polymorphism and MS4A6 novel do not appear to be trafficked to any particular location under these conditions.

3.5 MS4A ELECTROPHYSIOLOGY

3.5.1 Electrophysiology of baseline currents in transfected CHO cells

In order to determine whether any of the MS4A variants formed distinct ion channels which constitutively conducted ions, I first transfected GFP tagged MS4A cDNA into CHO cells using Fugene HD reagent. Using UV light I was able to identify and patch fluorescent cells. CHO cells were electrically quiet at rest (**Figure 3.39**). Transfection of CHO cells with the empty GFP vector (pEGFPN1) and MS4A2 had no effect on the baseline currents. However, transfection with the truncated MS4A2 induced a larger baseline current. This current had similar characteristics to the control cells but was larger in magnitude. Similarly, transfection with MS4A4 variant 1 had a similar effect (**Figure 3.39**). Transfection with MS4A6 variant 1 did not induce a larger current at baseline. However, there were occasional cells which displayed a very small $K_{Ca3.1}$ -like current.

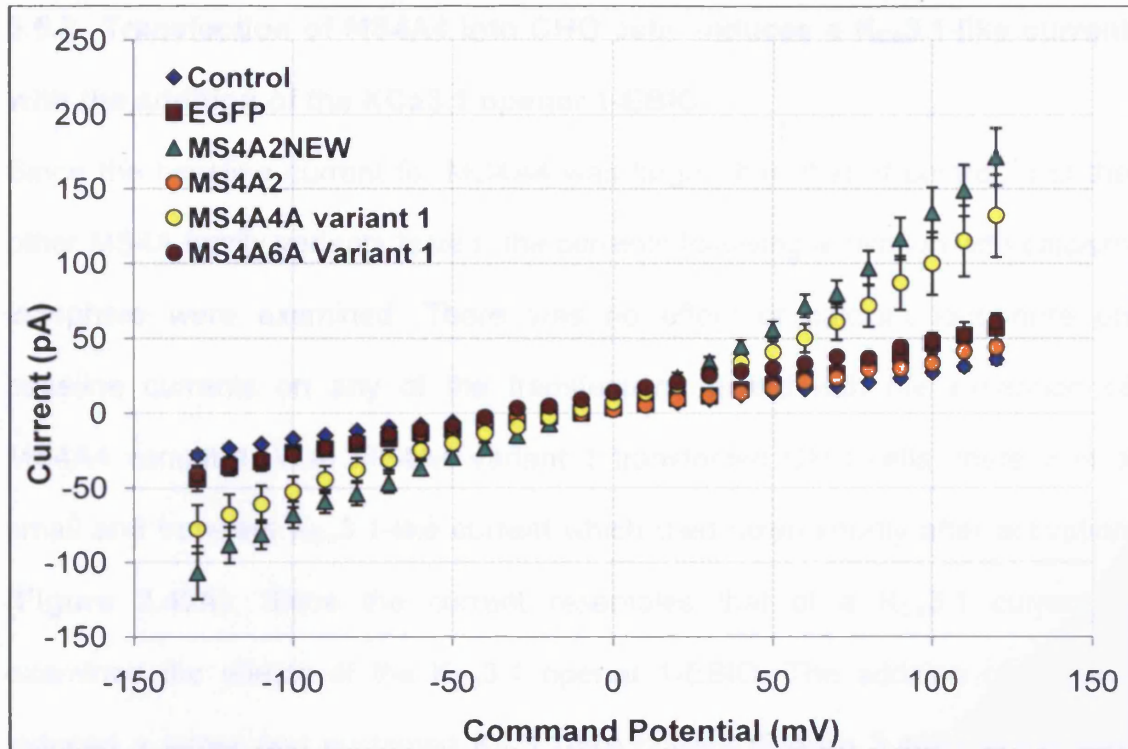


Figure 3.39: Effects of MS4A gene family transfection on baseline currents in CHO cells.

CHO cells exhibit a quiet baseline current (blue diamonds). This current was unaffected by transfection with the empty pEGFPN1 vector (brown squares). Similarly, transfection with MS4A2 had no effect of baseline current (orange circles). However, transfection of truncated MS4A2 significantly increased the magnitude of current (green triangles). A significant increase in baseline current was also evident in MS4A4 variant 1 transfected cells (yellow circles). Interestingly, there was occasional and very small shifts in current in MS4A6 variant 1 transfected cells which resembles a tiny K⁺ current (brown circles).

3.5.2 Transfection of MS4A4 into CHO cells induces a $K_{Ca3.1}$ -like current with the addition of the $K_{Ca3.1}$ opener 1-EBIO

Since the baseline current for MS4A4 was larger than that of control, and the other MS4A family variants tested, the currents following activation with calcium ionophore were examined. There was no effect of calcium ionophore on baseline currents on any of the transfections tested with the exception of MS4A4 variant 1. With MS4A4 variant 1 transfected CHO cells, there was a small and transient $K_{Ca3.1}$ -like current which died down shortly after activation (**Figure 3.40A**). Since the current resembles that of a $K_{Ca3.1}$ current, I examined the effects of the $K_{Ca3.1}$ opener 1-EBIO. The addition of 1-EBIO induced a larger and sustained $K_{Ca3.1}$ -like current (**Figure 3.40B**) which was not evident in controls. The reversal potential of the current was not as negative as would be expected for a pure K^+ current. Therefore, the presence of sodium was explored using NMDG perfusion. Perfusion of NMDG decreased the reversal potential from -45 to -70 mV which is closer to that expected from a pure K^+ current (**Figure 3.40C**) (pure K^+ has a reversal of -70 to -80 mV). This is suggestive of a sodium component to the current. However, this data should be treated as preliminary since further characterisation of these currents is required. This characterisation of currents is beyond the scope of this study as it requires in-depth electrophysiology.

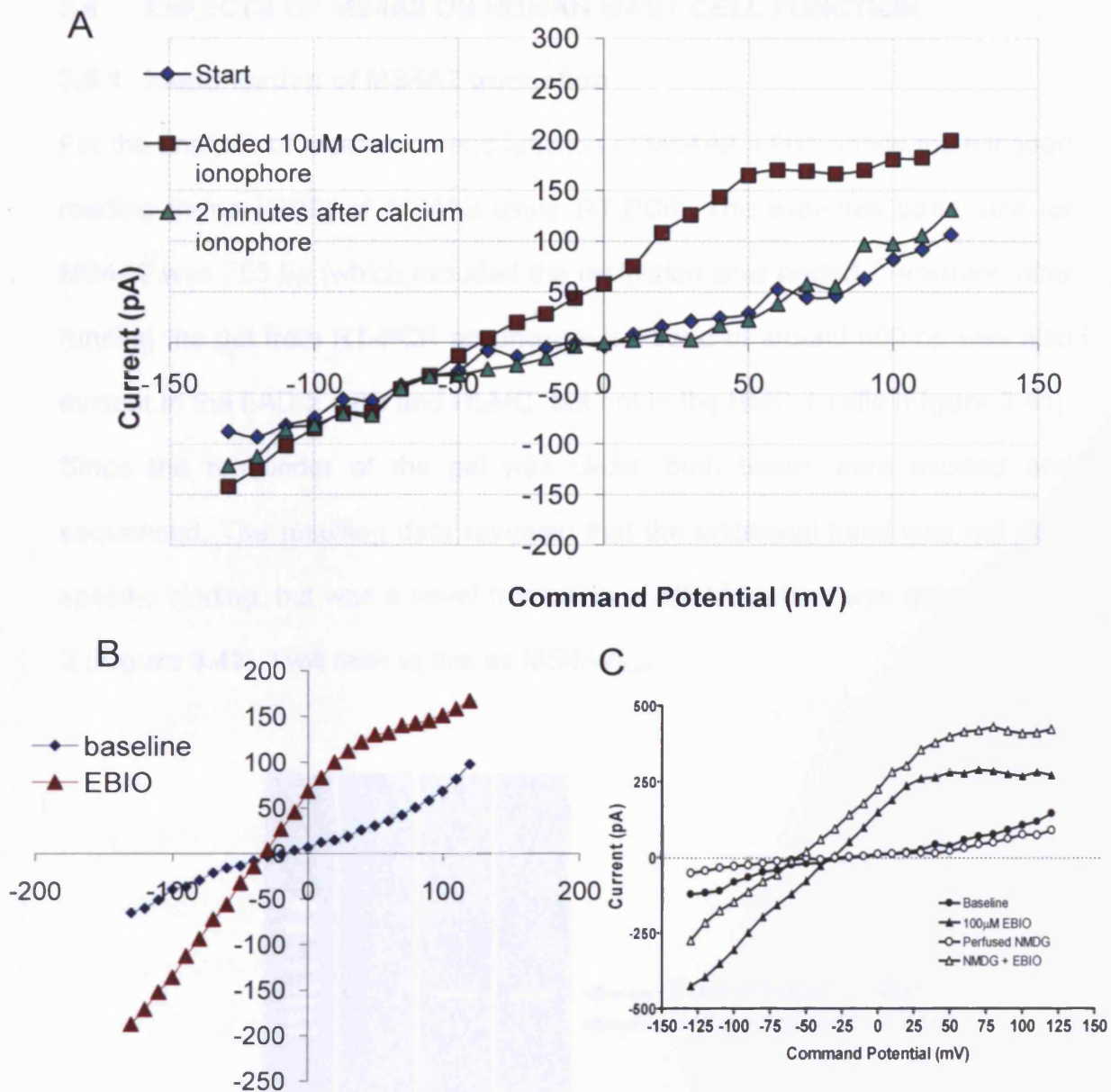


Figure 3.40: The $K_{Ca}3.1$ opener 1-EBIO induces a $K_{Ca}3.1$ -like current in CHO cells after transfection with MS4A4 variant 1.

A) The addition of 10 μ M calcium ionophore induced a transient $K_{Ca}3.1$ -like current in CHO cells transfected with MS4A4 variant 1. **B)** After transfection with MS4A4 variant 1, the addition of 100 μ M 1-EBIO induces a sustained $K_{Ca}3.1$ current. This current was not evident in untransfected cells, or in GFP control transfected cells. Data is the mean current from 18 cells. **C)** Perfusion of NMDG into the chamber caused a shift in reversal potential from -45 to -70 mV suggesting that there was a sodium component to the current.

3.6 EFFECTS OF MS4A2 ON HUMAN MAST CELL FUNCTION

3.6.1 Identification of MS4A2 truncation

For the analysis of expression and function of MS4A2, I first cloned the full open reading frame (ORF) of MS4A2 using RT-PCR. The expected band size for MS4A2 was 753 bp (which included the restriction sites added). However, after running the gel from RT-PCR an unexpected band of around 600 bp was also evident in the LAD-2 cells and HLMC, but not in the HMC-1 cells (**Figure 3.41**). Since the remainder of the gel was clean, both bands were excised and sequenced. The resulting data revealed that the additional band was not non-specific binding, but was a novel truncation of MS4A2 which was missing exon 3 (**Figure 3.42**). I will refer to this as MS4A2_{trunc}.

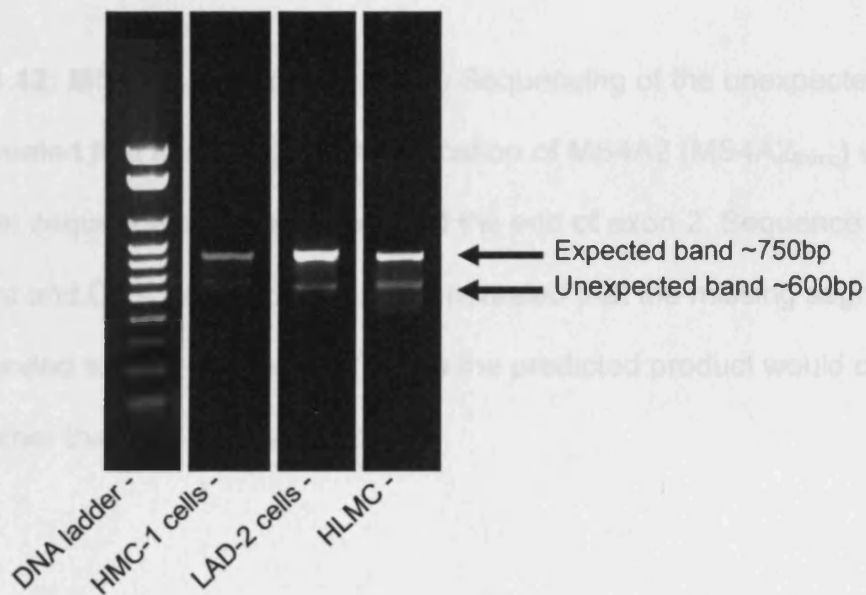


Figure 3.41: Human mast cells express a novel truncation of MS4A2. RT-PCR cloning of MS4A2 from HMC-1 cells, LAD-2 cells and HLMC. 2 bands were present in the LAD-2 cells and HLMC, but not in the HMC-1 cells.

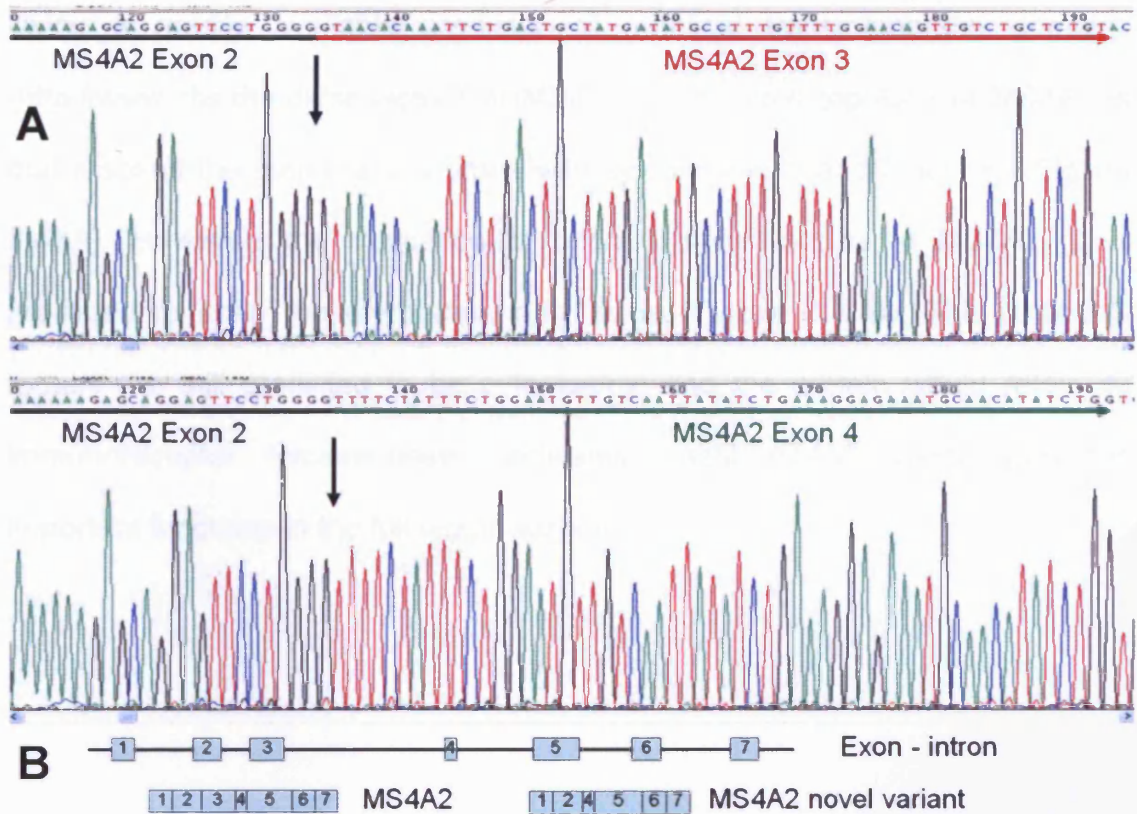


Figure 3.42: MS4A2_{trunc} sequencing **A)** Sequencing of the unexpected smaller band revealed that this was a novel truncation of MS4A2 (MS4A2_{trunc}) which differed in sequence at the exact point at the end of exon 2. Sequence alignment and DNA sequence searches revealed that the missing segment corresponded exactly to exon 3. **B)** Thus the predicted product would contain 6 exons rather than the 7 for MS4A2.

Using a readily available predictor of α -helical transmembrane domains (<http://www.cbs.dtu.dk/services/TMHMM/>), the predicted topology of MS4A2 is that it spans the membrane 4 times with cytoplasmic N and C termini (**Figure 3.43A**). However, the truncation of exon 3 which occurs in MS4A2_{trunc} is predicted to span the membrane only twice (**Figure 3.43B**). The N and C termini are still predicted to be cytoplasmic and the protein would retain its immunoreceptor tyrosine-based activation motif (ITAM) which performs important functions in the full length variant.

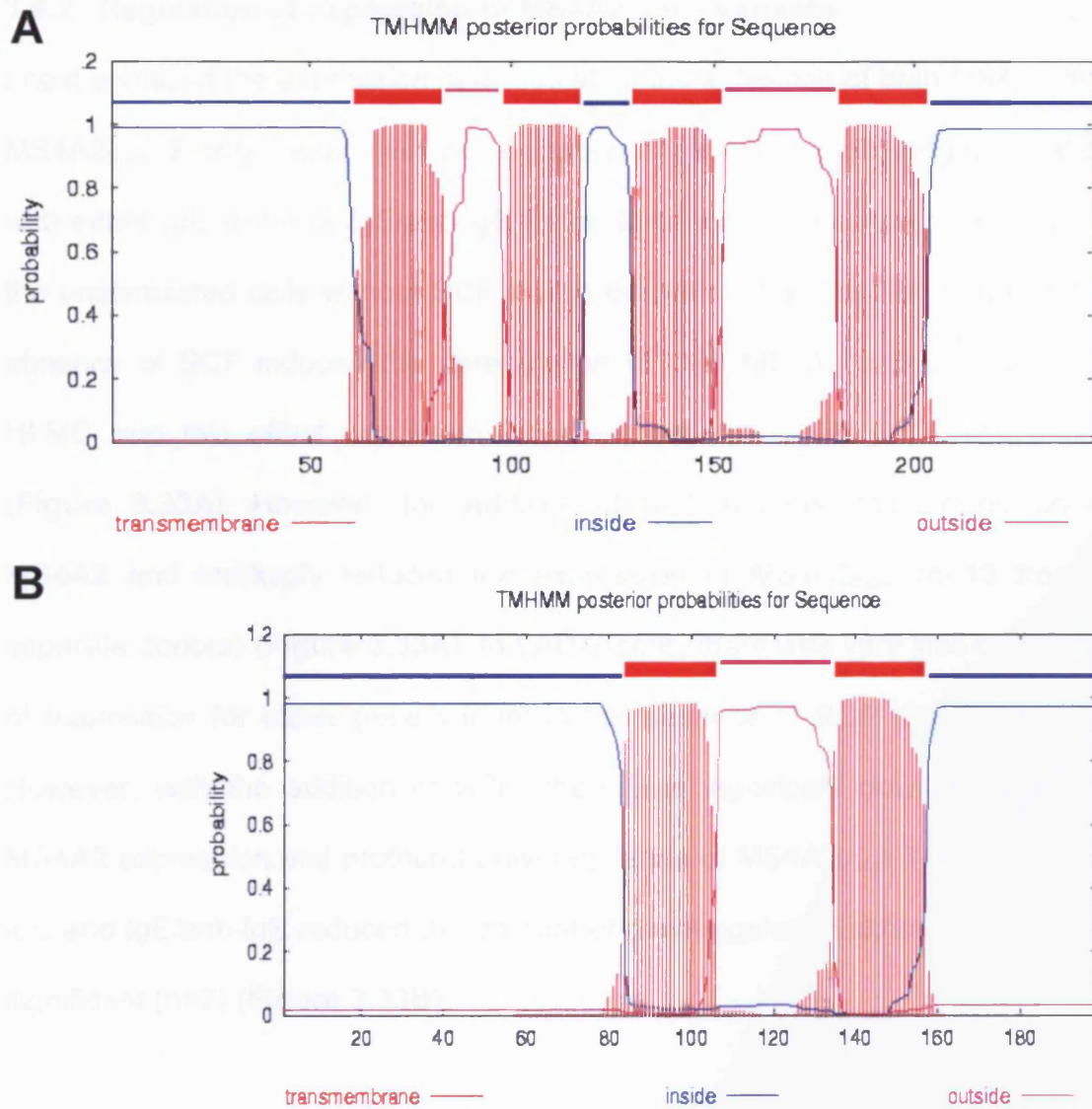


Figure 3.43: Transmembrane domain predictions A) The predicted amino acid sequence of MS4A2 spans the membrane four times. B) The predicted sequence of MS4A2_{trunc} loses the first 2 transmembrane regions spanning the membrane only twice.

3.6.2 Regulation of expression of MS4A2 gene variants

I next analyzed the expression and regulation of expression of both MS4A2 and MS4A2_{trunc}. Firstly, I examined the regulation of expression following stimulation with either IgE alone or IgE/anti-IgE in the absence or presence of SCF using the unstimulated cells without SCF as the calibrator. The addition of IgE in the absence of SCF induced the upregulation of both MS4A2 and MS4A2_{trunc} in HLMC and this effect was even more evident with IgE/anti-IgE stimulation (**Figure 3.33A**). However, the addition of SCF reduced the expression of MS4A2 and markedly reduced the expression of MS4A2_{trunc} (n=10 from 5 separate donors) (**Figure 3.33A**). In LAD-2 cells, there was very little regulation of expression for either gene variant in the absence of SCF (**Figure 3.33B**). However, with the addition of SCF, there was significant downregulation of MS4A2 expression and profound downregulation of MS4A2_{trunc}. The addition of IgE and IgE/anti-IgE reduced the amount of downregulation although it was still significant (n=7) (**Figure 3.33B**).

3.6.3 Transduction and overexpression of the MS4A2 variants in human mast cells

HLMC were efficiently transduced using an adenoviral delivery system ⁽²⁰⁵⁾. Thus using an MOI of 10 IU / HLHC I was able to achieve up to 100% transduction efficiency when using the eGFP control virus (**Figure 3.44A**). Thus to confirm the transduction of both MS4A2 and the MS4A2_{trunc} I first performed QPCR on transduced HLHC. HLHC transduced with both MS4A2 variants demonstrated marked upregulation of mRNA expression. Thus the relative expression of MS4A2 after transduction with cDNA was 141.6 ± 4.9 fold that of the GFP virus control (**Figure 3.44B**) (n=8, p<0.000001). The relative expression of MS4A2_{trunc} was more markedly upregulated with a relative expression of 410.3 ± 38.7 fold over the GFP virus control (**Figure 3.44B**) (n=8, p<0.000001). However, the overall level of expression for MS4A2 and MS4A2_{trunc} overexpression were similar, but since MS4A2_{trunc} expression was lower than MS4A2 at baseline, the relative expression after transduction was higher.

In order to confirm that the overexpression of MS4A2 variants was translated into MS4A2 protein, I next tested for MS4A2 variant protein expression using western blotting. I was able to demonstrate that both MS4A2 variants were overexpressed at the protein level as expected (**Figure 3.44C**).

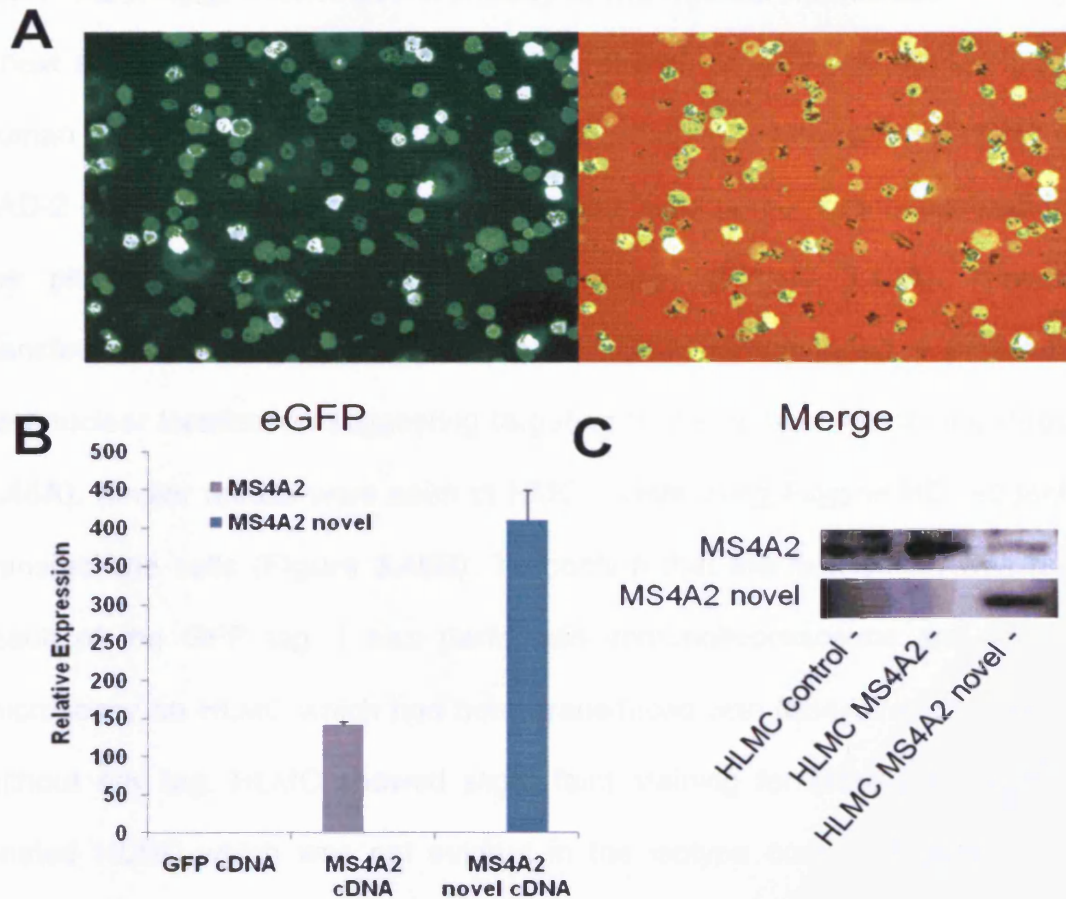


Figure 3.44: MS4A2 and MS4A2_{trunc} can be successfully transduced into human mast cells. A) The adenovirus Ad5C20Att01 efficiently transduces eGFP cDNA into primary *ex vivo* HLMC. B) Using viruses constructed to contain the full length open reading frame of MS4A2 and MS4A2_{trunc} leads to overexpression of the corresponding message for each variant assessed using quantitative real-time RT-PCR. Data is the mean \pm SEM of 8 experiments from 4 donors. C) Western blot demonstrating that transduction of the cDNA for each MS4A2 variant leads to the overexpression of the corresponding protein. Each panel is from a separate gel with different antibodies.

3.6.4 MS4A2_{trunc} traffics preferentially to the nuclear membrane

I next studied the intracellular localization of both MS4A2 and MS4A2 truncin human mast cells. As expected, transfection of chimeric GFP-MS4A2 cDNA into LAD-2 cells using nucleofection demonstrates plasma membrane localization of the protein when using confocal microscopy (**Figure 3.45A**). However, transfection of GFP- MS4A2_{trunc} chimeric cDNA demonstrated a preferential peri-nuclear localization suggesting targeting to the nuclear membrane (**Figure 3.45A**). Similar results were seen in HMC-1 cells using Fugene HD reagent to transfect the cells (**Figure 3.45B**). To confirm that the localisation was not a result of the GFP tag, I also performed immunofluorescence and confocal microscopy on HLMC which had been transduced with MS4A2 and MS4A2_{trunc} without any tag. HLMC showed slight faint staining for MS4A2 in the mock treated HLMC which was not evident in the isotype control (**Figure 3.45C**). However, the antibody worked best when used with the overexpression cells. MS4A2 overexpression did indeed increase the staining in the cytoplasmic membrane of HLMC, whilst MS4A2_{trunc} increased peri-nuclear staining (**Figure 3.45C**) confirming that the localisation of the proteins was different as a result of the truncation, and that GFP did not affect the trafficking of the proteins.

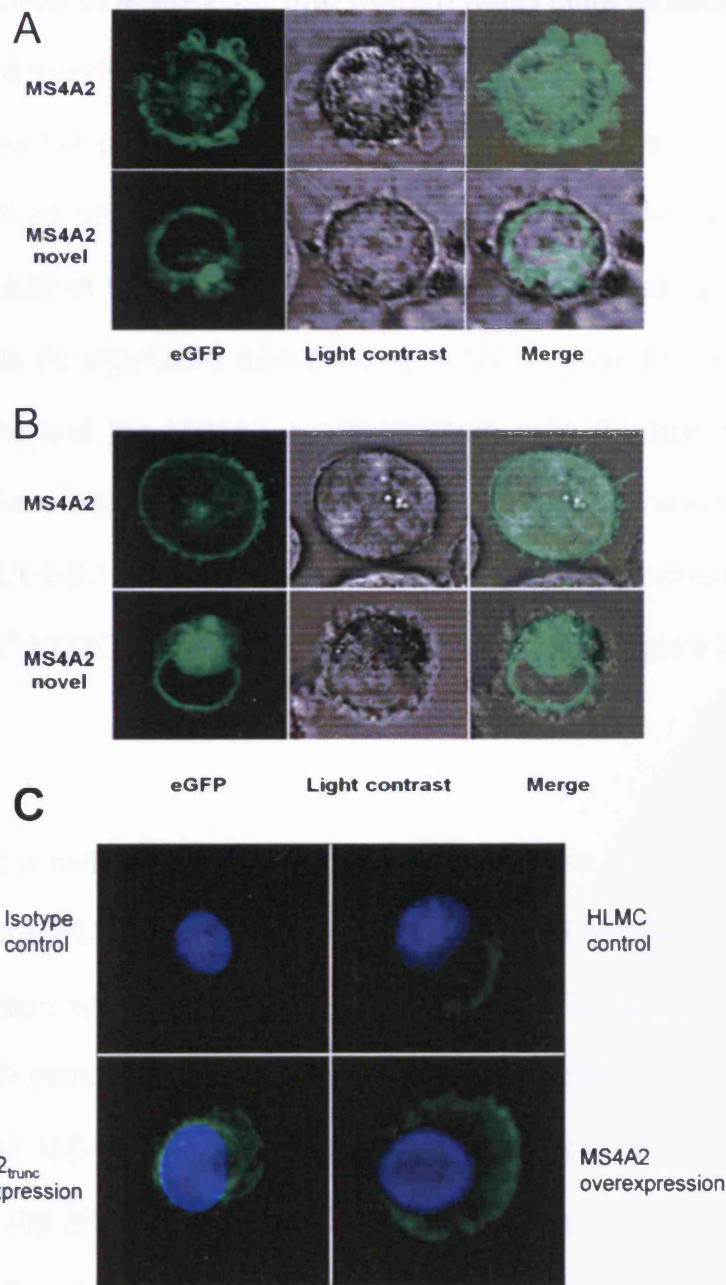


Figure 3.45: MS4A2_{trunc} localises to the nuclear membrane rather than the cytoplasmic membrane. A) Confocal micrographs of LAD-2 cells transfected with MS4A2 (top panels) and MS4A2_{trunc} (bottom panels) tagged with eGFP (pEGFP-N1) using nucleofection. MS4A2 localized to the cytoplasmic membrane. However, the MS4A2_{trunc} localised to the nuclear membrane. **B)** Similar results were seen using lipofection of HMC-1 cells. **C)** Immunofluorescence of HLMC with MS4A2 and MS4A2_{trunc} overexpression.

3.6.5 Transduction of MS4A2_{trunc} into human mast cells inhibits cell proliferation and survival

Having confirmed the overexpression of the MS4A2 variants in human mast cells, I next looked at the function of these proteins. I first examined any potential cytotoxicity of the viruses on the cells. After 7 days of culture with the viruses there was no significant difference in HLMC number between the GFP virus control cells and the MS4A2 overexpression cells (**Figure 3.46A**) (n=6, p=0.905). However, with the overexpression of MS4A2_{trunc} there was marked cell death with $0.1 \pm 0.1 \times 10^4$ HLMC in the MS4A2_{trunc} transductions compared to $7.3 \pm 1.2 \times 10^4$ HLMC in the GFP control transductions (**Figure 3.46A**) (n=6, p=0.001).

I next performed a cell survival and proliferation assay to obtain a time-course for the death of the HLMC. However, as expected the HLMC were killed by day 4 after transduction with MS4A2_{trunc} (**Figure 3.46C**). There was a significant effect of the GFP virus on HLMC survival and viability, although this was much less marked than MS4A2_{trunc} (**Figure 3.46C & E**). Since HMC-1 cells do not natively express the MS4A2_{trunc}, I also performed these experiments on HMC-1. Interestingly, I found that exogenous expression of MS4A2_{trunc} markedly inhibited the proliferation of HMC-1 cells when compared to untreated or GFP virus-treated cells (**Figure 3.46B**). The addition of the GFP virus had no significant effect on HMC-1 cell proliferation or viability (**Figure 3.46B & D**). HMC-1 cells transduced with MS4A2_{trunc} had significantly reduced viability after day 3 which was as low as 56.7 ± 3.4 % by day 7 (**Figure 3.46D**) (n=4, p=0.006).

In order to confirm that MS4A2_{trunc} was indeed anti-proliferative, I next performed ³H-thymidine incorporation assays on both HLMC and HMC-1 cells. HLMC proliferate slowly in culture and so have relatively low incorporation of ³H-thymidine. However, HLMC transduced with MS4A2_{trunc} incorporated considerably less ³H-thymidine than either untreated or GFP virus-treated HLMC (**Figure 3.46F**) (n=4, p=0.037 and 0.047 respectively). HMC-1 cells showed similar results (**Figure 3.46G**), but since HMC-1 cells proliferate more rapidly in culture when compared to HLMC, the effects were much more marked. Indeed, MS4A2_{trunc} was comparable to the negative controls in both HLMC and HMC-1 cells, whereas the GFP transduction control was comparable to untreated cells.

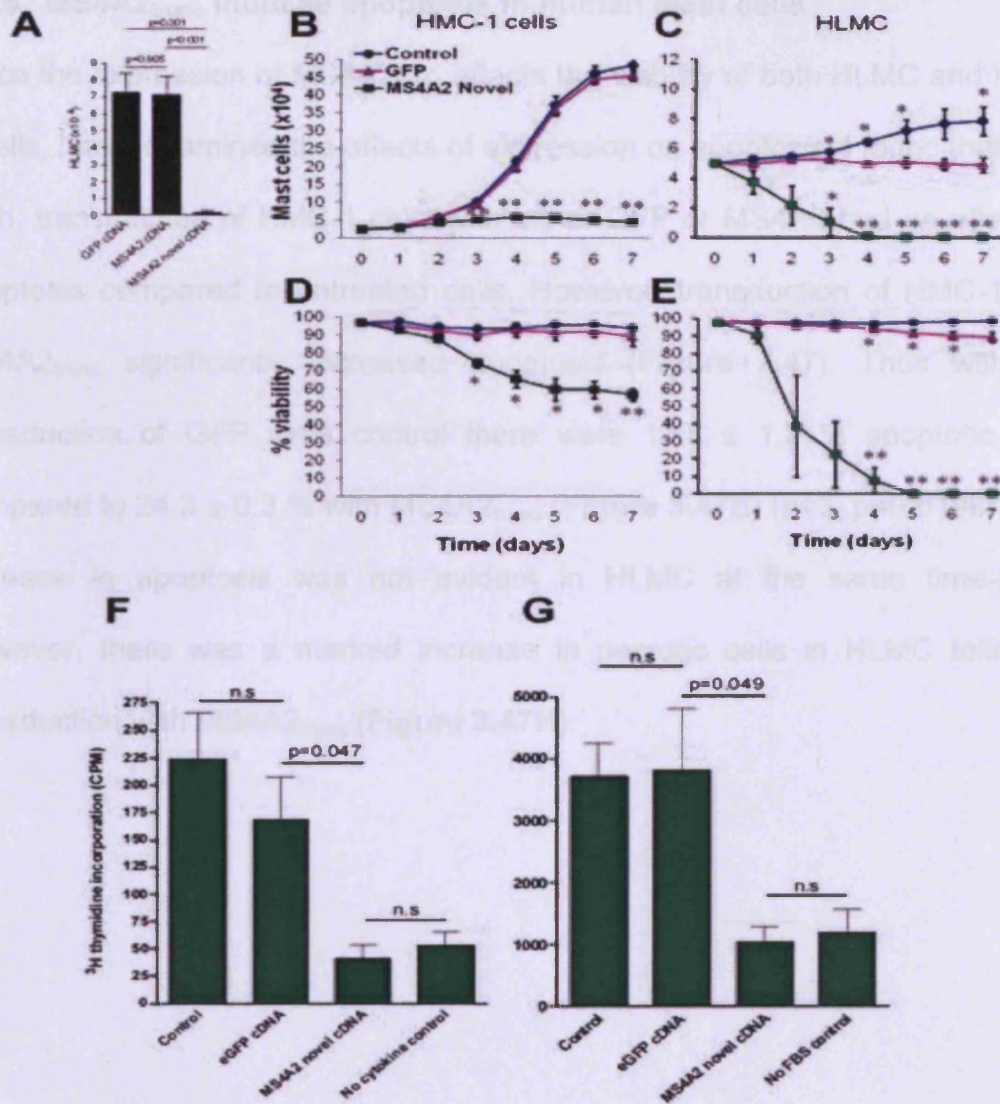


Figure 3.46: MS4A2_{trunc} prevents proliferation of HMC-1 cells and initiates cell death. **A)** Transduction of MS4A2 had no effect on the HLMC viability after 7 days when compared to the virus GFP control. However, transduction of MS4A2_{trunc} leads to cell death by day 7. **B)** In HMC-1 cells, transduction of MS4A2_{trunc} profoundly inhibits proliferation. **C)** In HLMC the cells were dead by day 4 after transduction of MS4A2_{trunc}. **D)** HMC-1 viability began to drop at 3 days after transduction of MS4A2_{trunc}. **E)** This drop in viability after MS4A2_{trunc} transduction was more evident in HLMC. **F)** To confirm the anti-proliferative effect of MS4A2_{trunc}, I next looked at ³H-thymidine incorporation into DNA. Both HLMC and HMC-1 cells (**G**). Data is the mean ± SEM from 6 (**A**) or 4 (**B-G**) experiments. * p<0.05, ** p<0.01, *** p<0.001, ANOVA with Tukey's post test.

3.6.6 MS4A2_{trunc} induces apoptosis in human mast cells

Since the expression of MS4A2_{trunc} affects the viability of both HLMC and HMC-1 cells, I next examined the effects of expression on apoptosis. I found that after 48 h, transduction of HMC-1 cells with either GFP or MS4A2 had no effect on apoptosis compared to untreated cells. However, transduction of HMC-1 with MS4A2_{trunc} significantly increased apoptosis (**Figure 3.47**). Thus with the transduction of GFP virus control there were 13.6 ± 1.2 % apoptotic cells compared to 24.3 ± 0.3 % with MS4A2_{trunc} (**Figure 3.47E**) ($n=3$, $p=0.0198$). This increase in apoptosis was not evident in HLMC at the same time-point. However, there was a marked increase in necrotic cells in HLMC following transduction with MS4A2_{trunc} (**Figure 3.47H**).

1897 The anti-proliferative effects of MS4A2_{trunc} are indicated via D, cell cycle arrest.

In order to determine the basic MS4A2_{trunc} 1 read expression by There was significantly lower MS4A2_{trunc} (0.9 ± 2.7%) when p40-D10), GFP transduction (transduction (32.7 ± 1.4%, n= GFP phase was entered by HMC-1 cells there were 44 2 MS4A2_{trunc} compared to 23 8 31.8 ± 0.2% in the GFP transduced MS4A2 transduction (n=3, p=0

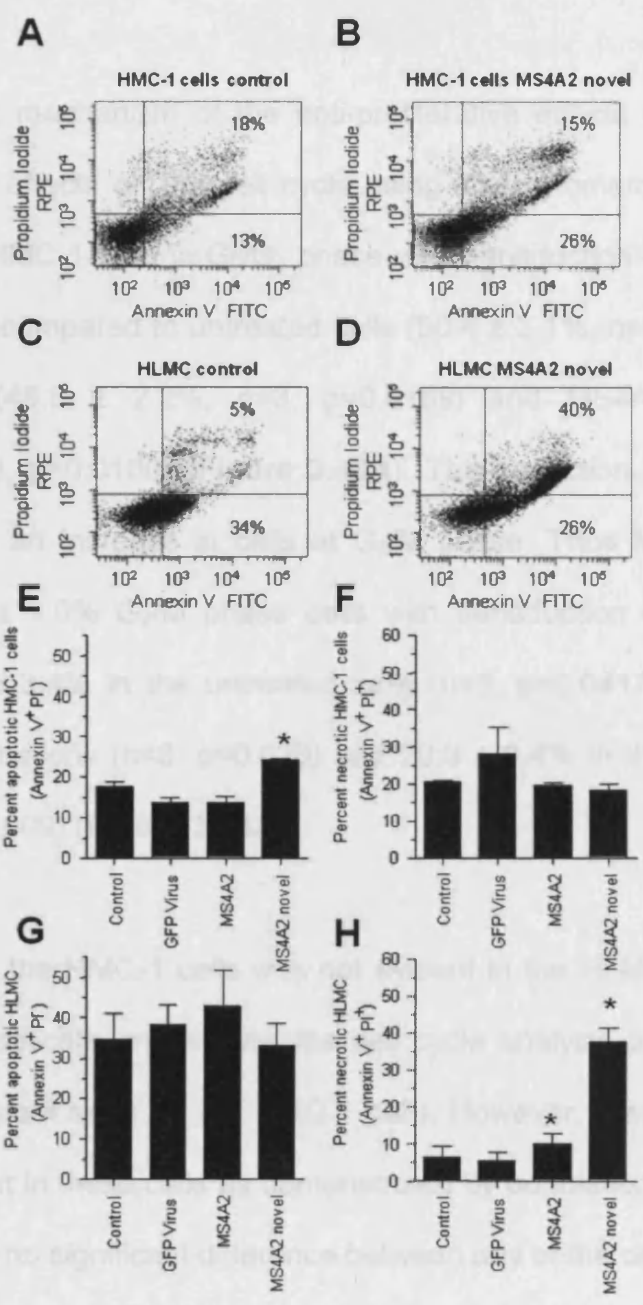


Figure 3.47: Transduction of MS4A2_{trunc} induces apoptosis. **A)** Scatter plot of HMC-1 control cells stained for annexin V (X axis) and propidium iodide (Y axis). **B)** Transduction of MS4A2_{trunc} leads to a greater population of annexin V positive, PI negative cells which is indicative of apoptosis. **C)** There was a high amount of HLMC which were apoptotic in the control cells and this did not change with the addition of MS4A2_{trunc} (**D**). However, there was an increase in necrotic cells with the addition of MS4A2_{trunc}. **E-H)** Graphical representation of the mean ± SEM of 3 separate experiments demonstrating the changes in the different populations of cells.

3.6.7 The anti-proliferative effects of MS4A2_{trunc} are mediated via G₂ cell cycle arrest

In order to delineate the basic mechanism of the anti-proliferative effects of MS4A2_{trunc} I next examined its effects on the cell cycle using flow cytometry. There were significantly fewer HMC-1 cells in G₀/G₁ phase with transduction of MS4A2_{trunc} (39.6 ± 3.1%) when compared to untreated cells (50.4 ± 3.1%, n=3, p=0.040), GFP transduction (48.8 ± 2.2%, n=3, p=0.0169) and MS4A2 transduction (52.7 ± 1.4%, n=3, p=0.0160) (**Figure 3.48A**). This reduction in G₀/G₁ phase was mirrored by an increase in cells at G₂/M phase. Thus for HMC-1 cells there were 44.2 ± 1.0% G₂/M phase cells with transduction of MS4A2_{trunc} compared to 28.8 ± 3.4% in the untreated cells (n=3, p=0.0417), 31.6 ± 0.8% in the GFP transductions (n=3, p=0.020) and 29.3 ± 0.4% in the MS4A2 transductions (n=3, p=0.009) (**Figure 3.48A**).

The clear effect on cell cycle in the HMC-1 cells was not evident in the HLMC (**Figure 3.48B**). Since HLMC replicate only slowly, the cell cycle analysis did not appear as the typical histogram seen for the HMC-1 cells. However, there was significant cell death evident in these cells as demonstrated by populations of cells in sub G₀/G₁. There was no significant difference between any of the cell cycle populations when comparing the virus conditions. However, all viruses increased the amount of cells in G₀ which is consistent with the increase in non-viable cells with the GFP virus in the survival assays.

Since HMC-1 cells are arrested in G₂/M phase with the exogenous expression of MS4A2_{trunc}, I next examined the regulatory phosphorylation of the cyclin

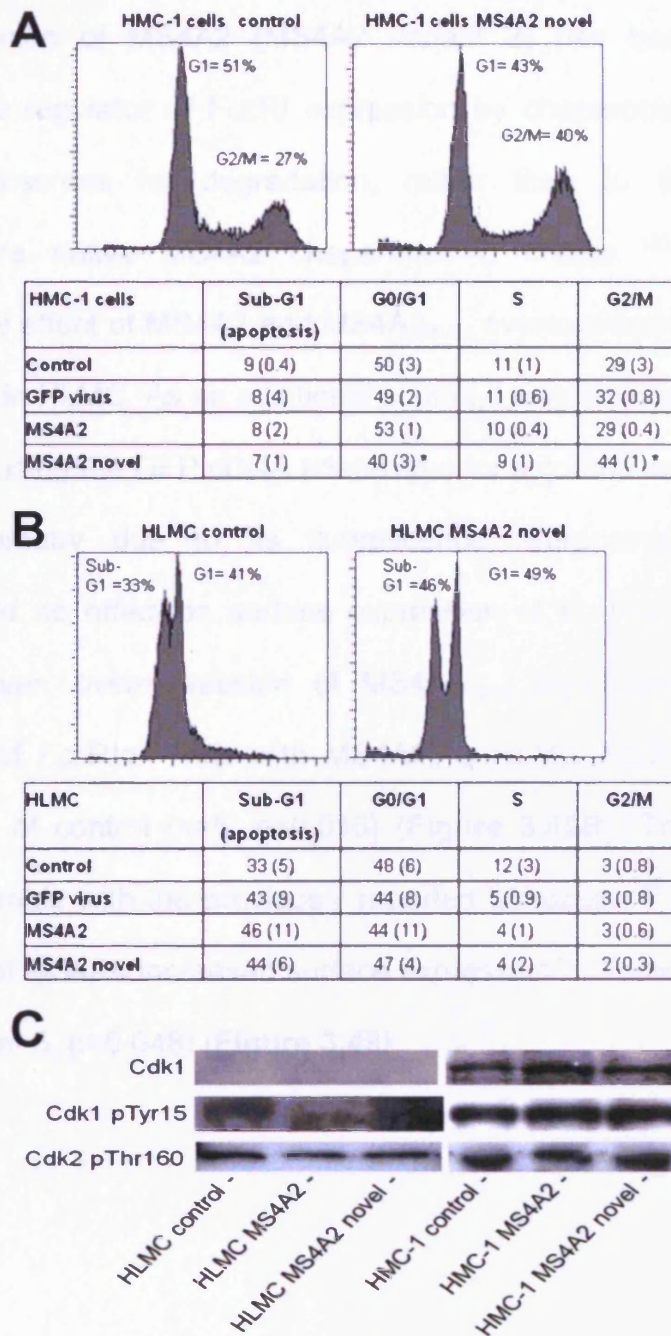
dependent kinases (cdk). There was no apparent difference in phosphorylated Thr160 on cdk2 in either HMC-1 cells or HLMC (**Figure 3.48C**). Similarly, there was no difference in total cdk1 between the conditions or in the amount of phosphorylated Tyr15 on cdk1 in HMC-1 cells transduced with MS4A2_{trunc} (**Figure 3.48C**). The expression of cdk1 was difficult to detect in the HLMC, possibly due to the lack of HLMC in G₂/M phase as demonstrated by the cell cycle analysis (**Figure 3.48B**).

3.5.9 MS4A2_{trunc} decreases surface FcγRIII expression

A previously reported mutation in the cytoplasmic membrane domain of FcγRIII reported to act as a dominant negative for the mature FcγRIII and to induce cytoplasmic membrane waves. Therefore, I next examined the effect of MS4A4 overexpression + knockdown of MS4A2 on surface FcγRIII expression in HLMC (Figure 3.49). However, MS4A4 overexpression + knockdown of MS4A2 had no effect on surface FcγRIII expression in HLMC (Figure 3.49). Therefore, I next examined the effect of MS4A2_{trunc} on surface FcγRIII expression in HLMC (Figure 3.49). However, MS4A2_{trunc} overexpression + knockdown of MS4A2 had no effect on surface FcγRIII expression in HLMC (Figure 3.49).

Figure 3.48: The antiproliferative effect of MS4A2_{trunc} was due to G₂/M phase arrest. A) Transduction of MS4A2_{trunc} induces an increase in the number of cells in G₂/M phase when compared to control. This was accompanied by a decrease in cells in G₁ phase consistent with G₂

arrest. Importantly, this effect was not evident with either GFP virus control or overexpression of MS4A2. Data in the table is the mean (SEM) of 3 separate experiments B) There was no significant difference in the cell cycle in HLMC. This was probably due to there being very few cells progressing through to S and G₂/M phases in these cells. C) There was no difference between the level of Cdk1, phosphorylated Cdk1 (Tyr15) or phosphorylated Cdk2 (Thr160) with the overexpression of either MS4A2 or MS4A2_{trunc}.



3.6.8 MS4A2_{trunc} decreases surface FcεR1α expression

A previously reported truncation of MS4A2 (MS4A2 variant 2) has been reported to act as a negative regulator of FcεRI expression by chaperoning immature α chains to endosomes for degradation, rather than to the cytoplasmic membrane where native MS4A2 chaperones α chains ⁽²¹¹⁾. Therefore, I next examined the effect of MS4A2 and MS4A2_{trunc} overexpression on surface FcεR1α expression in HLMC. As an additional control, I also included MS4A4 overexpression since using the GFP cDNA adenovirus for a control was incompatible with flow cytometry due to its fluorescence. Surprisingly, overexpression of MS4A2 had no effect on surface expression of FcεR1α in HLMC (**Figure 3.49**). However, overexpression of MS4A2_{trunc} significantly reduced surface expression of FcεR1α. Thus with MS4A2_{trunc} HLMC FcεR1α expression was $71.7 \pm 7.8\%$ of control (n=5, p=0.016) (**Figure 3.49B**). This level of reduction was comparable with the previously reported truncation ⁽²¹¹⁾. Interestingly, overexpression of MS4A4 increased surface expression of FcεR1α although to a modest degree (n=5, p=0.048) (**Figure 3.49**).

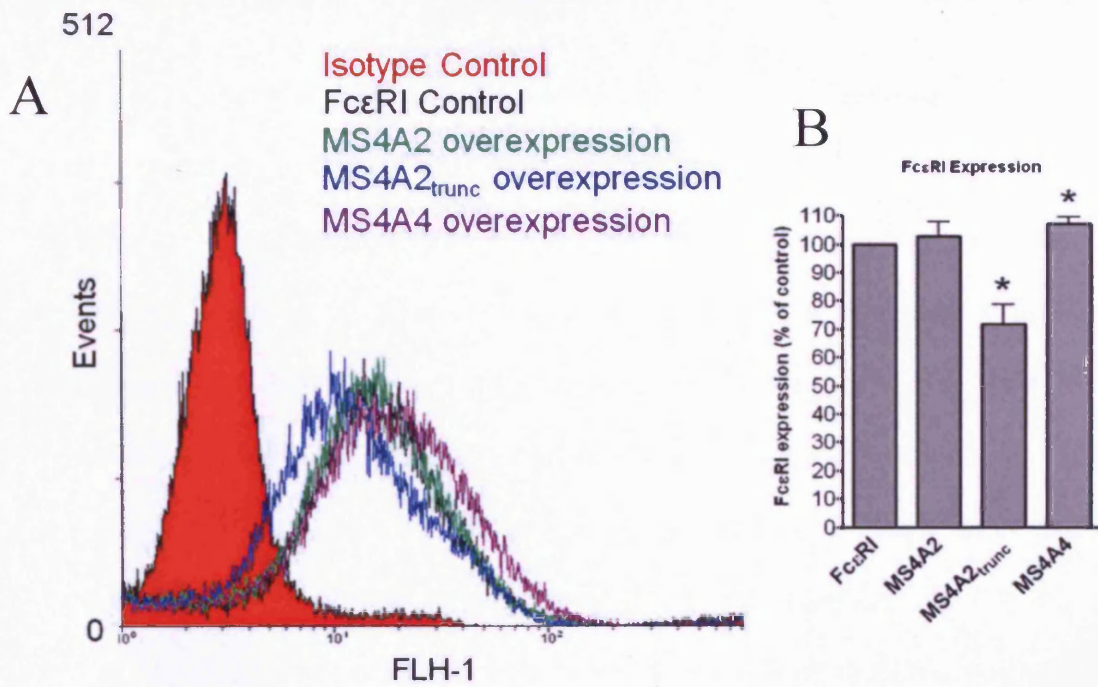


Figure 3.49: Overexpression of MS4A2_{trunc} decreases FcεRI expression in HLMC. **A)** Histogram showing the fluorescence intensity of cells stained for FcεRIα. There was no difference between MS4A2 overexpressing cells (green) compared to the virus treated controls (black). However, MS4A2_{trunc} overexpressing cells (blue) caused a left shift in fluorescence. Conversely, MS4A4 overexpressing cells demonstrated a modest right shift in fluorescence (purple). Histogram representative of 5 donors. **B)** The mean fluorescence intensity of each condition calculated as a percentage of control and represented as the mean ± SEM of 5 donors. * p<0.05.

CHAPTER 4: DISCUSSION

4 DISCUSSION

The primary aim of this study was to identify the expression of the MS4A gene family members in human mast cells and the secondary aim was to identify their function. I found that human mast cells expressed at least 4 MS4A family members, MS4A2, 4, 6 and 7. In addition, I also found that several splice variants of these genes were also expressed including 2 novel gene products. I have successfully cloned these variants and identified the regulation of gene expression, as well as the trafficking and localisation of each protein within the cell. I have also begun to elucidate important functions for MS4A family members in mast cells and identified several avenues for further study.

Human mast cells express MS4A2, a novel truncation of MS4A2 – MS4A2_{trunc}, MS4A4 variant 1, as well as both known variants of MS4A7. There were also several variants of MS4A6 present. When cloning MS4A6 there were multiple bands present with the cloning primers (**Figure 3.2A**). These bands proved to be alternative splice variants of MS4A6 including 1 novel variant (a novel truncation of MS4A6 variant 3) and a known truncated polymorphism of MS4A6 variant 1. Although these splice variants were positively identified, cloned and sequenced, it is the author's belief that other variants are likely to be expressed which were not identified in this study. Thus MS4A6 may represent a very diverse gene with many splice variants which have different biological roles. Indeed, it is believed that splice variants are an important contributor to genetic diversity⁽²¹²⁻²¹⁶⁾. In support of this, there was variable expression of the MS4A6 variants in the different cell types tested. In addition, MS4A6 polymorphism was often only expressed after stimulation in HLMC (**Figure 3.18**). Furthermore,

MS4A6 variants differed in their expression between HLMC donors where MS4A6 variant 1 was sometimes expressed well and sometimes not expressed at all. The novel variant of MS4A6 was also only expressed in the immortal cell lines. Therefore, further study of MS4A6 expression and function is warranted.

Also of great interest was MS4A7 variant expression. The 2 known variants of MS4A7 were expressed in all of the cell types examined. In HMC-1 cells, the full length variant was always more highly expressed than variant 2 (data not shown but evident in **Figure 3.16**). However, in HLMC and in the slowly replicating LAD-2 cells, MS4A7 variant 2 was always more highly expressed than the full length MS4A7 variant 1 (data not shown but evident in **Figures 3.15, 3.17 and 3.18**).

In addition, in HLMC SCF (which is so important in mast cell survival and proliferation) regulates the expression of the MS4A7 variants. Thus the full length MS4A7 variant 1 was often not expressed in HLMC in the absence of SCF, but MS4A7 variant 2 was present. With the addition of SCF, the predominant MS4A7 was often switched to MS4A7 variant 1 which was accompanied by a loss in expression of MS4A7 variant 2. This regulation of MS4A7 variant expression by SCF was also evident in the activation of HLMC with IgE and IgE + anti-IgE. IgE stimulation and IgE + anti-IgE upregulated the expression of both MS4A7 variants. However, SCF potentiated this upregulation of the full length MS4A7 variant 1, but reduced the amount of upregulation of MS4A7 variant 2 (**Figure 3.34**). Therefore, these data strongly suggest that MS4A7 variants may have opposing actions and that these actions are

regulated by SCF and related to proliferation and/or survival. This is particularly interesting since MS4A7 has been proposed to be involved in cell proliferation^(217;218) although differentiation between the splice variants was not performed⁽²¹⁸⁾. Thus the functions of MS4A7 protein variants are of great interest and will be studied further.

Elucidating the function of all the expressed MS4A family in human mast cells was beyond the scope, funding and timescale of this study. This study has been hindered by the paucity of antibodies available for the MS4A gene family. The only available antibodies that worked in any of the methods used in this study were for MS4A2. All other antibodies were tried and none of them worked. Thus it has not been possible to determine protein level expression of the MS4A gene family members. Therefore, gene silencing using shRNA functional knockdowns is of little benefit when knockdowns at the protein level cannot be validated using western blotting. Although it was possible to validate knockdowns at the mRNA level using quantitative real time PCR, this does not necessarily correspond to knockdown at the protein level. Thus the functional characterisation of the MS4A gene family depends on the production of reliable custom made antibodies. In addition, several antibodies will need to be produced for each gene family member in order to differentiate between the splice variants present which are identical except for exon removal truncations.

Despite these shortcomings, this study has made several novel and potentially important findings in the function of two MS4A gene products. HLMC and LAD-2 cells express a novel truncated variant of MS4A2, which I will term MS4A2_{trunc},

and MS4A4A variant 1, but I was unable to detect the expression of either gene in HMC-1 cells. This immediately raises two questions which arise from the known functional differences in these cell types. Firstly, both HLMC and LAD-2 cells express the high affinity IgE receptor FcεRI^(203;219), but HMC-1 cells do not⁽²¹⁰⁾. Therefore, does either or both of these genes have a role in FcεRI function? In addition, since HMC-1 cells replicate rapidly and both HLMC and LAD-2 cells only proliferate very slowly, does either or both of these genes have a role in cell proliferation?

I began to answer these questions with MS4A2_{trunc} which is a novel splice variant of the high affinity IgE receptor β subunit, MS4A2. MS4A2 is an integral subunit of FcεRI. Although its expression is not essential for IgE receptor signaling⁽¹⁸⁸⁾, MS4A2 is known to act as an amplifier of FcεRI signaling⁽¹⁸⁹⁾. Since the human genome project found that there were significantly fewer genes than expected, only around 35 000 genes accounting for around 100 000 proteins^(212;213), it is now considered that alternative splicing of genes accounts for much of the genetic diversity in the human genome and that up to 60% of human genes are alternatively spliced⁽²¹⁴⁻²¹⁶⁾. Indeed, Modrek and colleagues predicted that MS4A2 variants resulting from alternative splicing existed and that they may contribute to functional regulation of the FcεRI⁽²¹⁵⁾.

Although one of the possible functions of full-length (native) MS4A2 may be to act as an amplifier of FcεRI-dependent signaling⁽¹⁸⁹⁾, not much is known about other possible functions for this protein. Donnadieu and colleagues were the first to report a splice variant of MS4A2 (transcript variant 2) expressed in

human basophils and cord blood-derived mast cells ⁽²¹¹⁾. This splice variant was a truncation due to the retention of intron 5 which results in the encoding of several amino acids before an in-frame stop codon ⁽²¹¹⁾. Thus the C terminal domains of MS4A2 including the immunoreceptor tyrosine-based activation motif (ITAM) were lost ⁽²¹¹⁾. This truncation was shown to bind to immature α chains of Fc ϵ RI in the endoplasmic reticulum, and traffic them for endosomal degradation leading to downregulation of surface Fc ϵ RI expression. This would presumably reduce IgE-dependent mast cell activation. This protein has therefore been proposed to act as a naturally occurring negative-regulator of Fc ϵ RI-dependent cell activation, in direct competition with native MS4A2, and as such could determine the severity of allergic disease.

I was also able to demonstrate a reduction in Fc ϵ RI α surface expression with the overexpression of MS4A2_{trunc}. This may suggest a similar role for this truncation as the one reported previously ⁽²¹¹⁾. Indeed, the level of reduction in expression is comparable to that seen by Donnadieu and colleagues with their truncation ⁽²¹¹⁾. However, since I was measuring Fc ϵ RI α expression 48 h after transduction of MS4A2_{trunc}, the drop in cell viability which occurs in HLMC within 48 h may be a contributing factor for this reduction in expression. Nevertheless, MS4A2_{trunc} identified in this study appears to have an entirely novel role in mast cell biology unrelated to surface Fc ϵ RI expression since there was a profound effect on the proliferation of HMC-1 cells which do not express Fc ϵ RI ⁽²²⁰⁾.

MS4A2_{trunc} is generated due to a deletion of exon 3 and so retains both N and C termini thus retaining the C terminal ITAM. This deletion of exon 3 results in the

putative loss of transmembrane domains 1 and 2. The result of this truncation is that novel MS4A2 localizes to the peri-nuclear membrane rather than the cytoplasmic membrane. This event is likely to be critical for the function of the protein. MS4A2_{trunc} induced cell cycle arrest at G₂/M phase. An important regulator of G₂/M phase transition through the G₂ checkpoint is Cdk1 (cdc2). Cdk1 is dephosphorylated at Tyr15 and Thr14 with subsequent phosphorylation of Thr161 during the G₂/M phase checkpoint enabling transition through to M phase (For review see ⁽²²¹⁾). Dephosphorylation of Tyr15 is an absolute requirement for this transition. However, I was unable to identify any changes in the phosphorylated state of Cdk1 with transduction of MS4A2_{trunc}.

It is interesting that the rapidly dividing human mast cell line HMC-1 does not express MS4A2_{trunc}, while the slowly dividing cell line LAD2 and slowly dividing primary HLMC do express it. This provides a functional correlate of relevance to the proposed anti-proliferative effect of this protein. The downregulation of MS4A2_{trunc} gene expression by SCF is highly relevant to the action of this cytokine, and might provide an additional mechanism of action promoting SCF-dependent cell survival and proliferation. The HMC-1 cell line exhibits gain-of-function mutations at amino acid 816 and the juxtamembrane region of CD117 (SCF receptor), leading to constitutive receptor activity. These mutations are not present in primary HLMC or the LAD2 cell line, and might explain the differential expression of MS4A2_{trunc} in these cells.

In keeping with the proposed function of MS4A2_{trunc} discussed above, confocal microscopy using GFP tagged chimeric MS4A2 and MS4A2_{trunc} demonstrated

that MS4A2 trafficked to the cytoplasmic membrane, but MS4A2_{trunc} associates with the nuclear membrane. This is an interesting observation since I also show that both variants of MS4A7 are trafficked to the nuclear membrane, and as discussed above I have data to suggest that MS4A7 variants are regulated by the mast cell growth factor SCF and that they may have opposing actions on growth factor-dependent mast cell functions. In addition, MS4A7 is proposed to regulate the cell cycle and progression of proliferation ⁽²¹⁸⁾. Furthermore, another member of the MS4A gene family MS4A3, which is closely related to MS4A2, has also been shown to traffic to the nuclear membrane rather than the cytoplasmic membrane, where it binds directly to KAP, a cyclin-dependent kinase (Cdk) associated phosphatase which dephosphorylates human Cdk2 in the nucleus attenuating cell cycle progression ⁽²⁰⁰⁾. This dephosphorylation of Cdk2 at Thr160 by KAP is facilitated by MS4A3 binding directly to the complex which not only allows KAP greater access to dephosphorylate Thr160 on Cdk2, but also forces the dissociation and exclusion of cyclin A from this complex thus preventing G₁ – S phase transition ⁽²⁰¹⁾.

This study also shows that MS4A4 can induce a K_{Ca}3.1-like current when transfected into CHO cells. This is interesting since the current itself is blocked by the K_{Ca}3.1-specific blockers TRAM-34 and ICA 17043. Therefore, this current must be K_{Ca}3.1. However, the reversal potential of the current is too positive for a pure K_{Ca}3.1 current. There are a couple of possible explanations for the initiation of this current. Firstly, MS4A4 variant 1 has a region within the extracellular loop with amino acids YYG. The selectivity filter for K⁺ channels is GYG. However, the Weaver channel mutation in GIRK2 K⁺ channels (SYG –

although other amino acids may be in position 1) negates the K^+ selectivity of GIRK2 channels which are also able to carry Ca^{2+} and Na^+ making them non-selective cation channels ⁽²²²⁾. Therefore, it is possible that MS4A4 may form heteromeric complexes with $K_{Ca}3.1$ to form non-selective cation channels.

Alternatively, MS4A4 variant 1 may form distinct calcium channels which allow influx of calcium into the CHO cell which in turn activates native CHO $K_{Ca}3.1$ channels, since influx of extracellular calcium is critical for $K_{Ca}3.1$ function. Both of these hypotheses would be valid since CHO cells do express native K_{Ca} channels which do not always seem to be functional ^(223;224).

These proposed mechanisms for MS4A4 inducing a $K_{Ca}3.1$ current in CHO cells are entirely plausible. Indeed, MS4A1 has been proposed to act as a distinct and highly selective Ca^{2+} channel in B lymphocytes ⁽¹⁹⁰⁾. This hypothesis was drawn after the discovery that transfection of MS4A1 cDNA into human K562 erythroleukaemia cells and mouse NIH-3T3 fibroblasts induced an identical transmembrane Ca^{2+} conductance which was very similar to the native current evident in B cells ⁽¹⁹⁰⁾. More recently, Li and colleagues ⁽¹⁹¹⁾ demonstrated that MS4A1 may actually act as a store-operated calcium channel (SOCC) which associates within lipid rafts to couple B cell receptor signalling to store-operated calcium entry (SOCE) in cholesterol-dependent lipid microdomains ⁽¹⁹¹⁾.

In addition, MS4A12 may also act as a distinct calcium channel, which is colon specific and its expression was associated with colon cancer ⁽¹⁹⁷⁾. Subsequent functional knockdown of MS4A12 using siRNA in colon cancer cells significantly

attenuated cell proliferation, motility and chemotactic tissue infiltration ⁽¹⁹⁷⁾. Furthermore, cells expressing MS4A12 were more reactive to lower concentrations of growth factors than their counterpart cells not expressing MS4A12 ⁽¹⁹⁷⁾. Further evidence of a possible role of MS4A gene family members in cancer has been demonstrated with an increased expression of MS4A8B in small cell lung cancer although no mechanism was described ⁽¹⁸¹⁾. Thus a major role of the MS4A family appears to be to regulate cell cycle progression and therefore cellular proliferation and survival. The relative expression of pro- versus anti-proliferative MS4A family members may be important in determining the proliferative potential of a cell.

To briefly summarise, this study has given a great deal of insight into the expression and regulation of expression of MS4A gene family members in human mast cells. The complete characterization and functional analysis of an entire gene family is beyond the scope of a PhD thesis. However, this study has raised a great number of questions and opened several avenues of research for future projects. The molecular biology, which was such a big part of this study, has provided the tools for future research into the function of this gene family. In addition, the regulation of expression has identified possible candidates for study such as the MS4A7 variants and their putative opposing actions on mast cell proliferation.

In terms of functional data, this study has identified that MS4A4 variant 1 may play a role in ionic conductance which could be important in mast cell activation since it modulates, in one way or another, K⁺ efflux which directly effects Ca²⁺

conductance. However, the main functional aspect of this study was the identification of a novel MS4A2 gene variant, MS4A2_{trunc}, which has an entirely novel function. MS4A2_{trunc} inhibits mast cell proliferation and survival, and indicates that the MS4A2 gene has multiple roles, extending well beyond the regulation of acute allergic responses. By understanding the mechanisms regulating its function, it may one day be possible to induce its expression in mast cells *in vivo*, leading to better treatments for a number of mast cell-dependent or -associated diseases such as mastocytosis and asthma respectively.

4.1 Future work

As mentioned, this study has made several important observations that open further avenues of research into the MS4A gene family. Firstly, it is important to identify any differential expression between normal human mast cells and mast cells obtained from patients with mast cell-associated disease. Thus the mRNA and protein expression of MS4A family members in normal human mast cells (HLMC, primary human CD34+ blood-derived mast cells) and mast cells from patients with mastocytosis and anaphylaxis (obtained from blood and bone marrow progenitors), quantitative PCR, western blotting and flow cytometry will be performed.

Secondly, there are strong suggestions both in this study and in the literature that the MS4A gene family may have a role in proliferation and survival of not only mast cells, but also of other cell types in both normal and cancerous cells.

This role may also be associated with the modulation of calcium signalling and entry into the cell. Therefore, delineating the functional role of each of the expressed MS4A family members in mast cells, in terms of calcium signalling and proliferation/survival will be carried out using both cDNA overexpression and shRNA knockdown technologies. In order to validate the knockdowns, quantitative real time PCR and western blotting will be performed using custom-made antibodies which can differentiate between splice variants. Once validated, shRNA knockdowns will be used to determine the functional consequence of gene knockdown for each MS4A family member in terms of both normal mast cell biology and dysregulated mast cell functions.

Furthermore, the role of the MS4A family in other mast cell functions such as mediator release, degranulation, migration and chemotaxis will be studied. Thus overexpression and shRNA knockdown mast cells will be used for survival and proliferation assays such as ³H-thymidine incorporation and CFSE assays, transwell migration assays and mediator release assays (cytokine and eicosanoid ELISAs, beta hexosaminidase assays and histamine radioenzymatic assay).

4.2 Future aims

I aim to examine the expression and function of the MS4A gene family in normal human mast cells and aberrant human mast cell populations associated with disease states. The cellular localisation and protein trafficking will be established and regulation of gene expression examined. I will achieve this by using quantitative real-time RT-PCR, FACS analysis, western blotting,

immunofluorescence and confocal microscopy. Once the expression of the MS4A gene family in the different cell types has been established, I will begin to study their function. This will be achieved by assessing which mast cell responses are altered by protein overexpression, and which responses are altered with functional MS4A gene knockdown using shRNA adenoviral constructs. Once I have identified a function for each gene product in mast cell survival, proliferation, mediator release, and chemotaxis, I will identify the mechanisms involved. This will be achieved by studying calcium flux and ionic conductance, phosphorylation of receptor and adaptor molecules, activation of signalling enzymes such as PI3K, transcription factor regulation, pathways involved in apoptosis, proliferation and cell cycle regulation, such as the activation of caspases, cyclins, cyclin-dependent kinases and phosphatases. Growth factor-dependent responses will also be examined.

CHAPTER 5: REFERENCES

References

- (1) Iba Y, Shibata A, Kato M, Masukawa T. Possible involvement of mast cells in collagen remodeling in the late phase of cutaneous wound healing in mice. *Int Immunopharmacol* 2004; 4(14):1873-80.
- (2) Weller K, Foitzik K, Paus R, Syska W, Maurer M. Mast cells are required for normal healing of skin wounds in mice. *FASEB J* 2006.
- (3) Heissig B, Rafii S, Akiyama H, Ohki Y, Sato Y, Rafael T et al. Low-dose irradiation promotes tissue revascularization through VEGF release from mast cells and MMP-9-mediated progenitor cell mobilization. *J Exp Med* 2005; 202(6):739-50.
- (4) Echtenacher B, Mannel DN, Hultner L. Critical protective role of mast cells in a model of acute septic peritonitis. *Nature* 1996; 381(6577):75-7.
- (5) Gurish MF, Boyce JA. Mast cells: ontogeny, homing, and recruitment of a unique innate effector cell. *J Allergy Clin Immunol* 2006; 117(6):1285-91.
- (6) Hsieh FH, Sharma P, Gibbons A, Goggans T, Erzurum SC, Haque SJ. Human airway epithelial cell determinants of survival and functional phenotype for primary human mast cells. *Proc Natl Acad Sci U S A* 2005; 102(40):14380-5.
- (7) Ogasawara T, Murakami M, Suzuki-Nishimura T, Uchida MK, Kudo I. Mouse bone marrow-derived mast cells undergo exocytosis, prostanoid generation, and cytokine expression in response to G protein-activating

polybasic compounds after coculture with fibroblasts in the presence of c-kit ligand. *J Immunol* 1997; 158(1):393-404.

(8) Rubinchik E, Levi-Schaffer F. Mast cells and fibroblasts: two interacting cells. *Int J Clin Lab Res* 1994; 24(3):139-42.

(9) Swieter M, Midura RJ, Nishikata H, Oliver C, Berenstein EH, Mergenhagen SE et al. Mouse 3T3 fibroblasts induce rat basophilic leukemia (RBL-2H3) cells to acquire responsiveness to compound 48/80. *J Immunol* 1993; 150(2):617-24.

(10) Rothenberg ME, Austen KF. Influence of the fibroblast environment on the structure of mast cell proteoglycans. *Ann N Y Acad Sci* 1989; 556:233-44.

(11) Levi-Schaffer F, Austen KF, Gravallesse PM, Stevens RL. Coculture of interleukin 3-dependent mouse mast cells with fibroblasts results in a phenotypic change of the mast cells. *Proc Natl Acad Sci U S A* 1986; 83(17):6485-8.

(12) Valent P, Spanblochl E, Sperr WR, Sillaber C, Zsebo KM, Agis H et al. Induction of differentiation of human mast cells from bone marrow and peripheral blood mononuclear cells by recombinant human stem cell factor/kit-ligand in long-term culture. *Blood* 1992; 80(9):2237-45.

(13) Williams DE, Eisenman J, Baird A, Rauch C, Van Ness K, March CJ et al. Identification of a ligand for the c-kit proto-oncogene. *Cell* 1990; 63(1):167-74.

(14) Langley KE, Bennett LG, Wypych J, Yancik SA, Liu XD, Westcott KR et al. Soluble stem cell factor in human serum. *Blood* 1993; 81(3):656-60.

(15) Iemura A, Tsai M, Ando A, Wershil BK, Galli SJ. The c-kit ligand, stem cell factor, promotes mast cell survival by suppressing apoptosis. *Am J Pathol* 1994; 144(2):321-8.

(16) Berent-Maoz B, Piliponsky AM, Daigle I, Simon HU, Levi-Schaffer F. Human mast cells undergo TRAIL-induced apoptosis. *J Immunol* 2006; 176(4):2272-8.

(17) Tsujimura T, Morii E, Nozaki M, Hashimoto K, Moriyama Y, Takebayashi K et al. Involvement of transcription factor encoded by the mi locus in the expression of c-kit receptor tyrosine kinase in cultured mast cells of mice. *Blood* 1996; 88(4):1225-33.

(18) Li L, Krilis SA. Mast-cell growth and differentiation. *Allergy* 1999; 54(4):306-12.

(19) Frenz AM, Gibbs BF, Pearce FL. The effect of recombinant stem cell factor on human skin and lung mast cells and basophil leukocytes. *Inflammation Research* 1997; 46(2):35-9.

(20) Taylor AM, Galli SJ, Coleman JW. Stem-cell factor, the kit ligand, induces direct degranulation of rat peritoneal mast cells in vitro and in vivo: dependence of the in vitro effect on period of culture and comparisons of stem-cell factor with other mast cell-activating agents. *Immunology* 1995; 86(3):427-33.

(21) Columbo M, Horowitz EM, Botana LM, MacGlashan DW, Jr., Bochner BS, Gillis S et al. The human recombinant c-kit receptor ligand, rhSCF, induces mediator release from human cutaneous mast cells and enhances IgE-dependent mediator release from both skin mast cells and peripheral blood basophils. *J Immunol* 1992; 149(2):599-608.

(22) Cruse G, Kaur D, Yang W, Duffy SM, Brightling CE, Bradding P. Activation of human lung mast cells by monomeric immunoglobulin E. *Eur Respir J* 2005; 25(5):858-63.

(23) Lin TJ, Bissonnette EY, Hirsh A, Befus AD. Stem cell factor potentiates histamine secretion by multiple mechanisms, but does not affect tumour necrosis factor-alpha release from rat mast cells. *Immunology* 1996; 89(2):301-7.

(24) Petersen LJ, Brasso K, Pryds M, Skov PS. Histamine release in intact human skin by monocyte chemoattractant factor-1, RANTES, macrophage inflammatory protein-1 alpha, stem cell factor, anti-IgE, and codeine as determined by an ex vivo skin microdialysis technique. *J Allergy Clin Immunol* 1996; 98(4):790-6.

(25) Lukacs NW, Kunkel SL, Strieter RM, Evanoff HL, Kunkel RG, Key ML et al. The role of stem cell factor (c-kit ligand) and inflammatory cytokines in pulmonary mast cell activation. *Blood* 1996; 87(6):2262-8.

(26) Takaishi T, Morita Y, Hirai K, Yamaguchi M, Ohta K, Noda E et al. Effect of cytokines on mediator release from human dispersed lung mast cells. *Allergy* 1994; 49(10):837-42.

(27) Mierke CT, Ballmaier M, Werner U, Manns MP, Welte K, Bischoff SC. Human endothelial cells regulate survival and proliferation of human mast cells. *J Exp Med* 2000; 192(6):801-11.

(28) Yanagida M, Fukamachi H, Ohgami K, Kuwaki T, Ishii H, Uzunaki H et al. Effects of T-helper 2-type cytokines, interleukin-3 (IL-3), IL-4, IL-5, and IL-6 on the survival of cultured human mast cells. *Blood* 1995; 86(10):3705-14.

(29) Saito H, Ebisawa M, Sakaguchi N, Onda T, Iikura Y, Yanagida M et al. Characterization of cord-blood-derived human mast cells cultured in the presence of Steel factor and interleukin-6. *Int Arch Allergy Immunol* 1995; 107(1-3):63-5.

(30) Saito H, Ebisawa M, Tachimoto H, Shichijo M, Fukagawa K, Matsumoto K et al. Selective growth of human mast cells induced by Steel factor, IL-6, and prostaglandin E2 from cord blood mononuclear cells. *J Immunol* 1996; 157(1):343-50.

(31) Bradding P, Holgate ST. Immunopathology and human mast cell cytokines. *Crit Rev Oncol Hematol* 1999; 31(2):119-33.

(32) Furitsu T, Saito H, Dvorak AM, Schwartz LB, Irani AM, Burdick JF et al. Development of human mast cells in vitro. *Proc Natl Acad Sci USA* 1989; 86(24):10039-43.

(33) Levi-Schaffer F, Austen KF, Caulfield JP, Hein A, Gravalles PM, Stevens RL. Co-culture of human lung-derived mast cells with mouse 3T3 fibroblasts: morphology and IgE-mediated release of histamine, prostaglandin D2, and leukotrienes. *J Immunol* 1987; 139(2):494-500.

(34) Li L, Meng XW, Krilis SA. Mast cells expressing chymase but not tryptase can be derived by culturing human progenitors in conditioned medium obtained from a human mastocytosis cell strain with c-kit ligand. *J Immunol* 1996; 156(12):4839-44.

(35) Toru H, Eguchi M, Matsumoto R, Yanagida M, Yata J, Nakahata T. Interleukin-4 promotes the development of tryptase and chymase double-positive human mast cells accompanied by cell maturation. *Blood* 1998; 91(1):187-95.

(36) Okayama Y. Human cultured mast cells. *Clin Exp Allergy* 2000; 30(8):1053-5.

(37) Kanbe N, Kurosawa M, Miyachi Y, Kanbe M, Saitoh H, Matsuda H. Nerve growth factor prevents apoptosis of cord blood-derived human cultured mast cells synergistically with stem cell factor. *Clin Exp Allergy* 2000; 30(8):1113-20.

(38) Norrby K. Mast cells and angiogenesis. *APMIS* 2002; 110(5):355-71.

(39) Welker P, Grabbe J, Zuberbier T, Grutzkau A, Henz BM. GM-CSF downmodulates c-kit, Fc(epsilon)RI(alpha) and GM-CSF receptor expression as well as histamine and tryptase levels in cultured human mast cells. *Arch Dermatol Res* 2001; 293(5):249-58.

(40) Ishida S, Kinoshita T, Sugawara N, Yamashita T, Koike K. Serum inhibitors for human mast cell growth: possible role of retinol. *Allergy* 2003; 58(10):1044-52.

- (41) Church MK, Okayama Y, Bradding P. Functional mast cell heterogeneity. In: Busse WW, Holgate ST, editors. *Asthma and Rhinitis*. Boston: Blackwell Scientific Publications, Inc, 1994: 209-20.
- (42) Enerback L. Mast cells in rat gastrointestinal mucosa. 2. Dye-binding and metachromatic properties. *Acta Pathol Microbiol Scand* 1966; 66(3):303-12.
- (43) Gurish MF, Ghildyal N, McNeil HP, Austen KF, Gillis S, Stevens RL. Differential expression of secretory granule proteases in mouse mast cells exposed to interleukin 3 and c-kit ligand. *J Exp Med* 1992; 175(4):1003-12.
- (44) Craig SS, Irani AM, Metcalfe DD, Schwartz LB. Ultrastructural localization of heparin to human mast cells of the MCTC and MCT types by labeling with antithrombin III-gold. *Lab Invest* 1993; 69(5):552-61.
- (45) Pereira PJ, Bergner A, Macedo-Ribeiro S, Huber R, Matschiner G, Fritz H et al. Human beta-tryptase is a ring-like tetramer with active sites facing a central pore. *Nature* 1998; 392(6673):306-11.
- (46) Irani AM, Craig SS, DeBlois G, Elson CO, Schechter NM, Schwartz LB. Deficiency of the tryptase-positive, chymase-negative mast cell type in gastrointestinal mucosa of patients with defective T lymphocyte function. *J Immunol* 1987; 138(12):4381-6.
- (47) Trautmann A, Toksoy A, Engelhardt E, Brocker EB, Gillitzer R. Mast cell involvement in normal human skin wound healing: expression of monocyte chemoattractant protein-1 is correlated with recruitment of mast cells which synthesize interleukin-4 in vivo. *J Pathol* 2000; 190(1):100-6.

(48) Artuc M, Hermes B, Steckelings UM, Grutzkau A, Henz BM. Mast cells and their mediators in cutaneous wound healing--active participants or innocent bystanders? *Exp Dermatol* 1999; 8(1):1-16.

(49) Bradding P, Okayama Y, Howarth PH, Church MK, Holgate ST. Heterogeneity of human mast cells based on cytokine content. *J Immunol* 1995; 155(1):297-307.

(50) Horny HP, Greschniok A, Jordan JH, Menke DM, Valent P. Chymase expressing bone marrow mast cells in mastocytosis and myelodysplastic syndromes: an immunohistochemical and morphometric study. *J Clin Pathol* 2003; 56(2):103-6.

(51) Yamada M, Ueda M, Naruko T, Tanabe S, Han YS, Ikura Y et al. Mast cell chymase expression and mast cell phenotypes in human rejected kidneys. *Kidney Int* 2001; 59(4):1374-81.

(52) Anderson DF, Zhang S, Bradding P, McGill JI, Holgate ST, Roche WR. The relative contribution of mast cell subsets to conjunctival TH2-like cytokines. *Invest Ophthalmol Vis Sci* 2001; 42(5):995-1001.

(53) Dvorak AM. Ultrastructural studies of human basophils and mast cells. *J Histochem Cytochem* 2005; 53(9):1043-70.

(54) Dvorak AM, Morgan ES. Ribosomes and secretory granules in human mast cells: close associations demonstrated by staining with a chelating agent. *Immunol Rev* 2001; 179:94-101.

(55) Craig SS, Schechter NM, Schwartz LB. Ultrastructural analysis of human T and TC mast cells identified by immunoelectron microscopy. *Lab Invest* 1988; 58(6):682-91.

(56) Walls AF, Bennett AR, McBride HM, Glennie MJ, Holgate ST, Church MK. Production and characterization of monoclonal antibodies specific for human mast cell tryptase. *Clin Exp Allergy* 1990; 20(5):581-9.

(57) Aborg CH, Novotny J, Uvnas B. Ionic binding of histamine in mast cell granules. *Acta Physiol Scand* 1967; 69(4):276-83.

(58) Humphries DE, Wong GW, Friend DS, Gurish MF, Qiu WT, Huang C et al. Heparin is essential for the storage of specific granule proteases in mast cells. *Nature* 1999; 400(6746):769-72.

(59) Caulfield JP, Lewis RA, Hein A, Austen KF. Secretion in dissociated human pulmonary mast cells. Evidence for solubilization of granule contents before discharge. *J Cell Biol* 1980; 85(2):299-312.

(60) Caulfield JP, el Lati S, Thomas G, Church MK. Dissociated human foreskin mast cells degranulate in response to anti-IgE and substance P. *Lab Invest* 1990; 63(4):502-10.

(61) Begueret H, Berger P, Vernejoux JM, Dubuisson L, Marthan R, Tunon-De-Lara JM. Inflammation of bronchial smooth muscle in allergic asthma. *Thorax* 2007; 62(1):8-15.

(62) Djukanovic R, Lai CK, Wilson JW, Britten KM, Wilson SJ, Roche WR et al. Bronchial mucosal manifestations of atopy: a comparison of markers

of inflammation between atopic asthmatics, atopic nonasthmatics and healthy controls. *Eur Respir J* 1992; 5(5):538-44.

(63) Aoki M, Kawana S. The ultrastructural patterns of mast cell degranulation in Kimura's disease. *Dermatology* 1999; 199(1):35-9.

(64) Schwartz LB, Bradford TR. Regulation of tryptase from human lung mast cells by heparin. Stabilization of the active tetramer. *J Biol Chem* 1986; 261(16):7372-9.

(65) Bradding P, Walls AF, Church MK. Mast cells and basophils: their role in initiating and maintaining inflammatory responses. In: Holgate ST, editor. *Immunopharmacology of the Respiratory System*. New York Academic Press, 1995: 53-84.

(66) Boyce JA. Mast cells: beyond IgE. *J Allergy Clin Immunol* 2003; 111(1):24-32.

(67) Persinger MA, Lepage P, Simard JP, Parker GH. Mast cell numbers in incisional wounds in rat skin as a function of distance, time and treatment. *Br J Dermatol* 1983; 108(2):179-87.

(68) Egozi EI, Ferreira AM, Burns AL, Gamelli RL, DiPietro LA. Mast cells modulate the inflammatory but not the proliferative response in healing wounds. *Wound Repair Regen* 2003; 11(1):46-54.

(69) Thomas VA, Wheeless CJ, Stack MS, Johnson DA. Human mast cell tryptase fibrinogenolysis: kinetics, anticoagulation mechanism, and cell adhesion disruption. *Biochemistry* 1998; 37(8):2291-8.

(70) Valent P, Baghestanian M, Bankl HC, Sillaber C, Sperr WR, Wojta J et al. New aspects in thrombosis research: possible role of mast cells as profibrinolytic and antithrombotic cells. *Thromb Haemost* 2002; 87(5):786-90.

(71) Westphal E. Ueber mastzellen. In: Ehrlich P, editor. *Farbenanalytische Untersuchungen zur Histologie und Klinik des Blutes*. Verlag von Hirschwald, Berlin, 1891: 17.

(72) Hartveit F. Mast cells and metachromasia in human breast cancer: their occurrence, significance and consequence: a preliminary report. *J Pathol* 1981; 134(1):7-11.

(73) Welsh TJ, Green RH, Richardson D, Waller DA, O'Byrne KJ, Bradding P. Macrophage and mast-cell invasion of tumor cell islets confers a marked survival advantage in non-small-cell lung cancer. *J Clin Oncol* 2005; 23(35):8959-67.

(74) Rizzo V, DeFouw DO. Mast cell activation accelerates the normal rate of angiogenesis in the chick chorioallantoic membrane. *Microvasc Res* 1996; 52(3):245-57.

(75) Feoktistov I, Ryzhov S, Goldstein AE, Biaggioni I. Mast cell-mediated stimulation of angiogenesis: cooperative interaction between A2B and A3 adenosine receptors. *Circ Res* 2003; 92(5):485-92.

(76) Blair RJ, Meng H, Marchese MJ, Ren S, Schwartz LB, Tonnesen MG et al. Human mast cells stimulate vascular tube formation. Tryptase is a novel, potent angiogenic factor. *J Clin Invest* 1997; 99(11):2691-700.

(77) Bradding P, Holgate ST. Immunopathology and human mast cell cytokines. *Crit Rev Oncol Haematol* 1999; 31:119-33.

(78) Finkelman FD, Shea-Donohue T, Goldhill J, Sullivan CA, Morris SC, Madden KB et al. Cytokine regulation of host defense against parasitic gastrointestinal nematodes: lessons from studies with rodent models. *Annu Rev Immunol* 1997; 15:505-33.

(79) Madden KB, Urban JF, Jr., Ziltener HJ, Schrader JW, Finkelman FD, Katona IM. Antibodies to IL-3 and IL-4 suppress helminth-induced intestinal mastocytosis. *J Immunol* 1991; 147(4):1387-91.

(80) Malaviya R, Ikeda T, Ross E, Abraham SN. Mast cell modulation of neutrophil influx and bacterial clearance at sites of infection through TNF-alpha. *Nature* 1996; 381(6577):77-80.

(81) Supajatura V, Ushio H, Nakao A, Okumura K, Ra C, Ogawa H. Protective roles of mast cells against enterobacterial infection are mediated by Toll-like receptor 4. *J Immunol* 2001; 167(4):2250-6.

(82) Jippo T, Morii E, Ito A, Kitamura Y. Effect of anatomical distribution of mast cells on their defense function against bacterial infections: demonstration using partially mast cell-deficient tg/tg mice. *J Exp Med* 2003; 197(11):1417-25.

(83) Malaviya R, Ross EA, MacGregor JI, Ikeda T, Little JR, Jakschik BA et al. Mast cell phagocytosis of FimH-expressing enterobacteria. *J Immunol* 1994; 152(4):1907-14.

- (84) Malaviya R, Gao Z, Thankavel K, van der Merwe PA, Abraham SN. The mast cell tumor necrosis factor alpha response to FimH-expressing *Escherichia coli* is mediated by the glycosylphosphatidylinositol-anchored molecule CD48. *Proc Natl Acad Sci U S A* 1999; 96(14):8110-5.
- (85) Kulka M, Alexopoulou L, Flavell RA, Metcalfe DD. Activation of mast cells by double-stranded RNA: evidence for activation through Toll-like receptor 3. *J Allergy Clin Immunol* 2004; 114(1):174-82.
- (86) Fox CC, Jewell SD, Whitacre CC. Rat peritoneal mast cells present antigen to a PPD-specific T cell line. *Cell Immunol* 1994; 158(1):253-64.
- (87) Frandji P, Tkaczyk C, Oskeritzian C, Lapeyre J, Peronet, R et al. Presentation of soluble antigens by mast cells: upregulation by interleukin-4 and granulocyte/macrophage colony-stimulating factor and downregulation by interferon-gamma. *Cell Immunol* 1995; 163(1):37-46.
- (88) Bradding P, Feather IH, Howarth PH, Mueller R, Roberts JA, Britten K et al. Interleukin 4 is localized to and released by human mast cells. *J Exp Med* 1992; 176(5):1381-6.
- (89) Huels C, Germann T, Goedert S, Hoehn P, Koelsch S, Hultner L et al. Co-activation of naive CD4+ T cells and bone marrow-derived mast cells results in the development of Th2 cells. *Int Immunol* 1995; 7(4):525-32.
- (90) Burr ML, Wat D, Evans C, Dunstan FD, Doull IJ. Asthma prevalence in 1973, 1988 and 2003. *Thorax* 2006; 61(4):296-9.

(91) Galassi C, De Sario M, Biggeri A, Bisanti L, Chellini E, Ciccone G et al. Changes in prevalence of asthma and allergies among children and adolescents in Italy: 1994-2002. *Pediatrics* 2006; 117(1):34-42.

(92) Lack G, Chapman M, Kalsheker N, King V, Robinson C, Venables K. Report on the potential allergenicity of genetically modified organisms and their products. *Clin Exp Allergy* 2002; 32(8):1131-43.

(93) Madsen C. Prevalence of food allergy: an overview. *Proc Nutr Soc* 2005; 64(4):413-7.

(94) Carroll NG, Mutavdzic S, James AL. Distribution and degranulation of airway mast cells in normal and asthmatic subjects. *Eur Respir J* 2002; 19(5):879-85.

(95) de Magalhaes SS, dos Santos MA, da Silva OM, Fontes ES, Fernezlian S, Garippo AL et al. Inflammatory cell mapping of the respiratory tract in fatal asthma. *Clin Exp Allergy* 2005; 35(5):602-11.

(96) Pesci A, Foresi A, Bertorelli G, Chetta A, Olivieri D. Histochemical characteristics and degranulation of mast cells in epithelium and lamina propria of bronchial biopsies from asthmatic and normal subjects. *Am Rev Respir Dis* 1993; 147(3):684-9.

(97) Amin K, Janson C, Boman G, Venge P. The extracellular deposition of mast cell products is increased in hypertrophic airways smooth muscles in allergic asthma but not in nonallergic asthma. *Allergy* 2005; 60(10):1241-7.

(98) Bradding P, Roberts JA, Britten KM, Montefort S, Djukanovic R, Mueller R et al. Interleukin-4, -5, and -6 and tumor necrosis factor-alpha in normal and asthmatic airways: evidence for the human mast cell as a source of these cytokines. *Am J Respir Cell Mol Biol* 1994; 10(5):471-80.

(99) Chen FH, Samson KT, Miura K, Ueno K, Odajima Y, Shougo T et al. Airway remodeling: a comparison between fatal and nonfatal asthma. *J Asthma* 2004; 41(6):631-8.

(100) Carroll NG, Mutavdzic S, James AL. Increased mast cells and neutrophils in submucosal mucous glands and mucus plugging in patients with asthma. *Thorax* 2002; 57(8):677-82.

(101) Brightling CE, Bradding P, Symon FA, Holgate ST, Wardlaw AJ, Pavord ID. Mast-cell infiltration of airway smooth muscle in asthma. *N Engl J Med* 2002; 346(22):1699-705.

(102) Brightling CE, Ammit AJ, Kaur D, Black JL, Wardlaw AJ, Hughes JM et al. The CXCL10/CXCR3 axis mediates human lung mast cell migration to asthmatic airway smooth muscle. *Am J Respir Crit Care Med* 2005; 171(10):1103-8.

(103) Berger P, Girodet PO, Begueret H, Ousova O, Perng DW, Marthan R et al. Tryptase-stimulated human airway smooth muscle cells induce cytokine synthesis and mast cell chemotaxis. *FASEB J* 2003; 17(14):2139-41.

(104) El-Shazly A, Berger P, Girodet PO, Ousova O, Fayon M, Vernejoux JM et al. Fraktalkine Produced by Airway Smooth Muscle Cells

Contributes to Mast Cell Recruitment in Asthma. *J Immunol* 2006; 176(3):1860-8.

(105) Beasley R, Roche WR, Roberts JA, Holgate ST. Cellular events in the bronchi in mild asthma and after bronchial provocation. *Am Rev Respir Dis* 1989; 139(3):806-17.

(106) Casale TB, Wood D, Richerson HB, Zehr B, Zavala D, Hunninghake GW. Direct evidence of a role for mast cells in the pathogenesis of antigen-induced bronchoconstriction. *J Clin Invest* 1987; 80(5):1507-11.

(107) Kirby JG, Hargreave FE, Gleich GJ, O'Byrne PM. Bronchoalveolar cell profiles of asthmatic and nonasthmatic subjects. *Am Rev Respir Dis* 1987; 136(2):379-83.

(108) Flint KC, Leung KB, Hudspith BN, Brostoff J, Pearce FL, Johnson NM. Bronchoalveolar mast cells in extrinsic asthma: a mechanism for the initiation of antigen specific bronchoconstriction. *Br Med J (Clin Res Ed)* 1985; 291(6500):923-6.

(109) Wenzel SE, Fowler AA, III, Schwartz LB. Activation of pulmonary mast cells by bronchoalveolar allergen challenge. In vivo release of histamine and tryptase in atopic subjects with and without asthma. *Am Rev Respir Dis* 1988; 137(5):1002-8.

(110) Gilfillan AM, Tkaczyk C. Integrated signalling pathways for mast-cell activation. *Nat Rev Immunol* 2006; 6(3):218-30.

(111) Rivera J, Gilfillan AM. Molecular regulation of mast cell activation. *J Allergy Clin Immunol* 2006; 117(6):1214-25.

(112) Duffy SM, Lawley WJ, Conley EC, Bradding P. Resting and activation-dependent ion channels in human mast cells. *J Immunol* 2001; 167(8):4261-70.

(113) Cambier JC. Antigen and Fc receptor signaling. The awesome power of the immunoreceptor tyrosine-based activation motif (ITAM). *J Immunol* 1995; 155(7):3281-5.

(114) Dykstra M, Cherukuri A, Sohn HW, Tzeng SJ, Pierce SK. Location is everything: lipid rafts and immune cell signaling. *Annu Rev Immunol* 2003; 21:457-81.

(115) Siraganian RP. Mast cell signal transduction from the high-affinity IgE receptor. *Curr Opin Immunol* 2003; 15(6):639-46.

(116) Faeder JR, Hlavacek WS, Reischl I, Blinov ML, Metzger H, Redondo A et al. Investigation of early events in Fc epsilon RI-mediated signaling using a detailed mathematical model. *J Immunol* 2003; 170(7):3769-81.

(117) Church MK, Pao GJ, Holgate ST. Characterization of histamine secretion from mechanically dispersed human lung mast cells: effects of anti-IgE, calcium ionophore A23187, compound 48/80, and basic polypeptides. *J Immunol* 1982; 129(5):2116-21.

(118) Kim TD, Eddlestone GT, Mahmoud SF, Kuchtey J, Fewtrell C. Correlating Ca²⁺ responses and secretion in individual RBL-2H3 mucosal mast cells. *J Biol Chem* 1997; 272(50):31225-9.

(119) Lewis RS. Calcium oscillations in T-cells: mechanisms and consequences for gene expression. *Biochem Soc Trans* 2003; 31(Pt 5):925-9.

(120) Hoth M, Penner R. Depletion of intracellular calcium stores activates a calcium current in mast cells. *Nature* 1992; 355(6358):353-6.

(121) Feske S, Gwack Y, Prakriya M, Srikanth S, Puppel SH, Tanasa B et al. A mutation in Orai1 causes immune deficiency by abrogating CRAC channel function. *Nature* 2006; 441(7090):179-85.

(122) Vig M, Peinelt C, Beck A, Koomoa DL, Rabah D, Koblan-Huberson M et al. CRACM1 is a plasma membrane protein essential for store-operated Ca²⁺ entry. *Science* 2006; 312(5777):1220-3.

(123) Prakriya M, Feske S, Gwack Y, Srikanth S, Rao A, Hogan PG. Orai1 is an essential pore subunit of the CRAC channel. *Nature* 2006.

(124) Yeromin AV, Zhang SL, Jiang W, Yu Y, Safrina O, Cahalan MD. Molecular identification of the CRAC channel by altered ion selectivity in a mutant of Orai. *Nature* 2006.

(125) Artalejo AR, Ellory JC, Parekh AB. Ca²⁺-dependent capacitance increases in rat basophilic leukemia cells following activation of store-operated Ca²⁺ entry and dialysis with high-Ca²⁺-containing intracellular solution. *Pflugers Archiv - Eur J Physiol* 1998; 436(6):934-9.

(126) Chang WC, Parekh AB. Close functional coupling between Ca²⁺ release-activated Ca²⁺ channels, arachidonic acid release, and leukotriene C₄ secretion. *J Biol Chem* 2004; 279(29):29994-9.

(127) Bradding P, Okayama Y, Kambe N, Saito H. Ion channel gene expression in human lung, skin, and cord blood-derived mast cells. *J Leukoc Biol* 2003; 73(5):614-20.

(128) Panyi G, Varga Z, Gaspar R. Ion channels and lymphocyte activation. *Immunol Lett* 2004; 92(1-2):55-66.

(129) Lindau M, Fernandez JM. A patch-clamp study of histamine-secreting cells. *J Gen Physiol* 1986; 88(3):349-68.

(130) McCloskey MA, Qian YX. Selective expression of potassium channels during mast cell differentiation. *J Biol Chem* 1994; 269(20):14813-9.

(131) Cruse G, Duffy SM, Brightling CE, Bradding P. Functional KCa_{3.1} K⁺ channels are required for human lung mast cell migration. *Thorax* 2006; 61(10):880-5.

(132) Duffy SM, Cruse G, Lawley WJ, Bradding P. Beta₂-adrenoceptor regulation of the K⁺ channel iKCa₁ in human mast cells. *FASEB J* 2005; 19(8):1006-8.

(133) Duffy S.M., Berger P, Cruse G, Yang W, Bolton SJ, Bradding P. The K⁺ channel iKCA₁ potentiates Ca²⁺ influx and degranulation in human lung mast cells. *J Allergy Clin Immunol* 2004; 114(1):66-72.

(134) Duffy SM, Lawley WJ, Kaur D, Yang W, Bradding P. Inhibition of human mast cell proliferation and survival by tamoxifen in association with ion channel modulation. *J Allergy Clin Immunol* 2003; 112(5):965-72.

(135) Duffy SM, Leyland ML, Conley EC, Bradding P. Voltage-dependent and calcium-activated ion channels in the human mast cell line HMC-1. *J Leukoc Biol* 2001; 70(2):233-40.

(136) Kaur D, Berger P, Duffy SM, Brightling CE, Bradding P. Co-cultivation of mast cells and Fc epsilon RI alpha+ dendritic-like cells from human hip bone marrow. *Clin Exp Allergy* 2005; 35(2):226-33.

(137) Oka T, Hori M, Tanaka A, Matsuda H, Karaki H, Ozaki H. IgE alone-induced actin assembly modifies calcium signaling and degranulation in RBL-2H3 mast cells. *Am J Physiol Cell Physiol* 2004; 286(2):C256-C263.

(138) Kitaura J, Song J, Tsai M, Asai K, Maeda-Yamamoto M, Mocsai A et al. Evidence that IgE molecules mediate a spectrum of effects on mast cell survival and activation via aggregation of the Fc epsilon RI. *Proc Natl Acad Sci U S A* 2003; 100(22):12911-6.

(139) Liu Y, Furuta K, Teshima R, Shirata N, Sugimoto Y, Ichikawa A et al. Critical role of protein kinase C beta1 in activation of mast cells by monomeric IgE. *J Biol Chem* 2005; 280(47):38976-81.

(140) Nunomura S, Gon Y, Yoshimaru T, Suzuki Y, Nishimoto H, Kawakami T et al. Role of the Fc epsilon RI beta-chain ITAM as a signal regulator for mast cell activation with monomeric IgE. *Int Immunol* 2005; 17(6):685-94.

(141) Tanaka S, Mikura S, Hashimoto E, Sugimoto Y, Ichikawa A. Ca²⁺ influx-mediated histamine synthesis and IL-6 release in mast cells activated by monomeric IgE. *Eur J Immunol* 2005; 35(2):460-8.

(142) Pandey V, Mihara S, Fensome-Green A, Bolsover S, Cockcroft S. Monomeric IgE stimulates NFAT translocation into the nucleus, a rise in cytosol Ca²⁺, degranulation, and membrane ruffling in the cultured rat basophilic leukemia-2H3 mast cell line. *J Immunol* 2004; 172(7):4048-58.

(143) Matsuda K, Piliponsky AM, Iikura M, Nakae S, Wang EW, Dutta SM et al. Monomeric IgE enhances human mast cell chemokine production: IL-4 augments and dexamethasone suppresses the response. *J Allergy Clin Immunol* 2005; 116(6):1357-63.

(144) Kitaura J, Eto K, Kinoshita T, Kawakami Y, Leitges M, Lowell CA et al. Regulation of highly cytokinergic IgE-induced mast cell adhesion by Src, Syk, Tec, and protein kinase C family kinases. *J Immunol* 2005; 174(8):4495-504.

(145) Kalesnikoff J, Huber M, Lam V, Damen JE, Zhang J, Siraganian RP et al. Monomeric IgE stimulates signaling pathways in mast cells that lead to cytokine production and cell survival. *Immunity* 2001; 14(6):801-11.

(146) Huber M, Kalesnikoff J, Reth M, Krystal G. The role of SHIP in mast cell degranulation and IgE-induced mast cell survival. *Immunol Lett* 2002; 82(1-2):17-21.

(147) Gilchrest H, Cheewatrakoolpong B, Billah M, Egan RW, Anthes JC, Greenfeder S. Human cord blood-derived mast cells synthesize and release I-309 in response to IgE. *Life Sci* 2003; 73(20):2571-81.

(148) Burrows B, Martinez FD, Halonen M, Barbee RA, Cline MG. Association of asthma with serum IgE levels and skin-test reactivity to allergens. *N Engl J Med* 1989; 320(5):271-7.

(149) Sears MR, Burrows B, Flannery EM, Herbison GP, Hewitt CJ, Holdaway MD. Relation between airway responsiveness and serum IgE in children with asthma and in apparently normal children. *N Engl J Med* 1991; 325(15):1067-71.

(150) Sunyer J, Anto JM, Sabria J, Roca J, Morell F, Rodriguez-Roisin R et al. Relationship between serum IgE and airway responsiveness in adults with asthma. *J Allergy Clin Immunol* 1995; 95(3):699-706.

(151) Sunyer J, Anto JM, Castellsague J, Soriano JB, Roca J. Total serum IgE is associated with asthma independently of specific IgE levels. The Spanish Group of the European Study of Asthma. *Eur Respir J* 1996; 9(9):1880-4.

(152) Djukanovic R, Wilson SJ, Kraft M, Jarjour NN, Steel M, Chung KF et al. Effects of treatment with anti-immunoglobulin E antibody omalizumab on airway inflammation in allergic asthma. *Am J Respir Crit Care Med* 2004; 170(6):583-93.

(153) Ong YE, Menzies-Gow A, Barkans J, Benyahia F, Ou TT, Ying S et al. Anti-IgE (omalizumab) inhibits late-phase reactions and inflammatory cells

after repeat skin allergen challenge. *J Allergy Clin Immunol* 2005; 116(3):558-64.

(154) Holgate ST, Djukanovic R, Casale T, Bousquet J. Anti-immunoglobulin E treatment with omalizumab in allergic diseases: an update on anti-inflammatory activity and clinical efficacy. *Clin Exp Allergy* 2005; 35(4):408-16.

(155) D'Amato G, Liccardi G, Noschese P, Salzillo A, D'Amato M, Cazzola M. Anti-IgE monoclonal antibody (omalizumab) in the treatment of atopic asthma and allergic respiratory diseases. *Curr Drug Targets Inflamm Allergy* 2004; 3(3):227-9.

(156) He S, Aslam A, Gaca MD, He Y, Buckley MG, Hollenberg MD et al. Inhibitors of tryptase as mast cell-stabilizing agents in the human airways: effects of tryptase and other agonists of proteinase-activated receptor 2 on histamine release. *J Pharmacol Exp Ther* 2004; 309(1):119-26.

(157) Moormann C, Artuc M, Pohl E, Varga G, Buddenkotte J, Vergnolle N et al. Functional characterization and expression analysis of the proteinase-activated receptor-2 in human cutaneous mast cells. *J Invest Dermatol* 2006; 126(4):746-55.

(158) Sperr WR, Czerwenka K, Mundigler G, Muller MR, Semper H, Klappacher G et al. Specific activation of human mast cells by the ligand for c-kit: comparison between lung, uterus and heart mast cells. *Int Arch Allergy Immunol* 1993; 102(2):170-5.

(159) Brzezinska-Blaszczyk E, Pietrzak A. Tumor necrosis factor alpha (TNF-alpha) activates human adenoidal and cutaneous mast cells to histamine secretion. *Immunol Lett* 1997; 59(3):139-43.

(160) Yanagida M, Fukamachi H, Takei M, Hagiwara T, Uzumaki H, Tokiwa T et al. Interferon-gamma promotes the survival and Fc epsilon RI-mediated histamine release in cultured human mast cells. *Immunology* 1996; 89(4):547-52.

(161) Nilsson G, Johnell M, Hammer CH, Tiffany HL, Nilsson K, Metcalfe DD et al. C3a and C5a are chemotaxins for human mast cells and act through distinct receptors via a pertussis toxin-sensitive signal transduction pathway. *J Immunol* 1996; 157(4):1693-8.

(162) Ahamed J, Venkatesha RT, Thangam EB, Ali H. C3a enhances nerve growth factor-induced NFAT activation and chemokine production in a human mast cell line, HMC-1. *J Immunol* 2004; 172(11):6961-8.

(163) Forsythe P, McGarvey LP, Heaney LG, MacMahon J, Ennis M. Adenosine induces histamine release from human bronchoalveolar lavage mast cells. *Clin Sci* 1999; 96(4):349-55.

(164) Varadaradjalou S, Feger F, Thieblemont N, Hamouda NB, Pleau JM, Dy M et al. Toll-like receptor 2 (TLR2) and TLR4 differentially activate human mast cells. *Eur J Immunol* 2003; 33(4):899-906.

(165) Heaney LG, Cross LJ, Stanford CF, Ennis M. Substance P induces histamine release from human pulmonary mast cells. *Clin Exp Allergy* 1995; 25(2):179-86.

(166) Peachell PT, Morcos SK. Effect of radiographic contrast media on histamine release from human mast cells and basophils. *Br J Radiol* 1998; 71(841):24-30.

(167) Genovese A, Stellato C, Patella V, Lamparter-Schummert B, de Crescenzo G, Adt M et al. Contrast media are incomplete secretagogues acting on human basophils and mast cells isolated from heart and lung, but not skin tissue. *Int J Clin Lab Res* 1996; 26(3):192-8.

(168) Genovese A, Stellato C, Marsella CV, Adt M, Marone G. Role of mast cells, basophils and their mediators in adverse reactions to general anesthetics and radiocontrast media. *Int Arch Allergy Immunol* 1996; 110(1):13-22.

(169) Eggleston PA, Kagey-Sobotka A, Lichtenstein LM. A comparison of the osmotic activation of basophils and human lung mast cells. *Am Rev Respir Dis* 1987; 135(5):1043-8.

(170) Oskeritzian CA, Zhao W, Min HK, Xia HZ, Pozez A, Kiev J et al. Surface CD88 functionally distinguishes the MCTC from the MCT type of human lung mast cell. *J Allergy Clin Immunol* 2005; 115(6):1162-8.

(171) Marc MM, Korosec P, Kosnik M, Kern I, Flezar M, Suskovic S et al. Complement factors c3a, c4a, and c5a in chronic obstructive pulmonary disease and asthma. *Am J Respir Cell Mol Biol* 2004; 31(2):216-9.

(172) Applequist SE, Wallin RP, Ljunggren HG. Variable expression of Toll-like receptor in murine innate and adaptive immune cell lines. *Int Immunol* 2002; 14(9):1065-74.

(173) Matsushima H, Yamada N, Matsue H, Shimada S. TLR3-, TLR7-, and TLR9-mediated production of proinflammatory cytokines and chemokines from murine connective tissue type skin-derived mast cells but not from bone marrow-derived mast cells. *J Immunol* 2004; 173(1):531-41.

(174) Ikeda T, Funaba M. Altered function of murine mast cells in response to lipopolysaccharide and peptidoglycan. *Immunol Lett* 2003; 88(1):21-6.

(175) Supajatura V, Ushio H, Nakao A, Akira S, Okumura K, Ra C et al. Differential responses of mast cell Toll-like receptors 2 and 4 in allergy and innate immunity. *J Clin Invest* 2002; 109(10):1351-9.

(176) Okumura S, Kashiwakura J, Tomita H, Matsumoto K, Nakajima T, Saito H et al. Identification of specific gene expression profiles in human mast cells mediated by Toll-like receptor 4 and FcεRI. *Blood* 2003; 102(7):2547-54.

(177) Kraneveld AD, Kool M, van Houwelingen AH, Roholl P, Solomon A, Postma DS et al. Elicitation of allergic asthma by immunoglobulin free light chains. *Proc Natl Acad Sci U S A* 2005; 102(5):1578-83.

(178) MacDonald SM, Vonakis BM. Association of the Src homology 2 domain-containing inositol 5' phosphatase (SHIP) to releasability in human basophils. *Mol Immunol* 2002; 38(16-18):1323-7.

(179) Holgate ST, Corne J, Jardieu P, Fick RB, Heusser CH. Treatment of allergic airways disease with anti-IgE. *Allergy* 1998; 53(45 Suppl):83-8.

(180) Adra CN, Lelias JM, Kobayashi H, Kaghad M, Morrison P, Rowley JD et al. Cloning of the cDNA for a hematopoietic cell-specific protein related to CD20 and the beta subunit of the high-affinity IgE receptor: evidence for a family of proteins with four membrane-spanning regions. *Proc Natl Acad Sci U S A* 1994; 91(21):10178-82.

(181) Bangur CS, Johnson JC, Switzer A, Wang YH, Hill B, Fanger GR et al. Identification and characterization of L985P, a CD20 related family member over-expressed in small cell lung carcinoma. *Int J Oncol* 2004; 25(6):1583-90.

(182) Liang Y, Tedder TF. Identification of a CD20-, FcepsilonRIbeta-, and HTm4-related gene family: sixteen new MS4A family members expressed in human and mouse. *Genomics* 2001; 72(2):119-27.

(183) Ishibashi K, Suzuki M, Sasaki S, Imai M. Identification of a new multigene four-transmembrane family (MS4A) related to CD20, HTm4 and [beta] subunit of the high-affinity IgE receptor. *Gene* 2001; 264(1):87-93.

(184) Liang Y, Buckley TR, Tu L, Langdon SD, Tedder TF. Structural organization of the human MS4A gene cluster on Chromosome 11q12. *Immunogenetics* 2001; 53(5):357-68.

(185) Tedder TF, Klejman G, Disteché CM, Adler DA, Schlossman SF, Saito H. Cloning of a complementary DNA encoding a new mouse B lymphocyte differentiation antigen, homologous to the human B1 (CD20) antigen, and localization of the gene to chromosome 19. *J Immunol* 1988; 141(12):4388-94.

(186) Tedder TF, Engel P. CD20: a regulator of cell-cycle progression of B lymphocytes. *Immunol Today* 1994; 15(9):450-4.

(187) Uchida J, Lee Y, Hasegawa M, Liang Y, Bradney A, Oliver JA et al. Mouse CD20 expression and function. *Int Immunol* 2004; 16(1):119-29.

(188) Alber G, Miller L, Jelsema CL, Varin-Blank N, Metzger H. Structure-function relationships in the mast cell high affinity receptor for IgE. Role of the cytoplasmic domains and of the beta subunit. *J Biol Chem* 1991; 266(33):22613-20.

(189) Lin S, Cicala C, Scharenberg AM, Kinet JP. The Fc(epsilon)RIbeta subunit functions as an amplifier of Fc(epsilon)RIgamma-mediated cell activation signals. *Cell* 1996; 85(7):985-95.

(190) Bubien JK, Zhou LJ, Bell PD, Frizzell RA, Tedder TF. Transfection of the CD20 cell surface molecule into ectopic cell types generates a Ca²⁺ conductance found constitutively in B lymphocytes. *The Journal of Cell Biology* 1993; 121(5):1121-32.

(191) Li H, Ayer LM, Lytton J, Deans JP. Store-operated cation entry mediated by CD20 in membrane rafts. *J Biol Chem* 2003; 278(43):42427-34.

(192) Corcia A, Schweitzer-Stenner R, Pecht I, Rivnay B. Characterization of the ion channel activity in planar bilayers containing IgE-Fc epsilon receptor and the cromolyn-binding protein. *EMBO J* 1986; 5(5):849-54.

(193) Mazurek N, Dulic V, Pecht I, Schindler HG, Rivnay B. The role of the Fc epsilon receptor in calcium channel opening in rat basophilic leukemia cells. *Immunol Lett* 1986; 12(1):31-5.

(194) Berridge MJ, Lipp P, Bootman MD, Berridge MJ, Lipp P, Bootman MD. The versatility and universality of calcium signalling. *Nat Rev Mol Cell Biol* 2000; 1(1):11-21.

(195) Berridge MJ, Bootman MD, Lipp P. Calcium--a life and death signal. *Nature* 1998; 395(6703):645-8.

(196) Kanzaki M, Shibata H, Mogami H, Kojima I. Expression of calcium-permeable cation channel CD20 accelerates progression through the G1 phase in Balb/c 3T3 cells. *J Biol Chem* 1995; 270(22):13099-104.

(197) Koslowski M, Sahin U, Dhaene K, Huber C, Tureci O. MS4A12 is a colon-selective store-operated calcium channel promoting malignant cell processes. *Cancer Res* 2008; 68(9):3458-66.

(198) Anderson KC, Bates MP, Slaughenhaupt BL, Pinkus GS, Schlossman SF, Nadler LM. Expression of human B cell-associated antigens on leukemias and lymphomas: a model of human B cell differentiation. *Blood* 1984; 63(6):1424-33.

(199) Leget GA, Czuczman MS. Use of rituximab, the new FDA-approved antibody. *Curr Opin Oncol* 1998; 10(6):548-51.

(200) Donato JL, Ko J, Kutok JL, Cheng T, Shirakawa T, Mao XQ et al. Human HTm4 is a hematopoietic cell cycle regulator. *J Clin Invest* 2002; 109(1):51-8.

(201) Chinami M, Yano Y, Yang X, Salahuddin S, Moriyama K, Shiroishi M et al. Binding of HTm4 to cyclin-dependent kinase (Cdk)-associated phosphatase (KAP).Cdk2.cyclin A complex enhances the phosphatase activity of KAP, dissociates cyclin A, and facilitates KAP dephosphorylation of Cdk2. *J Biol Chem* 2005; 280(17):17235-42.

(202) Butterfield JH, Weiler DA, Hunt LW, Wynn SR, Roche PC. Purification of tryptase from a human mast cell line. *J Leukoc Biol* 1990; 47(5):409-19.

(203) Kirshenbaum AS, Akin C, Wu Y, Rottem M, Goff JP, Beaven MA et al. Characterization of novel stem cell factor responsive human mast cell lines LAD 1 and 2 established from a patient with mast cell sarcoma/leukemia; activation following aggregation of Fc[epsilon]RI or Fc[gamma]RI. *Leukaemia Res* 2003; 27(8):677-82.

(204) Clark JM. Novel non-templated nucleotide addition reactions catalyzed by procaryotic and eucaryotic DNA polymerases. *Nucleic Acids Res* 1988; 16(20):9677-86.

(205) Wykes RC, Lee M, Duffy SM, Yang W, Seward EP, Bradding P. Functional transient receptor potential melastatin 7 channels are critical for human mast cell survival. *J Immunol* 2007; 179(6):4045-52.

(206) Michiels F, van Es H, van Rompaey L, Merchiers P, Francken B, Pittois K et al. Arrayed adenoviral expression libraries for functional screening. *Nat Biotechnol* 2002; 20(11):1154-7.

(207) Hamill OP, Marty A, Neher E, Sakmann B, Sigworth FJ. Improved patch-clamp techniques for high-resolution current recording from cells and cell-free membrane patches. *Pflugers Archiv - Eur J Physiol* 1981; 391(2):85-100.

(208) Livak KJ, Schmittgen TD. Analysis of relative gene expression data using real-time quantitative PCR and the 2(-Delta Delta C(T)) Method. *Methods* 2001; 25(4):402-8.

(209) Kinet JP. The high-affinity IgE receptor (Fc epsilon RI): from physiology to pathology. *Annu Rev Immunol* 1999; 17:931-72.

(210) Butterfield JH, Weiler D, Dewald G, Gleich GJ. Establishment of an immature mast cell line from a patient with mast cell leukemia. *Leukaemia Res* 1988; 12(4):345-55.

(211) Donnadieu E, Jouvin MH, Rana S, Moffatt MF, Mockford EH, Cookson WO et al. Competing functions encoded in the allergy-associated F(c)epsilonRIbeta gene. *Immunity* 2003; 18(5):665-74.

(212) Venter JC, Adams MD, Myers EW, Li PW, Mural RJ, Sutton GG et al. The sequence of the human genome. *Science* 2001; 291(5507):1304-51.

(213) Lander ES, Linton LM, Birren B, Nusbaum C, Zody MC, Baldwin J et al. Initial sequencing and analysis of the human genome. *Nature* 2001; 409(6822):860-921.

- (214) Modrek B, Lee C. A genomic view of alternative splicing. *Nat Genet* 2002; 30(1):13-9.
- (215) Modrek B, Resch A, Grasso C, Lee C. Genome-wide detection of alternative splicing in expressed sequences of human genes. *Nucleic Acids Res* 2001; 29(13):2850-9.
- (216) Sorek R, Amitai M. Piecing together the significance of splicing. *Nat Biotechnol* 2001; 19(3):196.
- (217) Brink TC, Sudheer S, Janke D, Jagodzinska J, Jung M, Adjaye J. The origins of human embryonic stem cells: a biological conundrum. *Cells Tissues Organs* 2008; 188(1-2):9-22.
- (218) Gingras MC, Lapillonne H, Margolin JF. CFFM4: a new member of the CD20/FcepsilonRIbeta family. *Immunogenetics* 2001; 53(6):468-76.
- (219) Kaur D, Hollins F, Woodman L, Yang W, Monk P, May R et al. Mast cells express IL-13R alpha 1: IL-13 promotes human lung mast cell proliferation and Fc epsilon RI expression. *Allergy* 2006; 61(9):1047-53.
- (220) Nilsson G, Blom T, Kusche-Gullberg M, Kjellen L, Butterfield JH, Sundstrom C et al. Phenotypic characterization of the human mast-cell line HMC-1. *Scand J Immunol* 1994; 39(5):489-98.
- (221) Smits VA, Medema RH. Checking out the G(2)/M transition. *Biochim Biophys Acta* 2001; 1519(1-2):1-12.

(222) Harkins AB, Dlouhy S, Ghetti B, Cahill AL, Won L, Heller B et al. Evidence of elevated intracellular calcium levels in weaver homozygote mice. *J Physiol* 2000; 524 Pt 2:447-55.

(223) Pigozzi D, Tombal B, Ducret T, Vacher P, Gailly P. Role of store-dependent influx of Ca²⁺ and efflux of K⁺ in apoptosis of CHO cells. *Cell Calcium* 2004; 36(5):421-30.

(224) Skryma R, Prevarskaya N, Vacher P, Dufy B. Voltage-dependent ionic conductances in Chinese hamster ovary cells. *Am J Physiol* 1994; 267(2 Pt 1):C544-C553.

CHAPTER 6: APPENDIX

CHAPTER 6: APPENDIX

6.1 SOLUTIONS

Luria Broth (500mL)

5 grams tryptone

2.5 grams yeast extract

5 grams NaCl

Luria Broth Agar (500mL)

5 grams tryptone

2.5 grams yeast extract

5 grams NaCl

8.5 grams Agar

Tris-acetate electrophoresis (TAE) buffer (500mL) (50x solution)

121g of Tris base

28.55ml of glacial acetic acid

50ml 0.5M EDTA (pH 8)